Universitat de Lleida

Glutamatergic signaling in proximal tubular cells maintains the epithelial phenotype and decreases epithelial mesenchymal transition

Milica Božić Stanojević

Universitat de Lleida

Departament de Medicina

Glutamatergic signaling in proximal tubular cells maintains the epithelial phenotype and decreases epithelial-mesenchymal transition

Milica Božić Stanojević

Doctoral Thesis

Lleida, 2011

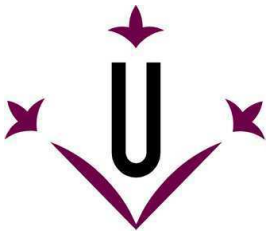

Universitat de Lleida

Programa de Doctorado de
Estudios Avanzados en Ciencias Biomédicas 2006-07
Salut 2009-10
Bioquímica y Biología Molecular

Supervisor

Dr. José Manuel Valdivielso Revilla

Principal Investigator
Director of the Experimental Nephrology Laboratory
Institute for Biomedical Research, Lleida

Supervisor

Dr. Elvira Fernández Giráldez

Director of Nephrology Service, HUAV
Professor at the Department of Medicine
University of Lleida

Lleida, 2011

Universitat de Lleida

José Manuel Valdivielso Revilla, PhD, Principal Investigator and Director of the Experimental Nephrology Laboratory at the Institute for Biomedical Research, Lleida, and **Elvira Fernández Giráldez**, MD, PhD, Director of Nephrology Service, HUAV and Professor at the Department of Medicine, University of Lleida, as supervisors of this thesis

Hereby state that,

Milica Božić Stanojević, with the BSc and MSc degrees in Biology, both acquired at the Faculty of Biology, University of Belgrade, Serbia, has performed under our direction and supervision, and within the Experimental Nephrology Laboratory of the Department of Medicine, the experimental work entitled ‘‘**Glutamatergic signaling in proximal tubular cells maintains the epithelial phenotype and decreases epithelial-mesenchymal transition**’’.

The work accomplishes the adequate conditions in order to be defended in front of the corresponding Thesis Committee and, if it is the case, to obtain the **Doctor degree** from the *University of Lleida*.

Signed

Dr. José Manuel Valdivielso Revilla **Dr. Elvira Fernández Giráldez**

Lleida, 2011

Give me a lever long enough and a fulcrum on which to place it,
and I shall move the world.

Archimedes

Acknowledgements

I would like to express my gratitude to those who made this thesis possible.

I wish to express my sincere appreciation to my supervisor Dr. José M. Valdivielso, who has supported me throughout my thesis with his patience, advices and open mind to diverse topics, while at the same time allowing me a privilege to work in my own way. I attribute the publication of my article in Journal of the American Society of Nephrology to his encouragement and enthusiasm, because without him this article would not have been published.

I wish to thank Professor Dr. Elvira Fernandez for giving me the opportunity to be a member of her laboratory and, although not always being in direct contact with her, for the help and support she has given me any time I asked for it.

I would like to thank AGAUR, University of Lleida and IRB Lleida for the financial support in realization of my doctoral studies.

I also thank members of the Experimental Nephrology Laboratory - Noelia, Petya, Ana M, Montse, Anna C, Eva, Sara, Vicki, Adriana and Jordi for their collaboration, humor and encouragement. In particular, I wish to thank Ana Martínez and Montse Freixenet for their technical skills, hard work and enthusiasm in helping me accomplish my tasks. Montse, thank you for being my friend from the first day we met and for the support you gave me in the most difficult moments of my life in Spain. Noelia, thank you for spreading *nirvāna* through the laboratory. It is a pleasure working with you!

I wish to thank Carme Gallego, Marti Aldea and Jordi Torres for accepting my PhD application and for directing me to the laboratory of Dr. José M. Valdivielso.

I would also like to show my gratitude to Dr. Johan de Rooij from the Department of Cell Biology, Netherlands Cancer Institute Antoni van Leeuwenhoek, Amsterdam, (present address at Hubrecht Institute and University Medical Center Utrecht), Netherlands, for his collaboration on our project and for enabling me to learn from him the fascinating Live Cell Imaging technique.

I wish to thank Dr. Marta Ruiz Ortega from the Laboratory of Nephrology, Foundation Jimenez Diaz, Madrid for her collaboration on our project.

Throughout whole my doctoral studies I have been surrounded with a friendly and joyful doctoral students and co-workers of IRB Lleida and ARNAU, who helped me in many different ways during my thesis: Nuria E, Anna Macia, Laura, Annabel, Cristina M, Nuria B, Andre, Arindam, Charumathi, Deepshikha, Junmei, Myriam, Gemma, Monica D, Cristina G, Mireia, Maria, Esmeralda, Anais, Manuel, Dolos, Ana V, Gordana, Monica D, Maya, Jisheng, Esteban, David. Thank you, guys and keep up the good work!

I would like to show my gratitude to Mario and Xavi for finding time for me every time I knocked at their door searching for advices, chemicals or antibodies.

I would like to thank Carles, Judit, Marta and Dani for their kindness and willingness to help each time they were asked.

I am grateful to Dr. Carme Piñol and the personnel of the animal facility for their help in manipulation with animals.

I would like to thank Dr. Peter Mundel for accepting my application for a short stay visit in the Division of Nephrology at Harvard Medical School and Massachusetts General Hospital, Boston and for giving me the opportunity to enrich my knowledge about podocyte cell biology. I am grateful to my colleagues from Mundel Lab from which I have learnt much and who made my stay in Boston very pleasant.

I would especially like to thank my mother, father and brother for their belief in me and for their wholehearted motivation through entire course of my studies at the University. This work is their accomplishment as much as mine, because it would not have happened without them caring so much.

Finally, I thank my wonderful and patient husband, Dejan, who supported every decision of mine and who helped me, unselfishly and in any meaning, accomplishing my goals throughout all nineteen years we spent together. In spite of many difficulties and trammels we had in the past in order to achieve what we wanted, those only made our love stronger and that’s why my heart will always belong to you!

Milica

Index

Abbreviations

ABD	Agonist-binding domain
AJ	Adherens junctions
Akt	Serine/threonine protein kinase
AMPA	α-amino-3-hydroxy-5-methyl-4-isoxazolepropionate
AngII	Angiotensin II
AP5	D-2-amino-5-phosphonopentanoic acid
BMP	Bone morphogenetic protein
CaMKII	Calcium/Calmodulin-dependent protein kinase II
cAMP	Cyclic adenosine monophosphate
Cdc42	Cell division control protein 42 homolog
CKD	Chronic kidney disease
CNS	Central nervous system
CTD	C-terminal domain
CTGF	Connective tissue growth factor
DAB	3, 3'-diaminobenzidine
DH5α	*E. coli* strain
ECM	Extracellular matrix
EGF	Epidermal growth factor
EMT	Epithelial-mesenchymal transition
EndMT	Endothelial–mesenchymal transition
Erk	Extracellular-signal-regulated kinase
FAK	Focal adhesion kinase
FAs	Focal adhesions
FBS	Fetal bovine serum
FGF	Fibroblast growth factor
FSP1	Fibroblast specific protein
GAP	GTPase-activating protein
GDP	Guanosine diphosphate
GEF	Guanine nucleotide-exchange factors
GFP	Green fluorescent protein
GRIN1	Human NMDAR1 subunit
GSK-3β	Glycogen synthase kinase 3β
GST	Glutathione-S-transferase
GTP	Guanosine triphosphate
HEK293T	Human embryonic kidney cell line
HGF	Hepatocyte growth factor
HK-2	Human renal proximal tubular epithelial cells
IGF-II	Insulin-like growth factor 2
iGluRs	Ionotropic glutamate receptors
IL-1	Interleukin 1

ILK	Integrin-linked kinase
IPTG	Isopropyl-β-D-thiogalactopyranoside
JNK	Jun N-terminal kinase
kDa	kiloDalton
MEK	MAPK/Erk kinase
MET	Mesenchymal-epithelial transition
MK-801	(+)-5-methyl-10,11-dihydro-5H-dibenzo[a,d]cyclohepten-5,10-imine maleate
MMP	Matrix metalloproteinases
MTT	3-(4,5-dimethylthiazol-2-yl)-2,5-diphenyltetrazolium bromide
NF-kB	Nuclear factor-kappaB
NMDA	N-methyl-D-aspartic acid
NMDAR	N-methyl-D-aspartate (NMDA) receptor
NOD	Non-obese diabetic
NSN	Nephrotoxic serum nephritis
NTD	N-terminal domain
p38MAPK	p38 mitogen-activated protein kinase
PBS	Phosphate buffer saline
PCP	Phencyclidine
PCT	Proximal convoluted tubule
PDGF	Platelet-derived growth factor
PEI	Polyethylenimine
PI3K	Phopshatidylinositol-3-kinase
PKA	Protein kinase A
PKB	Protein kinase B
PKC	Protein kinase C
PKCg	Protein kinase C gamma
PLCe	Phospholipase C epsilon
PTEC	Proximal tubular epithelial cell
Rac	Family member of the Rho-like GTPases
Raf	v-raf murine leukemia viral oncogene, protein kinase, effector of Ras
Ral	GDS, GEF for the Ral subfamily
Ras	RAt Sarcoma protein (Ras) subfamily of small GTPases
RBD	Ras binding domain
RhoA	Family member of the Rho-like GTPases
SARA	Smad anchor for receptor activation
shRNA	short hairpin RNA
Smad	Mammalian homolog of the *Drosophila* Mothers against dpp (Mad)
Snail 1	Snail homolog 1

SOS	Son of Sevenless
Src	v-src sarcoma (Schmidt-Ruppin A-2) viral oncogene homolog
TAK1	TGF-β-activated kinase 1
TBM	Tubular basement membrane
TCP 1	1-thienyl-cyclohexyl piperidine
TGF-β1	Transforming growth factor-β1
TIF	Tubulointerstitial fibrosis
TJ	Tight junctions
TNF-α	Tumor necrosis factor-alpha
Twist	Twist homolog 1
UUO	Unilateral ureteral obstruction
Wnt	Wingless-type MMTV integration site family
α-SMA	Alpha-smooth muscle actin

Abstract

Epithelial-mesenchymal transition (EMT) is a widely recognized molecular event of vital significance in the progression of renal tubulointerstitial fibrosis (TIF). EMT is characterized by the downregulation of E-cadherin, *de novo* expression of α-SMA and vimentin, actin cytoskeleton reorganization and increased cell migration. A number of factors have been stated as potential inducers of tubular EMT in diverse experimental models. Nevertheless, growing evidence establishes a crucial role for transforming growth factor-β1 (TGF-β1) signaling in mediating renal fibrosis. TGF-β1 plays an important role in altering the phenotype of renal epithelial cells and is capable of initiating and completing the whole process of EMT.

N-methyl-D-aspartate receptor (NMDAR) is an ionotropic glutamate receptor that acts as a calcium channel and its presence in proximal tubular epithelium is important in the maintenance of normal renal function. An important feature of NMDAR is its high permeability to calcium, placing this receptor in a unique position to control numerous calcium-dependent processes. Taking into consideration knowledge of multiple characteristics of NMDAR in a variety of tissues, including renal itself, we sought to examine the role of this receptor in the maintenance of the proximal tubular epithelial phenotype and its role in tubular EMT *in vitro*. Furthermore, we examined the role of channel activation in TIF induced by unilateral ureteral obstruction (UUO) in mice.

To assess the function of the NMDAR in HK-2 cells in basal conditions, we designed NR1 shRNA vector for lentiviral infection and the expression of the NMDAR1 subunit was disrupted by short hairpin RNA. Knockdown of an essential NR1 subunit of the NMDAR induced remarkable changes in epithelial phenotype of HK-2 cells, evident as a decrease of E-cadherin and an increase of α-SMA, alongside with the changes in cell morphology.

Having established that the basal NMDAR activation had a role in preserving the epithelial phenotype of HK-2 cells, we assessed if the activation of the channel could be a possible strategy in attenuating the phenotypic changes induced by TGF-β1. *In vitro*, HK-2 exposed to TGF-β1 demonstrated downregulation of E-cadherin and membrane-associated β-catenin, F-actin reorganization, *de novo* expression of mesenchymal markers such as α-SMA and vimentin, upregulation of Snail1 and elevated cell migration. Co-treatment with NMDA attenuated all described signs of

EMT induced by TGF-β1. Furthermore, TGF-β1 increased cell velocity on collagen and fibronectin matrices, which was inhibited by co-treatment with NMDA.

Once determined that the activation of NMDAR managed to attenuate EMT induced by TGF-β1 in HK-2 cells, we investigated the signaling events that had led to NMDAR-induced blockade of TGF-β1-initiated EMT. There is a growing body of evidence linking the activation of extracellular signal-regulated kinase Erk and serine/threonine kinase Akt pathways to the induction of TGF-β1-mediated EMT. Indeed, in our experimental set up, treatment of HK-2 cells with TGF-β1 resulted in a rapid increase in the phosphorylation of Erk1/2 and Akt within 30 min after stimulation, which was prevented by co-treatment with NMDA in the case of both investigated kinases. In addition, NMDAR activation remarkably blocked TGF-β1-mediated activation of Ras pointing to the inhibition of the Ras-MEK pathway as the mechanism by which NMDA antagonizes TGF-β1-induced EMT.

In vivo, administration of NMDA significantly inhibited expression of α-SMA in the obstructed mouse kidneys at 5 and 15 days after UUO. Collagen I expression was significantly diminished in obstructed kidneys of NMDA-treated mice at day 15 after UUO. Furthermore, administration of NMDA blunted the downregulation of E-cadherin and an increase of FSP1 induced by UUO.

Results obtained point to a paramount role of NMDAR in the preservation of normal epithelial phenotype of proximal tubular cells and in the modulation of important steps of tubular EMT.

La transición epitelio-mesenquimal (EMT) es un mecanismo molecular extensamente reconocido por su importante papel en la progresión de la fibrosis renal tubulointersticial (TIF). La EMT se caracteriza por la supresión de la expresión de E-cadherina, la expresión *de novo* de alpha-SMA y de vimentina, la reorganización del citoesqueleto y el aumento de migración celular. Se ha identificado un número de factores como inductores potenciales de EMT tubular en diversos modelos experimentales. Sin embargo, la creciente evidencia establece un papel crucial para la señalización por el factor de crecimiento transformante-beta1 (TGF-β1) en la mediación de la fibrosis renal. TGF-β1 juega un papel importante en la alteración del fenotipo de las células epiteliales renales y tiene la capacidad de iniciar y terminar todo el proceso de la EMT *in vitro*.

El receptor N-metil-D-aspartato (NMDAR) es uno de los receptores ionotrópicos de glutamato que funciona como canal de calcio de membrana. Su presencia en el epitelio de túbulo proximal es importante en el mantenimiento de la función renal normal. Una característica prominente de la NMDAR es su alta permeabilidad al calcio que coloca este receptor en una posición única para controlar los procesos dependientes del mismo. Teniendo en cuenta las características diversas del NMDAR en una variedad de tejidos, incluyendo tejido renal, hemos tratado de examinar el papel de este receptor en el mantenimiento del fenotipo epitelial de túbulo proximal y su papel en la EMT tubular *in vitro*. Además, hemos investigado el papel de la activación del NMDAR en la TIF inducida por la obstrucción ureteral unilateral (UUO) en ratones.

Para evaluar la función del receptor de NMDA en las células HK-2 en los condiciones basales, hemos diseñado un vector lentiviral (NR1 shRNA) y la expresión de la subunidad NMDAR1 fue interrumpida por la técnica de *short hairpin* RNA. La supresión de la expresión de NR1, una subunidad fundamental del receptor de NMDA, indujo cambios importantes en el fenotipo epitelial de las células HK-2, evidentes como una disminución de E-cadherina y un aumento de alpha-SMA, junto con cambios en la morfología celular.

Una vez establecido que la activación basal del NMDAR tiene un papel significativo en el mantenimiento del fenotipo epitelial de las células HK-2, investigamos si la activación del canal podría ser una estrategia eficaz para atenuar las

alteraciones fenotípicas inducidas por el TGF-β1. *In vitro*, el tratamiento de células HK-2 con el TGF-β1 indujo la supresión de E-cadherina, la translocación de beta-catenina al núcleo, la reorganización de F-actina, la expresión *de novo* de alpha-SMA y de vimentina, la elevación de Snail1 y el aumento de migración celular. El co-tratamiento con NMDA redujo todos los signos de la EMT inducidos por el TGF-β1. Además, el aumento de velocidad de células HK-2 inducido por el TGF-β1 en matriz de colágeno y de fibronectina fue inhibido por el co-tratamiento con NMDA.

Una vez determinado que la activación del NMDAR ha tenido la capacidad de atenuar la EMT inducida por el TGF-β1 en células HK-2, investigamos los eventos de señalización implicados en el efecto del NMDA inhibiendo la transición epitelio-mesenquimal. Hay una evidencia creciente que vincula la activación de la proteína cinasa regulada por señal extracelular (Erk) y la proteína cinasa serina/treonina (Akt) a la inducción de la EMT por el TGF-β1. En nuestro modelo experimental, el tratamiento de las células HK-2 con el TGF-β1 resultó en un aumento de la fosforilación de Erk1/2 y Akt 30 minutos después de la estimulación, que se inhibió por el co-tratamiento con el NMDA en el caso de ambas cinasas investigadas. Además, la activación del NMDAR bloqueó notablemente la activación de Ras inducida por el TGF-β1, apuntando a la inhibición de la vía Ras-MEK como el mecanismo por el cual NMDA antagoniza la EMT inducida por el TGF-β1.

In vivo, la administración de NMDA inhibió significativamente la expresión de alpha-SMA en los riñones obstruidos 5 y 15 días después de UUO. Los ratones tratados con NMDA demostraron una disminución significativa de fibras intersticiales de colágeno en sus riñones obstruidos en el día 15 después de UUO. Además, la administración de NMDA inhibió la supresión de la expresión de E-cadherina y el aumento de FSP1, ambos inducidos por la UUO.

Los resultados obtenidos apuntan a un papel fundamental del NMDAR en el mantenimiento del fenotipo epitelial de células de túbulo proximal y en la modulación de los pasos importantes de la EMT tubular.

La transició epiteli-mesenquimal (EMT) és un esdeveniment molecular àmpliament reconegut de vital importància en la progressió de la fibrosi túbul-intersticial renal (TIF). La EMT es caracteritza per la supressió de l'expressió d'E-cadherina, l'expressió *de novo* de l'alpha-SMA, de la vimentina, per la reorganització del citoesquelet d'actina i l'augment de la migració cel·lular. Una sèrie de factors han estat establerts com a potencials inductors de l'EMT tubular en diversos models experimentals. No obstant això, l'evidència creixent estableix un paper crucial per a la senyalització del factor de creixement transformant-β1 (TGF-β1) en la mediació de la fibrosi renal. El TGF-β1 juga un paper important en l'alteració del fenotip de les cèl·lules epitelials renals i té capacitat d'iniciar i finalitzar tot el procés de l'EMT.

El receptor N-metil-D-aspartat (NMDAR) és un dels receptors ionotròpics de glutamat, que actua com un canal de calci. La seva presència en l'epiteli tubular proximal és important en el manteniment de la funció renal normal. Una característica important del NMDAR és la seva alta permeabilitat al calci que posa aquest receptor en una posició única per controlar els processos dependents de calci. Tenint en compte les característiques múltiples del NMDAR en una varietat de teixits, incloent teixit renal, hem tractat d'examinar el paper d'aquest receptor en el manteniment del fenotip epitelial tubular proximal i el seu paper en l'EMT tubulars in vitro. A més, es va examinar el paper de l'activació del canals en la TIF induïda per l'obstrucció ureteral unilateral (UUO) en ratolins.

Per avaluar la funció del receptor NMDA en les cèl.lules HK-2 en conditions basals, hem dissenyat un vector lentiviral (NR1 shRNA) i l'expressió de la subunitat NMDAR1 va ser interrompuda per la forma de *short hairpin* RNA. La supressió de l'expressió de NR1, la subunitat fonamental del receptor de NMDA, va induir canvis notables en el fenotip epitelial de les cèl lules HK-2, evidenciant una disminució d'E-cadherina i un augment de l'alpha-SMA, juntament amb els canvis en la morfologia cel·lular .

Un cop establert que l'activació basal del receptor de NMDA va tenir un paper en el manteniment del fenotip epitelial de les cèl·lules HK-2, es va avaluar si l'activació del canal podria ser una estratègia eficaç per atenuar els canvis fenotípics induïts pel TGF-β1. *In vitro*, el tractament de les cèl·lules HK-2 amb el TGF-β1 va induir la supressió d'E-cadherina, la translocació de la beta-catenina al nucli, la

reorganització de la F-actina, l'expressió *de novo* de l'alpha-SMA i de la vimentina, l'elevació de Snail1 i l'augment de la migració cel·lular. El co-tractament amb NMDA va reduir tots els signes descrits de l'EMT induïda per TGF-β1. A més, l'increment de velocitat de cèl·lules HK-2 induït pel TGF-β1 en matriu de col·lagen i fibronectina va ser inhibit pel co-tractament amb NMDA.

Un cop determinat que l'activació del NMDAR ha tingut la capacitat d'atenuar l'EMT induïda pel TGF-β1 en cèl·lules HK-2, hem investigat els esdeveniments de senyalització implicats en l'efecte del NMDA inhibint la transició epiteli-mesenquimal. Hi ha una gran evidència que vincula l'activació de la proteïna cinasa regulada per senyal extracel·lular (Erk) i la proteïna cinasa serina/treonina (Akt) en la inducció de l'EMT pel TGF-β1.En efecte, en el nostre model experimental, el tractament de les cèl·lules HK-2 amb el TGF-β1 va produir un augment de la fosforilació de Erk1/2 i Akt dins els 30 minuts després de l'estimulació, la qual cosa es va impedir amb el co-tractament amb NMDA en el cas de les dues cinases investigades. A més, l'activació del receptor de NMDA va bloquejar notablement l'activació de Ras induïda pel TGF-β1 que apunta a la inhibició de la via Ras-MEK com a mecanisme pel qual el NMDA antagonitza l'EMT induïda pel TGF-β1.

In vivo, l'administració de NMDA va inhibir significativament l'expressió de l'alpha-SMA en els ronyons obstruïts als 5 i 15 dies després de la UUO. Els ratolins tractats amb NMDA van demostrar una disminució significativa de les fibres intersticials de col·lagen en els seus ronyons obstruïts el dia 15 després de la UUO. A més, l'administració de NMDA va inhibir la supressió de l'expressió d'E-cadherina i l'augment de FSP1, induïda per la UUO.

Els resultats obtinguts apunten a un paper fonamental del NMDAR en el manteniment del fenotip epitelial de les cèl·lules del túbul proximal i en la modulació dels passos importants de l'EMT tubular.

Introduction

1. The Kidney

Kidneys are essential excretory and homeostatic organs of the body that are responsible for preserving the internal environment of the organism. Glomerular filtration, tubular reabsorption, and tubular excretion are the three mechanisms by which kidneys accomplish the homeostasis of the internal environment. Every kidney performs an essential function such as excretion of most of the end products of metabolism by filtering the blood, reabsorbing necessary substances while excreting toxins and other waste products through urine. Furthermore, kidney controls the concentration of certain constituents of the body's fluids, such as sodium salt and uric acid, by controlling their excretion and reabsorption[1].

The kidney can be divided into three segments: cortex, outer medulla and inner medulla (Figure 1).

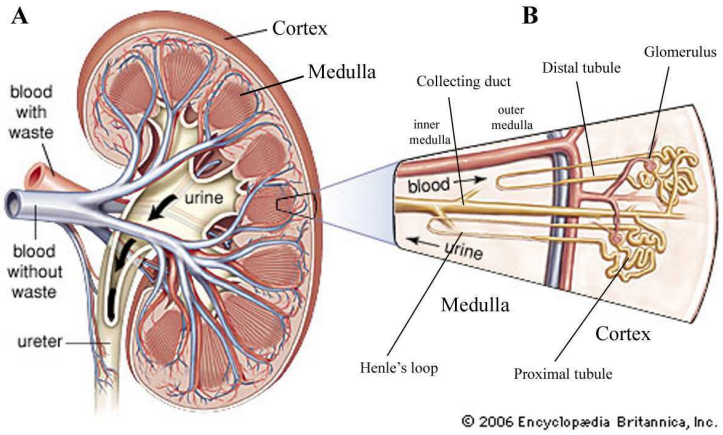

Figure 1. **Schematic representation of the kidney and nephron**. *The kidney consists of a papilla, inner and outer medulla and the cortex (**A**). Each kidney consists of about*

one million nephrons (B), which contain the glomerulus, proximal tubule, Loop of Henle, distal tubule and the collecting duct.

1.1. Nephron – basic urine-producing unit of kidney

Nephron (from Greek νεφρός – nephros, meaning ‘‘kidney’’) is the basic structural and functional unit of the kidney. In humans, a normal kidney contains about one million nephrons[2]. The nephron takes the responsibility of nearly all of the kidney’s functions, especially functions concerning reabsorption and secretion of different soluble substances such as ions (e.g., sodium salts), carbohydrates and amino acids. Each nephron is composed of the principal filtering component – the *renal corpuscle* and a part specialized for reabsorption and secretion – the *renal tubule*.

1.1.1. Renal corpuscle

The renal corpuscle is the initial filtering component of the kidney nephron (Figure 2). The renal corpuscle of each nephron has two parts – *glomerulus*, which represents the network of small blood vessels called capillaries, and the *Bowman’s capsule*, which is the double-walled epithelial cup composed of visceral inner layer formed of specialized cells called podocytes and a parietal outer layer composed of squamous epithelium. Glomerulus is located in the Bowman’s capsule. Glomerulus receives blood from an afferent arteriole of the renal circulation; fluids in the glomerulus are filtered through the visceral layer of podocytes, and the remaining blood is drained away from the glomerulus by the efferent arteriole (Figure 2). The resulting glomerular filtrate is further processed along the renal tubule of the nephron.

1.1.2. Renal tubule

The renal tubule is the part of the kidney nephron into which the glomerular filtrate passes after it has reached the Bowman's capsule (Figure 2). The first part of the renal tubule is the *proximal convoluted tubule (PCT)*. The water and solutes that have passed through the proximal convoluted tubule enter the U-shaped tube called *Loop of Henle*, which consists of two portions - a descending branch and an ascending branch.

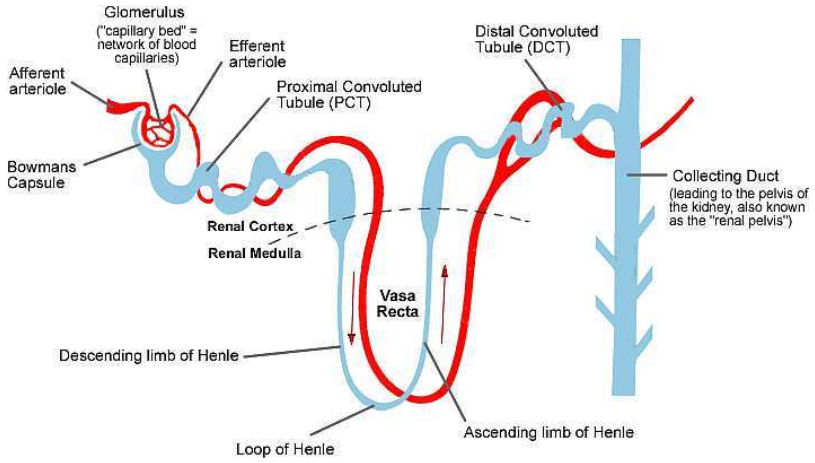

Figure 2. **Schematic representation of the nephron – basic urine-producing unit of kidney**. *Each nephron is composed of the renal corpuscle and the renal tubule. The renal corpuscle has two parts – glomerulus and the Bowman's capsule. The renal tubule starts with proximal convoluted tubule (PCT), continues as the Loop of Henle and through the ascending branch connects to the distal convoluted tubule. Many distal convoluted tubules converge into a single collecting duct leading to the pelvis of the kidney, also known as the ''renal pelvis''.*

The Loop of Henle begins in the cortex where it extends from the proximal tubule. After receiving the filtrate from the proximal tubule, it continues into the

medulla as a descending branch, and then returns to the cortex as an ascending branch where it connects to the *distal convoluted tubule* (Figure 2). The distal convoluted tubules of many individual nephrons converge into a single collecting duct while many collecting ducts join together to form several hundred papillary ducts. The content of the papillary ducts drain into specialized channels, and via the major calyx passes into the centre of the kidney called *renal pelvis*, and finally into the urinary bladder via ureter.

1.1.2.1. Proximal tubular epithelial cells (PTECs)

Proximal tubular cells lining the proximal convoluted tubule form a polarized monolayer of cells tightly connected to each other through intercellular junctional complexes. On their basal side, PTECs are connected with the tubular basement membrane (TBM) via cell-extracellular matrix (ECM) interactions (Figure 3A, B). Both the cell-ECM and cell-cell adhesion complexes are linked to the actin cytoskeleton through a complex of cytoskeletal/signalling proteins[3]. Regulation of these two types of adhesion is important in the maintenance of cell polarity[4] and influences pathological events in the renal interstitium.

1.1.2.1.1. Intercellular adhesion complexes

Proximal tubular epithelial cells form multiple cell-cell interactions which consist of adherens junctions (AJ) and tight junctions (TJ). Adherens junctions are composed of cadherin-catenin complexes linked to the actin cytoskeleton[5]. Having a single transmembrane-spanning region, an extracellular domain and an intracellular domain, *cadherins* mediate Ca^{2+}-dependent homotypic interactions between adjacent cells. The extracellular part of an E-cadherin protein binds to the extracellular domain

of an E-cadherin protein from an adjacent cell, thereby linking two cells in a zipper-like way[6] (Figure 3 B). The intracellular/cytoplasmic domain of the cadherin interacts with either β- or γ-catenin. α-catenin binds with β-catenin and γ-catenin, forming a link with the actin cytoskeleton[5]. Within the complex, β-catenin binds directly to the F-actin cytoskeleton, which is required for the formation of cell-cell junctions[3,7] (Figure 3 B). The stability of cell-cell interactions is essential for the maintenance of the epithelial phenotype of PTECs. Loss of cell-cell junctions via disruption of the cadherin-catenin complex results in loss of adhesiveness, which leads to renal PTEC detachment, and, in the end, loss of renal tubular function[8,9].

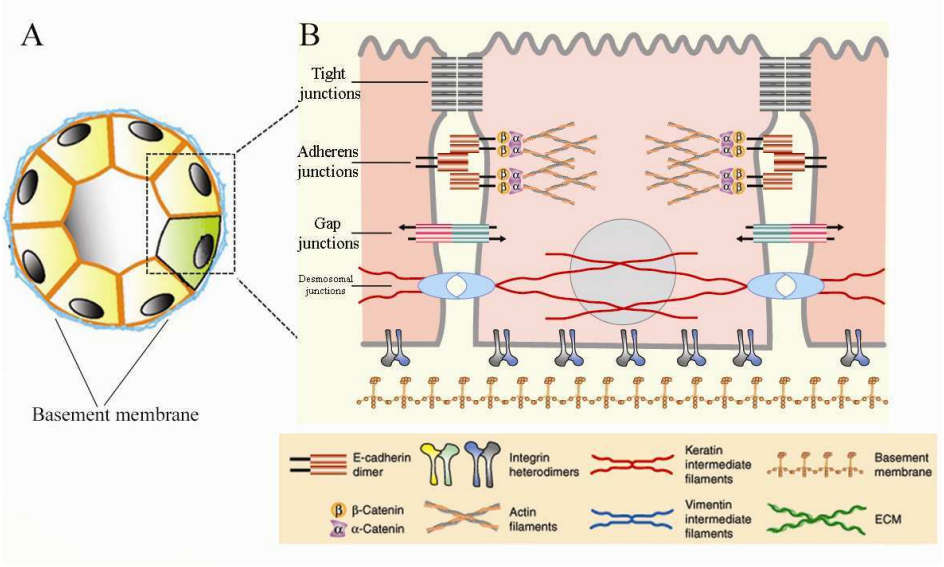

Figure 3. **Tubular cell-cell and cell-ECM adhesion complexes.** ***(A)*** *Proximal tubule.* ***(B)*** *Tubular cell adhesion is mediated via cell-cell adhesion complexes and cell-extracellular matrix (ECM) interactions. Intercellular adherens junctions are composed of cadherin-catenin complexes linked to the actin cytoskeleton. Adhesion of PTECs to the tubular basement membrane is mediated through focal adhesions (FAs)*

consisted of integrins interacting with different signaling- and cytoskeletal-related proteins such as FAK, Src and paxilin (scheme modified from Radisky, 2005[10]).

1.1.2.1.2. Cell-ECM adhesion complexes

Another type of interactions necessary for maintaining the normal function of proximal tubular cells is their adhesion to the tubular basement membrane (TBM). The adhesion is mediated by heterodimeric transmembrane proteins called *integrins* (Figure 3B). After binding to the extracellular matrix, integrins cluster leading to the formation of a specialized structure known as focal adhesion (FA) through an interaction of cytoplasmic domain of integrins with a large complex of signalling- and cytoskeletal-related proteins[11]. These FAs mediate cell attachment to the ECM and serve as anchor points for organization and remodelling of actin filaments. The loss of interaction between PTECs and the basement membrane leads to denudation of the proximal tubule which alongside with the tubular obstruction, induced by aggregation of detached cells in the tubular lumen, could lead to an impairment in renal function[8].

Properties of the cells that line the nephron vary considerably along its length, but each segment of the nephron has highly specialized functions and contributes to the transport function of the kidney. As a result of this transport function, cells within the particular segments of the nephron may be extensively exposed to different toxins. The cells of the PTEC layer are believed to be the major target for cellular injury, due to an intensive reabsorption of large volumes of fluid and the high activity of several enzymes within these cells. Persistent injury of kidney cells could lead to chronic progressive renal fibrosis which results in formation of a scar in the kidney and disruption of renal function.

2. Chronic kidney disease (CKD)

Chronic kidney disease (CKD) is a gradual loss of renal function over a period of months or years which finally leads to well known complications such as cardiovascular disease, anemia or pericarditis[12]. CKD is a growing epidemic worldwide, primarily driven by the rise of obesity, hypertension and diabetes[13] and over the past decade it has become an area of intensive clinical and epidemiological research. Chronic kidney disease is defined by a sustained reduction in glomerular filtration rate or evidence of structural or functional abnormalities of the kidneys on urinalysis, biopsy or imaging[14]. On 2002, the National Kidney Foundation's Kidney Disease Outcomes Quality Initiative (KDOQI) created guidelines that define CKD as the presence of kidney damage or glomerular filtration rate (GFR) of < 60 ml/min/1.73m^2 for 3 month[15].

Regardless of the fact that a range of diseases such as glomerulonephritis, diabetes mellitus, atherosclerosis, obstructive nephropathy, interstitial nephritis, and polycystic kidney disease can be the major causes of CKD, *renal fibrosis* is always the common pathologic result/pathway in nearly every type of chronic kidney disease[16-18].

2.1. Renal fibrosis

Renal fibrosis, as the final manifestation of CKD, represents a dynamic and complex spectrum of changes in the renal tissue that engage constituents of extracellular matrix and different renal and infiltrating cell types[19]. The involved cells exhibit enormous plasticity or phenotypic variability[19]. It is generally accepted that renal fibrosis initiates as a beneficial reaction to injury of the renal tissue[17]. Nevertheless, if an injurious condition is sustained, which is the situation in most

progressive renal diseases, pathologic renal fibrosis sets up developing in a disorder characterized by glomerulosclerosis, tubulointerstitial fibrosis, inflammatory cell infiltration and loss of renal parenchyma denoted by tubular atrophy, capillary loss and podocyte depletion[16,17].

2.1.1. Pathogenesis of renal fibrosis

The pathogenesis of renal fibrosis is a progressive process that finally leads to an end-stage renal failure, a severe disorder that requires dialysis or kidney transplantation[17]. The pathogenic mechanisms underlying renal fibrosis are extremely complex and not entirely understood. After an initial injury such as high ambient glucose, protein overload, hypoxia, persistent infection, autoimmune reaction, or chemical insults, the affected renal tissue undergoes a series of events in an attempt to recover from the damage[17,20]. First of all, resident tubular epithelial cells become activated which subsequently leads to the production of proinflammatory molecules that contribute to renal fibrosis[17,19-21]. Due to the activation of various chemokines and chemoattractants, many inflammatory cells such as monocytes/macrophages and lymphocytes (T cells) are becoming directed to the glomerular or interstitial areas, depending of the site of injury (Figure 4). Arriving to their final destination, these inflammatory cells become activated leading to the secretion of inflammatory and fibrogenic cytokines, as well as injurious molecules such as reactive oxygen species (ROS)[16,17]. As a final outcome, these challenging stimuli induce activation of mesangial cells, fibroblasts and especially tubular epithelial cells to undergo phenotypic transition via common pathway known as epithelial-mesenchymal transition (EMT), all together leading to an excessive production of ECM components

(Figure 4). As the process progresses, ECM proteins are deposited in the extracellular compartment, they become crosslinked and resistant to degradation. The continuation of the process leads to the formation of fibrous scars, distorts the subtle architecture of the kidney, leading to the destruction of renal parenchyma and the loss of kidney function[17].

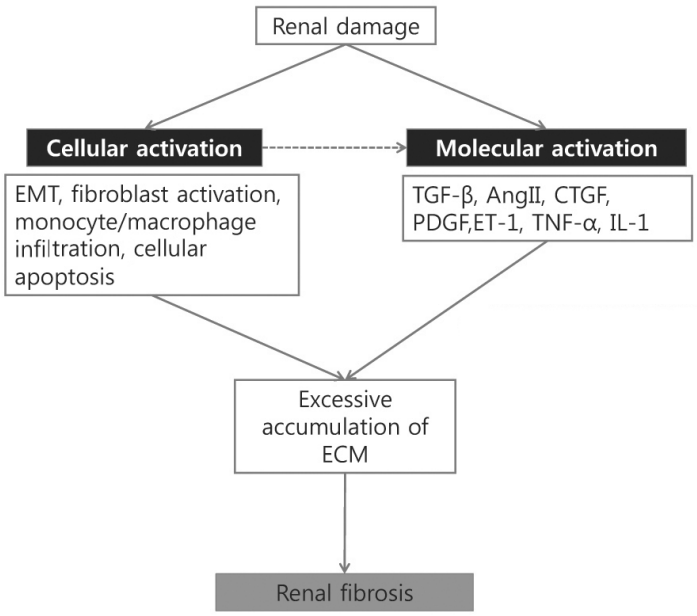

Figure 4. **Pathogenic mechanism underlying renal fibrosis.** *Initial injury of renal tissue leads to activation of different cell types and diverse signalling molecules. Cellular activation, from its side, could provoke activation of many profibrotic cytokines. Synergistic effect of fibroblast activation, EMT, monocyte infiltration, apoptosis, on one side, and molecular activation such as TGF-β1, Angiotensin II and other profibrotic molecules, on another side, result in excessive accumulation and deposition of extracellular matrix components which subsequently leads to loss of renal function (scheme modified from Cho, 2010[16]).*

Epithelial-mesenchymal transition, fibroblast activation, monocyte/macrophage infiltration and cellular apoptosis, together with the activation of different signalling molecules lead to the final pathologic result of renal fibrosis – accumulation of extracellular matrix (ECM) components.

2.1.2. The origin of fibroblasts and ECM production in renal fibrosis

Normal kidney with proper tubular structure contains small amount of fibroblasts in the renal interstitium[19,21]. During kidney fibrosis, activated fibroblasts or myofibroblasts are the primary collagen-producing cells[22]. A variety of mechanisms, including paracrine signals derived from lymphocytes and macrophages, autocrine factors secreted by myofibroblasts, as well as mechanical stress, could all be potential sources of myofibroblast activation[22].

The origin of myofibroblasts has long been a matter of debate and still remains unclear as they demonstrate poor antigenicity and a lack of reliable cell markers[23]. Until the late 1980s, resident interstitial fibroblasts were considered the only source of ECM in the fibrotic kidney[24]. However, it is now believed that fibroblasts during kidney fibrosis can also derive from other sources. In addition to resident mesenchymal cells, around 36% of myofibroblasts in fibrotic kidney originate from epithelial cells through process of epithelial-mesenchymal transition (EMT)[20,21,25] (Figure 5). Furthermore, it has been suggested that a similar process occurs with endothelial cells, termed endothelial-mesenchymal transition (EndMT)[21]. More recently, it has been proposed that bone-marrow-derived cells may also give rise to the population of ECM-producing cells in kidney fibrosis[26]. These, so called, “fibrocytes”- marrow-derived and blood-borne cells are capable to leave the blood, penetrate into

tissue and become fibroblasts[24] (Figure 5). They share markers of both leukocytes and mesenchymal cells and their contribution to the myofibroblast population has been reported to account for ~14-15% of all tubulointerstitial fibroblasts in the fibrotic kidney[25].

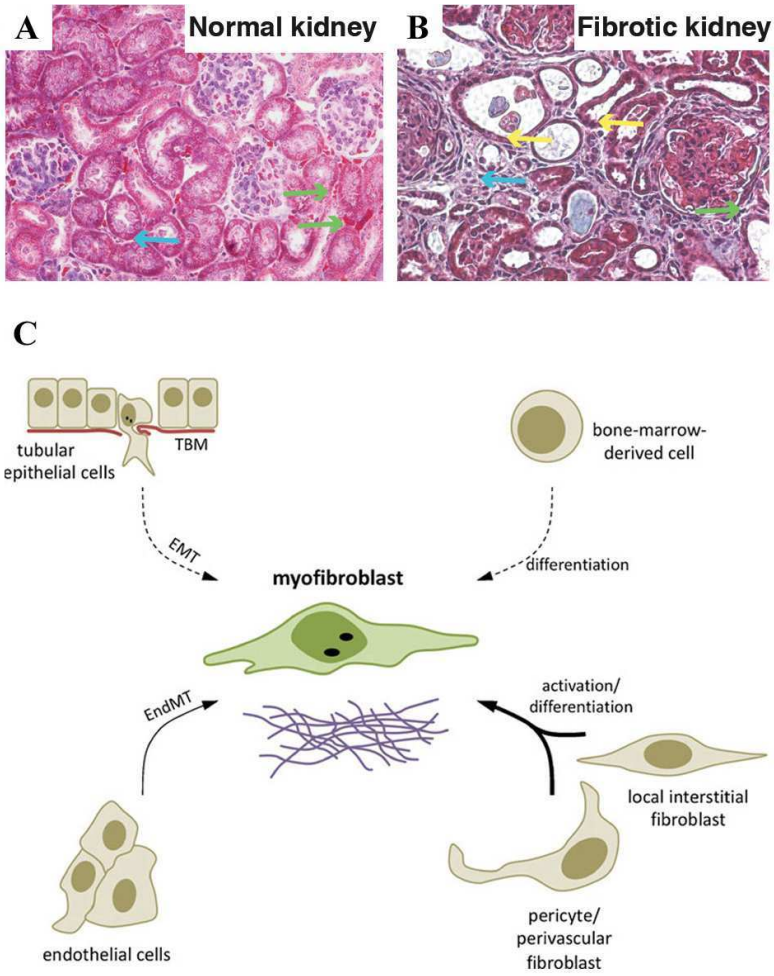

Figure 5. **Origin of fibroblasts during kidney fibrosis.** *(**A**) Normal kidney with proper tubular structures contains very few fibroblasts. (**B**) Fibrotic kidney displays accumulation of numerous fibroblasts (blue arrow), damaged kidney tubules (yellow arrow), and blood vessels (green arrow). (**C**) Schematic illustration of possible*

mechanisms via which fibroblasts can originate during kidney injury. The traditional concept states that myofibroblasts primarily derive from local stromal cells in the kidney such as resident fibroblasts and pericytes/perivascular fibroblasts. Recent data suggest that approximately 36% of fibroblasts can arise via local EMT involving tubular epithelial cells under inflammatory stress[21,24]. Other possible mechanism of myofibroblast engaging includes endothelial cells (via endothelial-mesenchymal transition, EndMT). The current literature suggests that about 14–15% of fibroblasts derive from bone marrow (scheme modified from Kalluri et al. 2003[21] and Grgic et al. 2011[24]).

In this work the main attention will be focused on the role of tubular epithelial-mesenchymal transition (EMT) in interstitial fibrosis, pointing out at the most important key steps of EMT and the possibility for these EMT steps to be attenuated as a therapeutic target to prevent progressive kidney disease.

2.1.3. Epithelial-Mesenchymal Transition (EMT)

Epithelial-mesenchymal transition represents a dynamic course of events that characterizes physiological developmental processes, but it also denotes pathological conditions such as fibrosis and carcinogenesis[21,27].

2.1.3.1. EMT in embryogenesis and adults

EMT was initially defined as an early embryonic event enabling primitive epithelia to migrate as mesenchymal cells forming the mesoderm and allowing primitive neuroepithelia to move as neural crest cells[28]. Without the mechanism of EMT, complex organisms could not exist[28]. EMTs are classified into three different subtypes based on the phenotype of the output cells (Figure 6)[29,30]. EMT associated with implantation, embryo formation, and organ development constitutes one EMT

subtype termed type 1 EMT[28,29,31]. Type 1 EMT generates cells with the mesenchymal phenotype to create new tissue(s) with diverse functions and never leads to fibrosis nor to unsuppressed systemic invasion of epithelial cancer cells (Figure 6 A)[29,31].

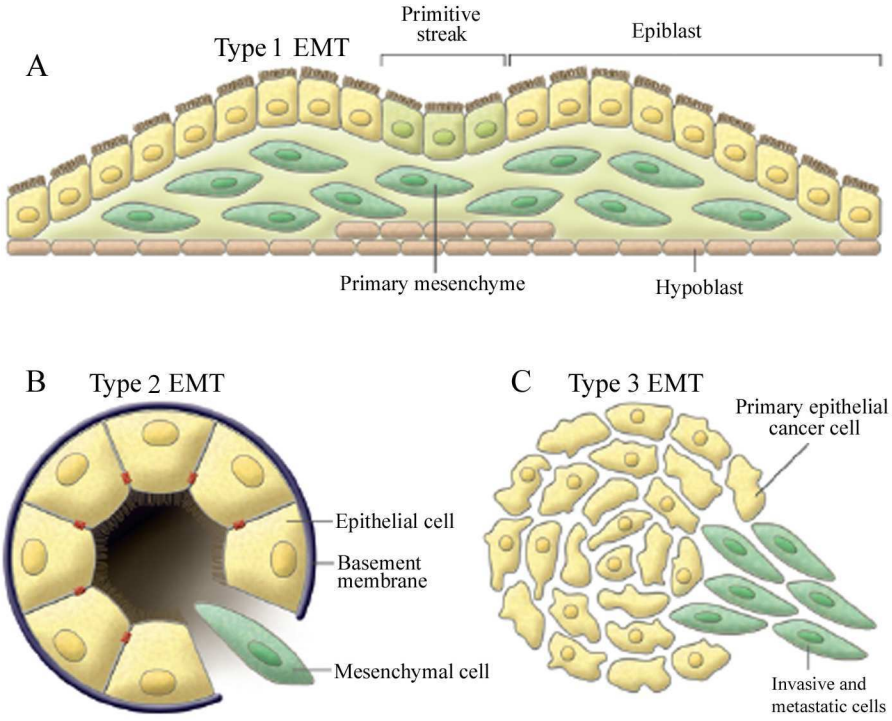

Figure 6. **Different subtypes of epithelial-mesenchymal transition**. *(**A**) Type 1 EMT is associated with implantation of the embryo, embryonic gastrulation and organ development. Among other outcomes, type 1 EMT can produce mesenchymal cells (primary mesenchyme) that are capable of undergoing a mesenchymal-epithelial transition (MET) generating secondary epithelia[30]. (**B**) Type 2 EMT is associated with wound healing, tissue regeneration and organ fibrosis and could subsequently lead to organ destruction if the primary inflammatory insult is not abolished. (**C**) Type 3 EMT is the part of the metastatic process where secondary epithelia transform into cancer cells and metastasize via circulation into distant organs (from Kalluri and Weinberg 2009[30]).*

During development, primitive epithelium, specifically the epiblast, gives rise to the first set of mesenchymal cells, which are known as the primary mesenchyme via an EMT[29]. Following tissue expansion, primary mesenchyme gives rise to secondary epithelia via mesenchymal-epithelial transition (MET), as seen during kidney development[29]. It is believed that secondary epithelia can undergo further differentiation giving rise to other types of epithelial tissues and could subsequently undergo EMT forming the cells of connective tissue and muscle cells[30].

The second EMT subtype refers to adult epithelial and endothelial cells transitioning into fibroblasts. Type 2 EMT is associated with wound healing, tissue regeneration, and organ fibrosis and it begins as a part of a renewal process where new fibroblasts are generated to repair the damage of the tissue (Figure 6 B)[29-31]. Type 2 EMT associated with wound healing and tissue regeneration stops when the repair is achieved and inflammation attenuated[29]. Type 2 EMT related with organ fibrosis can continue to respond to current inflammation, leading eventually to organ destruction[29].

Type 3 EMT is the third proposed subtype of EMT[30,31] and is part of the metastatic process (Figure 6 C). Cells generated by type 3 EMT may invade and metastasize via circulation creating systemic manifestations of malignant cancer progression[29].

2.1.3.2. Tubular epithelial-mesenchymal transition in renal fibrosis

Tubular epithelial-mesenchymal transition, a process by which differentiated tubular epithelial cells undergo a phenotypic conversion that gives rise to the matrix-producing fibroblasts and myofibroblasts[20], has been described as one of the key mechanisms in the pathogenesis of renal tubulointerstitial fibrosis[32] and an important

pathway for progression of CKD[28,33]. It has been proposed that tubular EMT is an orchestrated, highly regulated, step-wise process that relies on an excitable transforming growth factor-β1 (TGF-β1) signaling, and is composed of several key events necessary for the fulfillment of the entire EMT process *in vivo*[3]. In response to injury and local activation, renal tubular cells lose cell-cell contacts and apical-basal polarity, leading to separation and destabilization of neighboring cells (Figure 7)[3,13].

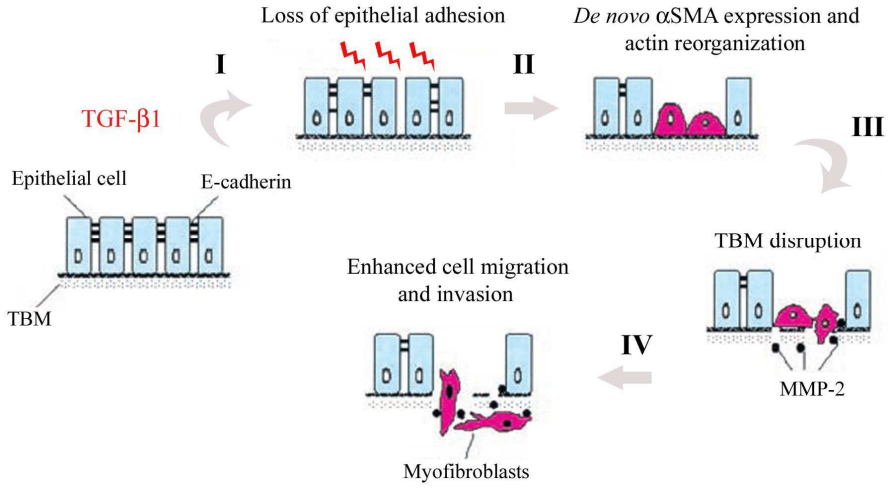

Figure 7. **Schematic illustration of four key events essential for the fulfillment of the entire process of tubular epithelial-mesenchymal transition at cellular level.** *Four key events of EMT include: 1) loss of epithelial adhesion properties, 2) de novo expression of α-SMA and actin reorganization, 3) disruption of the TBM that surrounds the renal tubule, and 4) enhanced cell migration and invasion toward the interstitial compartments of the kidneys (scheme taken and modified from Yang and Liu, 2001[3]).*

This step is associated with the loss of epithelial adherent junction proteins, such as E-cadherin. While losing their epithelial markers, tubular cells acquire *de novo*

synthesis of mesenchymal markers, such as α-smooth muscle actin (α-SMA), vimentin and fibroblast specific protein-1 (FSP1) which now defines their new morphology and phenotype. This stage is also associated with the reorganization of the cytoskeleton which provides a structural foundation in defining the morphology of the transformed migratory cell[3,13]. The third step of tubular EMT is characterized by the upregulation of matrix metalloproteinases (MMP-2 and MMP-9)[3,13,21,34] that disrupt the TBM. TBM is the substantial component of renal tubules that promotes diverse cell-matrix interactions crucial for the maintenance of the epithelial phenotype and normal function of tubular epithelial cell[34]. Disruption of TBM is a delayed event that follows the loss of epithelial adhesion and *de novo* expression of α-SMA and it is of vital importance because it facilitates the subsequent step of tubular EMT - process of invasion and migration of transformed cells toward the interstitial compartments of the kidneys.

2.1.3.3. Induction of epithelial-mesenchymal transition in the kidney

In the past few decades, EMT has become one of the most fascinating topics in the studies of embryonic development, organ fibrosis and tumor metastasis[20]. The concept that epithelial cells can undergo conversion after stress/injury, giving rise to fibroblasts and contributing to the pathogenesis of kidney fibrosis, became a very attractive and intensively investigated matter. It has already been reported that the healthy tubular epithelium is composed of highly polarized cells closely attached to each other by adherens junctions containing specialized cadherins and catenins[11,35], while basal actin cortex attaches the cells, through integrins, to the underlying ECM[11]. Change of phenotype of tubular epithelial cells during EMT, toward the loss of cell

polarity, adherens and tight junctions and actin cytoskeleton rearrangement, requires specific molecular shift of tubular epithelium in the direction of a new biochemical and transcriptional program. A growing list of different extracellular and intracellular factors and mediators that could induce EMT has been identified recently, but despite this progress many questions regarding mechanisms that control EMT still remain unanswered.

EMT could be efficiently employed through the miscellany of diverse growth factors (e.g. TGF-β1, EGF, IGF-II or FGF) and enzymes which promote proteolitic degradation of the basement membrane (e.g. MMPs)[4,21]. It has been reported that at the place of injury versatile factors could be cooperatively expressed, which makes difficult to distinguish their priority in contribution to EMT. In general, TGF-β1 has been identified as the main inducer of EMT in the kidney, as well as, in other organs. In addition, participation of other cytokines alongside with TGF-β1 has been reported to contribute in completing the process of EMT. For instance, cultured cells exposed to epidermal growth factor (EGF) or fibroblast growth factor (FGF) exhibit only a mild EMT transition, whereas EGF and FGF have an important synergistic affect when combined with TGF-β1[36,37]. Additionally, many other cytokines seem to have effects on EMT on an indirect way via the induction of TGF-β1. Interleukin-1 was shown to induce tubular EMT through a TGF-β1-dependent mechanism while incubation with a neutralizing TGF-β1 antibody prevented this outcome[38]. Similarly, angiotensin II, a central component of the renin-angiotensin system, when combined with TGF-β1 increased TGF-β1's ability to induce EMT, while when used alone failed to induce conversion of epithelial cells to mesenchymal[39,40]. It is of interest to mention that hepatocyte growth factor (HGF) induces EMT during somitogenesis through its c-

Met/Crk adaptor proteins[41,42], but in the tissue affected by fibrosis it has completely opposite effect of protecting epithelium from EMT[21,43]. In addition to stimulation by growth factors, disruption of the underlying tubular basement membrane by MMP-2 or other MMPs, can also induce EMT of tubular epithelial cells[32] and it is suggested that MMP-2 is both necessary and sufficient for induction of EMT[44]. Except of soluble factors, some components of interstitial matrix and TBM such as collagens may play an important role in regulating EMT. It is reported that type I collagen promoted EMT[37,45,46], while type IV collagen suppressed it[47]. TBM integrity is essential for normal cell functioning and disruption of its composition induces EMT *in vitro*[47].

2.1.3.4. Transforming growth factor-β1-induced EMT in the kidney

Although a number of factors have been stated as potential inducers of tubular EMT in diverse experimental models[13,46,48], a growing evidence establishes a crucial role for TGF-β1 signaling in mediating EMT[20,49-51] and tissue fibrosis[52]. In particular, it has been previously shown that TGF-β1 plays an important role in *altering* the phenotype of renal epithelial cells[48] and it appears to be able to both initiate and complete the whole course of EMT[3,45]. Transforming growth factor-β1 (TGF-β1) is the prototypic member of the TGF-β1 super family and exerts a broad range of biological activities. Taking into account an evident increase of its expression in the fibrotic kidney, TGF-β1-induced EMT is especially pertinent to the pathogenesis of kidney fibrosis[20]. It has been reported that in the diseased kidneys TGF-β1 receptors are quickly up-regulated specifically in tubular epithelium[3,53], implicating that tubular cells are the natural targets of TGF-β1 under pathological conditions *in vivo*[3]. Expression of exogenous TGF-β1, either via gene delivery *in vivo* or in transgenic

mice, causes renal fibrosis[17]. Conversely, inhibition of TGF-β1 by multiple strategies suppresses renal fibrotic lesions and prevents progressive loss of kidney function[17]. Recent results from Yang et al (2001) point to a pro-fibrogenic role of TGF-β1 in promoting myofibroblast activation via tubular epithelial-myofibroblast transition[3].

TGF-β exerts its various biological and immunological functions via complex signaling pathways[54,55]. The 3 isoforms of TGF-β (TGF-β1, TGF-β2, and TGF-β3) are generally expressed in almost every cell type in mammals. Nearly all renal studies to date have analyzed TGF-β1 in the context of kidney fibrosis and other isoforms, β2 and β3, possibly have similar profibrotic effects on kidney cells, but their exact role remains to be elucidated[55]. TGF-β binds to cell surface type II receptors (TβRII), which then recruit the type I receptors (TβRI) with kinase activity. The activated receptor complex phosphorylates downstream proteins of the Smad pathway but also of other pathways (e.g. p38MAPK, JNK or Rho, etc).

2.1.3.5. Signaling pathways leading to EMT

EMT is a dynamic and complex process that requires the cooperation and conjunction of multiple signaling pathways at different stages therefore the current comprehension of the molecular mechanism underlying EMT is generally incomplete. A plethora of intracellular signal transduction pathways have been implicated in mediating EMT in different model systems. From the point of CKD, it is believed that TGF-β1/Smad, integrin/ ILK, and Wnt/-β-catenin signaling pathways are essential for conferring tubular epithelial-mesenchymal transition[20] (Figure 8).

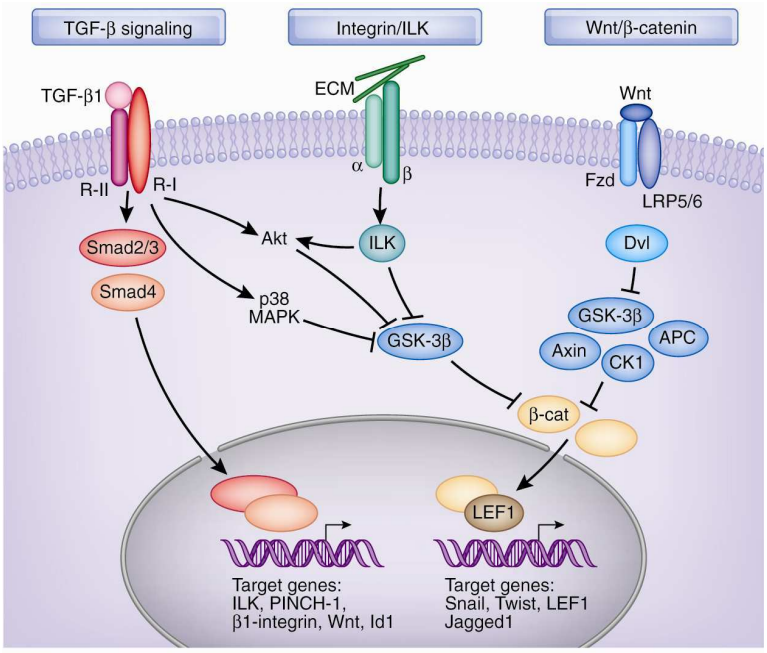

Figure 8. **Scheme of major intracellular signaling pathways and mediators involved in the regulation of EMT in the fibrotic kidney**. *It has been proposed that three major signaling pathways (i.e., TGF-β/Smad, integrin/ILK, and Wnt/β-catenin signaling) are characteristic in mediating tubular EMT. These pathways are connected and integrated at different levels (from Liu, 2010[20]).*

These pathways correlate and integrate in a complex way and it has been proposed that they could converge at the point of activation of β-catenin which subsequently leads to the activation of EMT transcriptional programs[20] (Figure 8).

In this work, the main attention regarding the intracellular signaling pathways of epithelial-mesenchymal transition was focused on TGF-β1–induced EMT and the downstream cascades/routes that this cytokine subsequently activates.

2.1.3.5.1. TGF-β1/Smad signaling pathway

One of the most important mediators of TGF-β1 signaling seems to be the Smad family of transcriptional activators (Figure 9). The Smad family consists of three groups of Smad proteins: the ***R-Smads*** (receptor-regulated Smads) which include Smad2 and 3 (recognized by TGF-β1 and activin receptors) and Smad1, 5 and 8 (recognized by BMP receptors), the ***Co-Smads*** (common-partner Smads) including Smad4, and the ***I-Smads*** (inhibitory Smads) which includes Smads6 and 7[13,56]. Upon stimulation by TGF-β, transmembrane type II TGF-β receptor forms tight complexes with the type I receptor which results in the phosphorylation and activation of the type 1 receptor (Figure 9)[20,56]. The activated type 1 receptor phosphorylates Smad2 and/or 3, which subsequently heterodimerizes with common partner Smad4, which is not subject of phosphorylation by the TGF-β type I receptor[51,57,58]. Complex composed of R-Smads and Smad4 translocates into the nucleus where it controls the transcription of diverse genes implicated in EMT[54,59] such as connective tissue growth factor, ILK, β1-integrin, Wnt, Snail, Id1, α-SMA, collagen IA2, and MMP-2[60-62].

The importance of Smad molecules in TGF-dependent signaling during EMT was demonstrated by Sato et al. (2003)[63] in an *in vivo* experiments with Smad3 knockout mice. Mice lacking Smad3 were protected from EMT and subsequently from renal interstitial fibrosis and showed reduced collagen accumulation after unilateral ureteral obstruction[63]. Consistent with previous finding, primary tubular epithelial cell from the Smad3 null mice were resistant to induction of EMT and activation of key EMT regulatory genes[63,64].

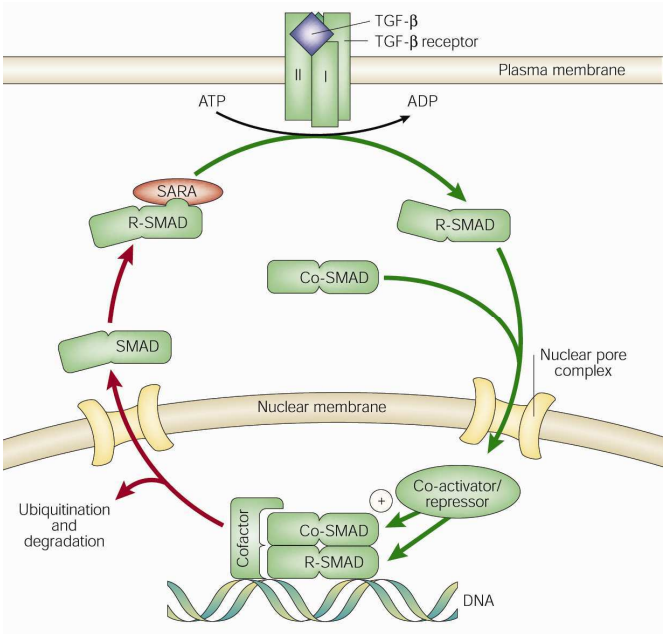

Figure 9. **Activation of the Smad pathway through TGF-β1 signaling.** *Activation of the transmembrane TGF-β receptor occurs when TGF-β induces the activation of two type I and two type II receptors. Type II receptor phosphorylates the GS domain of type I receptor and activates it. Activated type I receptor phosphorylates R-Smads, which decreases the affinity of R-Smads for SARA (Smad anchor for receptor activation) and increases their affinity for co-SMADs. R-Smads form a complex with co-Smad (Smad4) and the activated complex translocates into the nucleus, where it regulates transcription of target genes and associates with transcriptional coactivators or corepressors. Smads can contact DNA, but effective binding to particular gene regulatory sites is enabled by specific DNA-binding cofactors. R-Smads that shift into the nucleus may return to the cytoplasm, but their ubiquitylation- and proteasome-dependent degradation in the nucleus provide a way to terminate TGF-β responses*[65,66] *(from Massagué 2000*[65]*).*

2.1.3.5.2. Non-Smad pathways of TGF-β1 signaling

Alongside with Smad signaling, TGF-β1 is capable of activating several other signaling cascades in epithelial cells leading to manifestations characteristic for epithelial-mesenchymal transition. TGF-β1 can rapidly activate Ras pathway[66], extracellular-signal-regulated kinase (Erk1/2)[67] and phopshatidylinositol-3-kinase (PI3K)/Akt pathway[68,69], the Rho-GTPase RhoA[70], Jun N-terminal kinase (JNK)[67] and p38 mitogen-activated protein kinase (p38MAPK)[71] (Figure 10). Oftentimes activation of these non-Smad pathways could give a background for induction and specification of EMT and is necessary for some points of EMT[20].

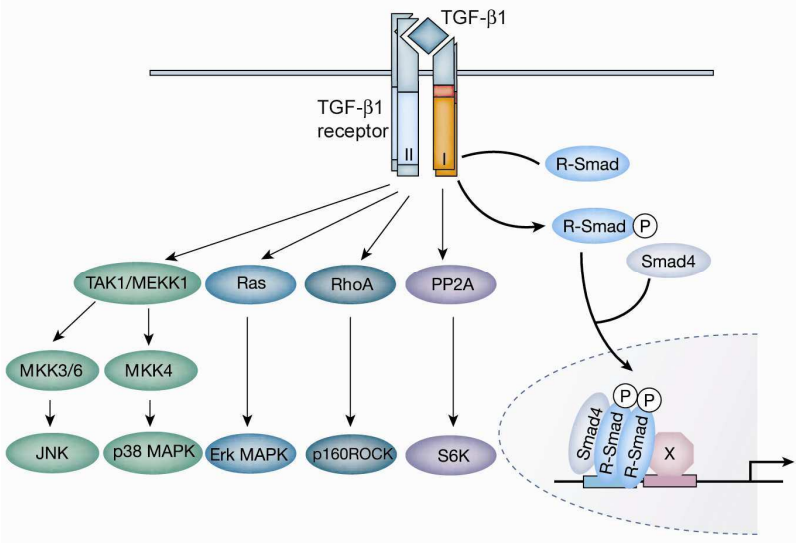

Figure 10. **Non-Smad pathways of TGF-β1 signaling**. *Apart from Smad signaling pathway, TGF-β1 activates other signaling cascades such as MAPK/Erk, JNK, p38MAPK, RhoA, PP2A/p70S6K and TAK1/MEKK1 (from Derynck and Zhang, 2003)*[66].

Extracellular-signal-regulated kinase (Erk) is one of the three major kinase cascades that belong to the MAPK family of signaling molecules that serves to connect extracellular stimuli to intracellular responses[72]. Two other members are c-Jun N-terminal kinase and p38MAPK[73]. It has been demonstrated that tubular levels of pErk correlate with renal dysfunction and interstitial fibrosis in human glomerulopathies[74]. It is proposed that the Erk signaling activation is one of the crucial pathways whereby TGF-β1 promotes EMT[67] and fibrosis[54,75-77]. There are different mechanisms proposing the ways of activation of Erk, JNK or p38 MAPK by TGF-β1 in different cell types and one of them suggests that the rapid activation of Ras by TGF-β1 in epithelial cells may associate Ras in TGF-β1-induced MAPK/Erk signaling[78,79].

Phosphatidylinositol-3-kinase (PI3K) could also be activated by TGF-β1, as indicated by the phosphorylation of its effector serine/threonine protein kinase Akt[69,80]. The activation of Akt could be direct, with possible involvement of RhoA[69], or it can be a result of TGF-β-induced TGF-α expression and consequent EGF receptor activation[66,80]. Phosphatidylinositol 3-kinase (PI3K), signaling through the Akt/PKB, is required for TGF-ß–induced disassembly of cell-cell junctions and F-actin remodeling[69,70]. Evidence indicates that Akt could subsequently mediate β-catenin accumulation in EMT through inhibition of GSK-3β[20]. Both PI3K/Akt and MAPK/Erk signaling pathways have been implicated in TGF-β1-induced EMT[69,81].

Ras is one of the most common pathways leading to the activation of Erk and Akt, which represent important signalling events responsible for TGF-β1-induced EMT in different epithelial cell types[67,69,79,82]. A growing body of evidence describes

the role of TGF-β1 in activation of Ras pathway[83-87]. Ras proteins are small GTPases that control a wide number of biological functions including proliferation and apoptosis in physiological conditions. Ras cycle between their two conformational states, a guanosine diphosphate (GDP)-bound inactive state, and active, guanosine triphosphate (GTP)-bound state (Figure 11). Conversion of the inactive to active state is mediated by guanine nucleotide-exchange factors (GEFs) that stimulate the exchange of GDP for GTP[88]. In the active GTP-bound form, Ras proteins activate a wide spectrum of signaling pathways and effector proteins such as already mentioned PI3K/Akt and MAPK/Erk, as well as Raf[89] and GEF[90] (Figure 11).

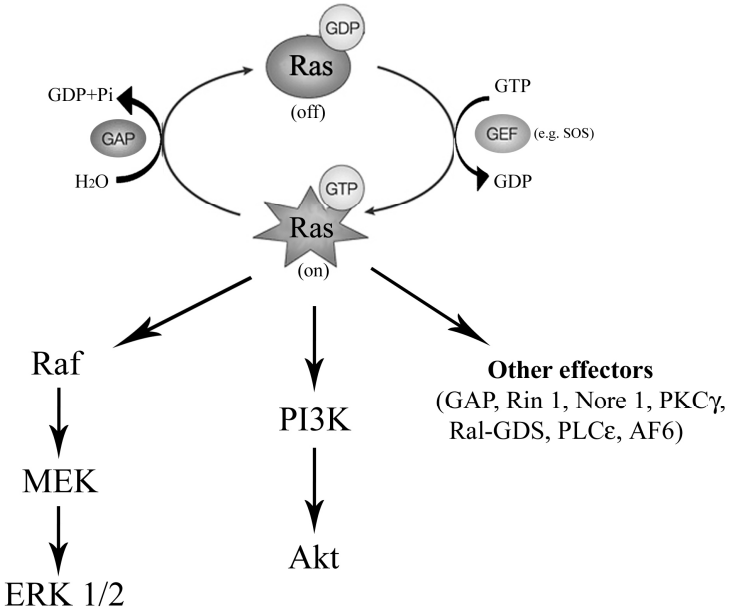

Figure 11. **Ras activation and its effector proteins.** *(ERK, extracellular signal regulated kinase; GAP, GTPase-activating protein; GEF, guanine nucleotide exchange factor;GDP, guanosine diphosphate; GTP, guanosine triphosphate; MEK, mitogen-activated protein kinase kinase; PI3K, phosphatidylinositol 3-kinase; PKCg,*

protein kinase C gamma; PLCe, phospholipase C epsilon; Ral-GDS, GEF for the Ral subfamily; SOS, Son of Sevenless (modified from Martinez-Salgado et al. 2008[88]).

TGF-β1 can quickly activate Rho-like GTPases (Figure 10), including RhoA, Rac and Cdc42[66] which are important for TGF-β1-induced changes in cytoskeletal organization and epithelial-mesenchymal transition. Rac and Cdc42 regulate JNK and p38 MAPK pathway activation, presumably by directly interacting with MAPKKKs upstream of JNK and p38 MAPK, whereas Rho, Rac and Cdc42 affect the cytoskeletal organization[66]. Activation of Rac and RhoA signaling has been implicated in TGF-β1-induced stress-fiber formation during process of EMT, while RhoA is important for the activation of α-SMA promoter and for the rapid membrane ruffling and lamellipodia formation in response to TGF-β1[70,91-94].

2.1.3.6. Markers of epithelial-mesenchymal transition

Turning an epithelial cell into a mesenchymal cell through process of epithelial-mesenchymal transition requires a multitude of changes in cellular morphology and architecture, cell adhesion and migration capacity. This phenotypic conversion requires a completely new molecular program in the cell. A diversity of biomarkers has been used to determine the presence of epithelial-mesenchymal transition and fibrosis in different *in vitro* or *in vivo* experimental settings. Table 1 represents common markers used in different studies of EMT.

Commonly used markers of EMT include increased expression of N-cadherin and vimentin, nuclear localization of β-catenin and increased production of the transcription factors such as Snail1, Snail2, Twist that inhibit E-cadherin production[95].

Additionally, proteins that have an evident increase in their expression/activity during EMT process are matrix metalloproteinases (MMP-2, MMP-9), fibronectin, collagen type I and type III, ILK and GSK-3β. A change in expression of E-cadherin toward its decrease in epithelial cells affected by EMT is the typical marker of EMT[31] and the loss of E-cadherin function promotes EMT[21]. Cytoskeletal markers of EMT are also dramatically changed during process of transition.

Table 1. **EMT markers** *(taken from Lee at all., 2006[95]).*

Proteins that increase in abundance	**Proteins that decrease in abundance**
N-cadherin	E-cadherin
Vimentin	Desmoplakin
Fibronectin	Cytokeratin
Snail 1 (Snail)	Occludin
Snail 2 (Slug)	
Twist	**Proteins that accumulate in the nucleus**
Goosecoid	
FOXC2	β-catenin
Sox10	Smad-2/3
MMP-2	NF-κB
MMP-3	Snail 1
MMP-9	Snail 2
Integrin αvβ6	Twist
Proteins whose activity increases	*In vitro* **functional markers**
ILK	Increased migration
GSK-3β	Increased invasion
Rho	Increased scattering
	Elongation of cell shape
	Resistance to anoikis

FSP1, a member of the family of Ca^{2+}-binding S100 proteins[96], is a prototypical fibroblast marker for detection of EMT in cancer and fibrogenesis[31]. FSP1 identifies tubular epithelial cells undergoing transition in nephrons affected by

interstitial injury[97], that are capable to traverse through damaged tubular basement membrane (TBM) and accumulate in the interstitium of the kidney[21]. Another marker of EMT is the intermediate filament vimentin which is expressed in various cells, including fibroblasts, endothelial cells and cells of the hematopoietic lineage, and glial cells[98,99].

Alpha-smooth muscle actin (α-SMA) is the member of the actin family of cytoskeletal proteins and is normally expressed in vascular smooth muscle cells and myoepithelial cells. α-SMA is very often used for detection of activated fibroblasts (myofibroblasts) in *in vitro* and *in vivo* experimental models of EMT and fibrosis. β-catenin, a binding partner for E-cadherin, plays a dual role in EMT: it links cadherins to the cytoskeleton promoting cell-cell adhesion and also serves as a transcriptional coactivator upon entry into the nucleus[31,100]. Other proteins that accumulate in the nucleus alongside with β-catenin are Smad2/3, NF-kB, Snail1, Snail2 and Twist, all of which are used as important markers of EMT.

Phenotypic markers of an EMT process include an increased ability for cell migration and invasion, elongation of cell shape, as well as resistance to anoikis[95] (Table 1).

2.1.4. Experimental models of renal fibrosis

Current knowledge regarding the pathogenesis of renal fibrosis is generally based on experimental studies of kidney fibrosis in animals. Typical experimental models of kidney fibrosis in mice or rats include progressive glomerulonephritis from anti-glomerular basement membrane disease[101], Alport syndrome[102] with an intended disruption of the COL4A3 gene, nephrotoxic serum nephritis (NSN)[103], and NOD or

db/db nephritic mice (models for diabetic nephropathy)[104]. The closest human analogue is pediatric obstructive nephropathy, that is, an infrequent, usually nonproteinuric and normotensive disease[19]. The most widely used and well-established model of renal interstitial fibrosis is unilateral ureteral obstruction (UUO). Similar to human obstructive nephropathy, UUO is induced by the ligation of a ureter of one kidney, while the contralateral kidney serves as a normal control. It has been reported that as early as 3 days after UUO surgery, it is possible to detect interstitial fibrosis associated with interstitial deposition of type IV collagen and tubular cell apoptosis[25]. UUO is characterized by interstitial infiltration of macrophages, tubular atrophy, and subsequent interstitial fibrosis[105]. A study by Iwano et al.[25] using mice with a LacZ reporter expression system, under proximal tubule-specific γ-glutamyl transferase promoter control, is the most frequently cited as providing functional evidence for EMT in UUO. Following obstruction, 36% of activated (fibroblast-specific protein-1 positive) fibroblasts in the interstitium appeared to derive from epithelium (fibroblast-specific protein-1 positive and LacZ positive), suggesting a large contribution of proximal tubular EMT. Mechanisms by which UUO gives rise to renal damage include mechanical stretch from urine accumulation and tubular distension[106], increased oxidative stress[107], hypoxia caused by reduced renal perfusion[108] and upregulation of inflammatory factors such as monocyte chemoattractant peptide[109], vasoconstrictors including angiotensin II[110] and endothelin[111] as well as transforming growth factor-β1[112] which together contribute to obstruction-induced renal damage[113].

3. N-methyl-D-aspartate receptor (NMDAR)

3.1. Introduction and general background

NMDAR (N-methyl-D-aspartate (NMDA) receptor) is a cation channel which belongs to a large family of excitatory ionotropic glutamate receptors (iGluRs) that has been extensively studied in the nervous system. The most rapid excitatory synaptic transmission in the central nervous system (CNS) is mediated by GluR channels[114-121] that are classified into two major groups termed ionotropic and metabotropic glutamate receptors[122]. Based on their electrophysiological and pharmacological properties, the ionotropic receptors can be subdivided into three distinct types of receptors[118]: N-methyl-D-aspartate (NMDA) receptors, α-amino-3-hydroxy-5-methyl-4-isoxazolepropionate (AMPA) receptors and kainate receptors[122-124]. Dysfunction of the glutamatergic pathways has been implicated in many progressive degenerative diseases, such as Huntington's disease, Alzheimer's disease, Parkinson's disease, encephalopathy, lathyrism, acquired immunodeficiency syndrome, dementia complex and pain/hyperalgesia, as well as schizophrenia and other psychiatric disorders[118,125-131].

The NMDAR is a crucial receptor for the neurotransmitter glutamate, which is the most important excitatory transmitter in the brain[132]. NMDAR is characterized by a specific molecular composition and unique pharmacological and functional properties[133,134]. An essential feature of the NMDAR is that its activation and subsequent influx of calcium (Ca^{2+}) ions could trigger a series of Ca^{2+}-mediated intracellular events and via this Ca^{2+} entry NMDAR performs its important physiological functions. High permeability to calcium ions is thought to be responsible

for the NMDAR's important role in neuronal plasticity under physiological conditions and neuronal death under excitotoxic pathological conditions[135,136].

3.2. Structural characteristics of the NMDAR

NMDAR is a heteromeric protein complex composed of different subunits from two separate protein families, termed as NMDAR1 (NR1; zeta 1 for mice) and NMDAR2 (NR2; epsilon for mice) protein family[137,138] (Figure 12). There is a 99% amino acid homology between the rat and human NR1 and the mouse zeta 1 subunit[139-141]. There are at least four members of the NR2 family of subunits that show high homology between species[139,140,142] and are designated as NR2A-D for the rat[143,144] and human[140] and as epsilon 1-4 for the mouse[137,139,145,146].

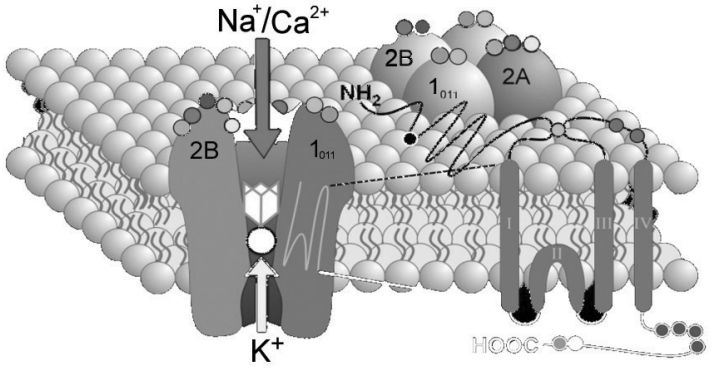

Figure 12. **Schematic representation of the N-methyl-D-aspartate receptor.** *NMDARs are tetramers that most often comprise of two NR1 and two NR2 subunits of the same or different subtypes. The NR1 subunit is the essential subunit for the activity of the NMDAR, while NR2 subunits have important modulatory properties. The NMDAR is a non-specific cation channel which allows the flow of Ca^{2+} and Na^{+} ions into the cell and K^{+} ions out of the cell. Nevertheless, the main function of the NMDAR is transmission of calcium ions into the cell.*

The channel properties are highly dependable on the subunit composition of the receptor[147]. Functional NMDARs usually require members from each family and probably exist as a tetramer or a pentamer *in vivo*[138]. The stoichiometry of NMDARs has not yet been definitely established, but the consensus is that NMDARs are tetramers that most often comprise of two NR1 and two NR2 subunits of the same or different subtypes[133,136,136,148] (Figure 12). The NR1 subunit is the main subunit of the NMDAR and it is essential for channel activity[118,149,150], whereas the NR2 subunits, although not essential for function, can confer modulatory properties[151]. The diversity of the NMDAR NR1 subunit is created by alternative splicing from a single gene giving eight functional splice forms of NR1 subunit[152]. Splice variants arise via the insertion or deletion of three short exon cassettes in the N-terminal (N1) and C-terminal (C1, C2) domains of the subunit protein[152,153]. The NR1 subunit family consists of eight different splice variants (NR1a–h) that can influence the properties of the channel[153-155]. The splice variants are now designated by several nomenclatures based on the presence or absence of these specific cassettes[156].

The NR2 subunit family is composed of four members (NR2A, 2B, 2C and 2D) produced from separate but related genes[139,143,157]. Within recent years, a novel subunit of the NMDAR family has been cloned and characterized[156,158]. This subunit, initially termed chi-1 or NMDAR-L, is now reviewed in the literature as NR3. The NR3 subunit, found in the form of NR3A and NR3B, has been demonstrated to be developmentally and spatially regulated, as all other NMDAR subunits[159]. It has been shown that NR3A subunit, when forming the NMDAR complex together with NR1 and NR2 subunits, has the ability to decrease NMDA-evoked current[160] and Ca^{2+} permeability of the NMDAR in heterologous cells[135,161].

According to their conductance properties, NMDARs can be subdivided into two classes: '*high conductance channels*' that are composed of NR2A or NR2B subunits and '*low conductance channels*' that are composed of NR2C and NR2D subunits. The low conductance channels are characterized by reduced sensitivity to Mg^{2+} block[118,132,134].

3.2.1. Functional domains in NMDAR subunits

Every subunit of the NMDAR contains a long extracellular N-domain, a membrane region composed of three transmembrane segments plus a re-entrant pore loop, an extracellular loop and an intracellular C-domain, which varies in size depending of the receptor subunit[133,136,148,148,162,163] (Figure 13). The N-terminal domain (NTD; first 350 amino acids) plays an important role in subunit assembly[164]. In NR2A and NR2B, the NTD contains binding sites for Zn^{2+} and ifenprodil, known allosteric inhibitors of the channel[136]. The cytoplasmic C-terminus of both NR1 and NR2 subunits is subject to phosphorylation and may link the receptor to calcium-activated intracellular signaling pathways[165]. The interactions of the receptor with signal transduction systems may be modulated by the association of the NMDAR C-terminal domain with anchoring proteins or other cytoskeletal elements[166,167]. By providing multiple sites of interaction with different intracellular proteins, C-terminal domain is involved in the regulation of receptor trafficking and function[148].

The NMDAR is a ligand-gated ion channel that requires simultaneous binding of two agonists, glutamate and glycine, for the proper channel activation and its opening[133,168]. Glutamate binds to the NR2 subunit while the co-agonist glycine binds to the allosteric site located at NR1 subunit[169,170] (Figure 13). Magnesium (Mg^{2+}) acts

as a voltage-dependent antagonist of the NMDAR, within the M2 domain of NR2 subunits (Figure 13), and depolarization of the membrane will relieve this block.

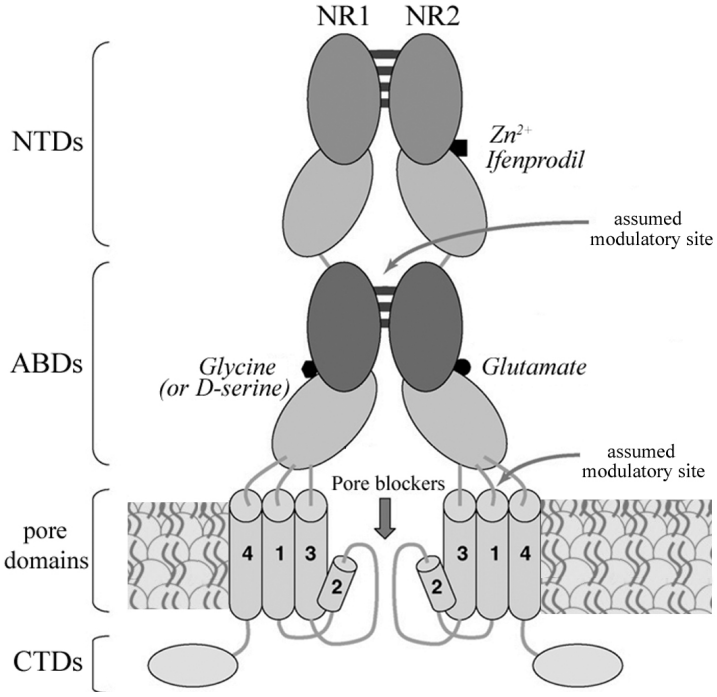

Figure 13. **Functional domains of NMDAR and potential sites for ligand binding**. *NMDAR subunits are characterized by a large extracellular N-domain, a membrane region comprising three transmembrane segments (TM1, 3 and 4) plus a re-entrant pore loop (M2), an extracellular loop between TM3 and TM4, and a cytoplasmic C-terminus*[136]*. The extracellular N-domain of each subunit is made up of a tandem of domains, the NTD and the ABD. The NR2 ABD binds glutamate, whereas the NR1 ABD binds the co-agonist glycine (or D-serine). Allosteric modulators such as endogenous zinc (Zn^{2+}) bind to sites on NTDs of NR2A and NR2B, while ifenprodil-like compounds bind to NR2B NTDs, both acting as non-competitive antagonists. The ion-channel domain forms binding sites for pore blockers such as endogenous Mg^{2+}, MK-801, memantine or ketamine, acting as uncompetitive antagonists*[136]*. Arrows indicate assumed modulatory sites for either positive or negative allosteric*

modulators. For better understanding only one of the two NR1/NR2 heterodimers is shown in this schematic representation. NTDs – N-terminal domains; ABDs – agonist-binding domains; CTDs – C-terminal domains (taken and modified from Paoletti and Neyton, 2007[136]).

Therefore, it has been suggested that the opening of the NMDAR requires at least 3 distinct events to happen - binding of two agonists, glutamate and glycine, and membrane depolarization[156]. N-methyl-D-aspartic acid (NMDA), a non-metabolic agonist of NMDAR mimics the action of glutamate thus regulating only this receptor. NMDA binding site is located at NR2 subunit.

3.3. Localization of the NMDAR

NMDAR is the receptor widely investigated in the CNS; therefore the significant amount of data describes the presence and its localization in the neuronal tissues. Nevertheless, over the past few years, NMDAR and its presence outside of the central nervous system have emerged as an interesting subject worldwide. Growing evidence implicate that the functional NMDAR is also expressed in a variety of non-neuronal cells and tissues.

3.3.1. Localization of the NMDAR in embryonic and adult brain

Regarding the distribution of the NMDAR in the brain, NR1 subunit is expressed in nearly all neurons and at all developmental stages in the brain[171]. On the other hand, NR2 subunit genes display diverse regional and developmental expression patterns. While NR2B and NR2D are predominant subunits of the NMDAR in the embryonic brain, NR2A and NR2C are absent[154]. On the contrary, in the adult brain

NR2A predominates as a widely expressed subunit, while NR2B expression is restricted to forebrain areas, and NR2C is highly enriched in the cerebellum[154,171,172].

In the mature nervous system, NMDARs are presented as complexes composed primarily of NR1, NR2A, NR2B and NR2C subunits. Certain receptors contain only NR1 subunit combined with either NR2A or NR2B[118]. In very rare occasions, receptor could contain the NR2D subunit. The presence of NR2B reflects a high affinity for glycine and its agonists and the interaction between the NR1 and NR2 subunits regulates glycine affinity. Presence of NR2A subunit brings high affinity for glutamatergic agonists[118]. The NR3 subunit (NR3A and NR3B) has been shown to be developmentally and spatially regulated, as all other NMDAR subunits, with the highest levels of mRNA expression during the first 2 postnatal weeks[156,159]. NR3A is widely expressed subunit, while NR3B is predominantly expressed in motor neurons in the spinal cord, pons and medulla[160,161]. NMDARs are also present in oligodendrocytes and astrocytes[154], but their function in these localizations is not completely understood.

3.3.2. Localization of the NMDAR in peripheral tissues

In addition to NMDAR's broad distribution in neurons, it has become evident that functional NMDAR is also expressed in a variety of non-neuronal cells and tissues such as human keratinocytes[173,174], lymphocytes[175], bone cells[176,177], rat heart, lung, thymus, stomach[151], parathyroid gland[178] and the kidney[151,179]. According to the study of differential binding of NMDAR's antagonists, Nasstrom et al. (1993) suggested the presence of this receptor in various tissues outside the central nervous system, such as heart, stomach, pancreas, and kidney[180]. For instance, it was reported that the NR2C

subunit was present in the adult rat pancreas[181], while the NR2B subunit was transiently expressed in the newborn rat heart[182]. Leung et al. (2002) demonstrated presence of NR1 in total rat kidney, cortex and medulla, while of other subunits of NMDAR, only NR2C was detectable in the rat kidney[151]. Both NR1 and NR2C are present in Madin-Darby canine kidney, opossum kidney and LLC-PK1 cells[151]. The same authors showed presence of an essential NR1 subunit in the rat heart while the expression of NR2 subunits was not detected in this organ[151].

Importance of NMDAR in peripheral tissues, such as kidney, and its functional role is becoming an interesting research topic worldwide. It has been shown that the abundance of an essential NR1 subunit of the NMDAR increases with kidney development[151]. Results from Deng et al.[179] showed the presence of NR1 subunit of NMDAR in the basolateral proximal tubules of the rat kidney where it plays a role in regulation of the normal kidney function[183]. Furthermore, functional NMDAR was found present in human[184] and mouse[184,185] podocytes, where glutamatergic signaling driven by these visceral epithelial cells contributes to the integrity of the glomerular filtration barrier[185]. Sproul et al. (2011) showed high expression of NMDAR subunits NR3A and NR3B in the neonatal kidney and suggested that there is continued expression of NR3A in the renal medulla and papilla of the adult mouse. These authors showed specific presence of NR3A in basolateral membrane of collecting duct cells where this subunit may play an important reno-protective role[186].

3.4. Modulation of N-methyl-D-aspartate receptor activity

The NMDAR is a complex protein assembly with multiple binding sites for different ligands that could be modulated by endogenous and exogenous factors[118]

(Figure 14). NMDAR contains the NMDA binding site, a glycine binding site and a binding site within the channel for specific non-competitive antagonists[137,187].

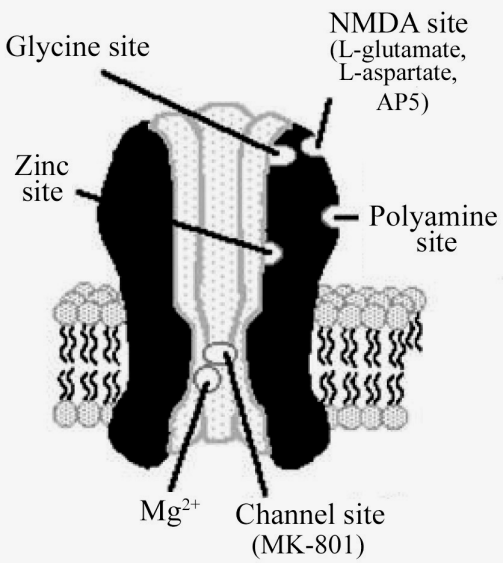

Figure 14. **Binding sites for different modulators of the NMDAR complex.** *NMDAR complex has numerous binding sites for various ligands. NMDAR contains NMDA binding site which also binds L-glutamate, L-aspartate (endogenous agonists) and AP5 (antagonists). The glycine site binds, except of glycine, serine and D-cycloserine (agonists) and certain antagonists of this site. Within the channel there is a binding site for some non-competitive antagonists such as MK-801, ketamine, etc. Diagram adapted from Corsi, et al. (9). (taken and modified from Magnusson 1998[137]).*

L-glutamate and L-aspartate both interact with *NMDA binding site* and represent endogenous agonists of this receptor[137]. NMDA site is also specifically recognized by a competitive antagonist of NMDAR, D-2-amino-5-phosphonopentanoic acid (AP5)[137]. The *glycine site* binds serine and D-cycloserine, which act as agonists and 7-chlorokynurenic acid (7-Cl-KYNA) which is an antagonist

for this site[137,188]. Non-competitive antagonists, such as *(+)-5-methyl-10,11-dihydro-5H-dibenzo[a,d]cyclohepten-5,10-imine maleate* (MK-801), ketamine, phencyclidine (PCP) and 1-(1-thienyl-cyclohexyl) piperidine (TCP) can bind within the channel[137].

3.4.1. Agonists of the NMDAR

As already mention above, extracellularly, NMDARs can be modulated by glycine and D-serine, which act as co-agonists to stimulate NMDAR function[148,169]. Binding site for glycine is located on the NR1 subunit wile glutamate binds to the NR2 subunits. Structural variation among diverse NR2 subtypes could explain the heterogeneity in glutamatergic effects among native NMDARs[156].

Activation of Src family of protein kinases could increase phosphorylation of NR2A and NR2B and therefore could upregulate NMDAR function[118,148]. Furthermore, PKC could potentiate NMDAR function through activation of subunits NR2A and NR2B alone or in conjunction[189]. NR2C and NR2D are unaffected by PKC[118]. The C-terminal domain of NMDAR subunits contains many serine/threonine phosphorylation sites, which are substrates not only for protein kinase C (PKC), but also for cAMP-dependent protein kinase A (PKA), protein kinase B (PKB), CaMKII, cyclin-dependent kinase-5 (Cdk5) and casein kinase II (CKII)[190]. For instance, PKC and PKA activation increase NMDAR-mediated currents and Ca^{2+} permeability[148,191,192]. Activation of Ephrin B receptors could be another mechanism for the regulation of NMDAR Ca^{2+} permeability, through tyrosine phosphorylation of NR2A/B subunits[118,193]. Activation of numerous G protein-coupled receptors enhances NMDAR function via phosphorylation of the NMDAR[194]. Different G protein-coupled

receptors seem to coincide onto Src-family kinases which constitute a molecular hub for signaling pathways that enhance NMDAR activity[194].

3.4.2. Antagonists of the NMDAR

One of the important characteristics of the NMDAR ion channel is the voltage-dependent block by *magnesium* (Mg^{2+}), which varies developmentally[156]. Magnesium is capable of blocking NMDARs both intracellularly and extracellularly[195] and this property is subunit specific. It has been demonstrated that NMDARs with a predominant composition of NR1/NR2A and NR1/NR2B are susceptible to a stronger block by magnesium than NR1/NR2C or NR1/NR2D receptors[156,196]. Mg^{2+} blocks the NMDA channels in a voltage dependent manner[118,168]. At positive membrane potential, Mg^{2+} acts as a potentiator of NMDA-induced responses. The blocking action of Mg^{2+} is determined by specific residues within the M2 domain of NR2 subunits[197]. The residues mediating this block have been identified as asparagines and serine.

NMDARs could be partially inhibited by ambient H^{+}[118]. Zinc (Zn^{2+}) is both voltage dependent and independent inhibitor of NMDAR. The NR1 subunit is important in mediating the inhibitory effect of Zn^{2+} and H^{+}, as well as responses to polyamines[118,198-200]. Extracellular zinc (Zn^{2+}) can inhibit NMDAR function by binding to the N-terminal domain of NR1 or NR2 subunits[148,201] of the NMDAR and mediates both voltage dependent and voltage independent NMDAR blockade[148,201].

The lead (Pb^{2+}) cation is also an inhibitor of NMDAR. Inhibition by Pb^{2+} is most potent in NR2A receptors containing NR2A subunit and less potent with receptors with predominant composition of NR2C and NR2D[118,202,203].

In excitatory CNS synapses, Ca^{2+} transients result in Ca^{2+}-dependent inactivation of the NMDAR activity. This inactivation is mediated by Ca^{2+}/calmodulin interaction with α-actinin at the C-terminus of NR1 subunits, which is essential for inactivation. The NR2 subunit modulates Ca^{2+}-dependent inactivation since this does not occur in NR2C-containing receptors, but does occur in the presence of NR2A.

Ethanol is a potent inhibitor of NMDARs, but its precise mode of action remains obscure[118,204].

Polyamines are polybasic aliphatic amines that have been reported to influence NMDAR function. Polyamines are widely distributed throughout the body and are found at high intracellular levels, where they interact with nucleic acids and proteins, including plasma membrane ion channels[171]**.** Polyamines, such as spermine and spermidine, block the channel in a voltage-dependent manner at higher concentrations[156], while the low micromolecular concentrations promote channel opening by increasing the affinity of the receptor for glycine[133,168].

The NMDAR complex contains several potential binding sites for extracellular modulators. The highly selective NMDAR blocker dizolcipine (MK-801) is more potent at inhibiting NR1/NR2A and NR1/NR2B receptors than NR1/NR2C and NR1/NR2D receptors[136]. Except for dizocilpine, there are other antagonists that directly block the ion channel such as phencyclidine, ketamine, dextromethorphan and amantidine[156,205,206].

Ifenprodil is a selective inhibitor of the NMDAR. This compound selectively inhibit NR2B-containing NMDARs by binding to the NR2B N-terminal domain[207-209]. Ifenprodil and related drugs appear to work through enhancement of proton

inhibition[156]. These compounds are non-competitive antagonists because their action requires prior pore opening[207-209].

3.5. Functional properties and physiological roles of the NMDAR

The NMDAR is a non-specific cation channel with a specific property of voltage-dependent activation. Activation of NMDAR allows the flow of Ca^{2+} and sodium (Na^{+}) ions into the cell and potassium (K^{+}) ions out of the cell. However, the main function of this receptor is transmission of calcium ions into the cell[210]. Due to its high Ca^{2+} permeability[122,133,134,211], NMDAR plays an essential role in neuronal developmental and many neurophysiological and neuropathological processes[161].

NMDAR has an affinity to interact with a variety of intracellular molecules such as cytoskeletal proteins and components of signal transduction pathways, which is important for its structural function and activity modulation[212]. Association of NMDAR with the actin cytoskeleton through α-actinin, has been shown to be important for channel activity[212,213].

3.5.1. Physiological roles of the NMDAR in neuronal tissues

NMDARs are vital for the brain function[214]. They play a principal role in synaptic plasticity during development[215,216], learning and memory[138,154]. NMDAR is essential for induction of long term potentiation, a long lasting change in neuronal responsiveness that is thought to underlie learning and memory[122,143]. Recent evidence suggests that NMDARs are critical for corticogenesis, neuronal migration, and synaptogenesis during brain development[152]. NMDAR is crucial for a process known as excitotoxicity where excessive release of glutamate leads to over-excitation of

neurons producing neuronal injury and death[156,217]. According to Hardingham & Bading (2003), physiological levels of synaptic NMDAR activity are very important for the survival of many types of neurons[216] (Figure 15).

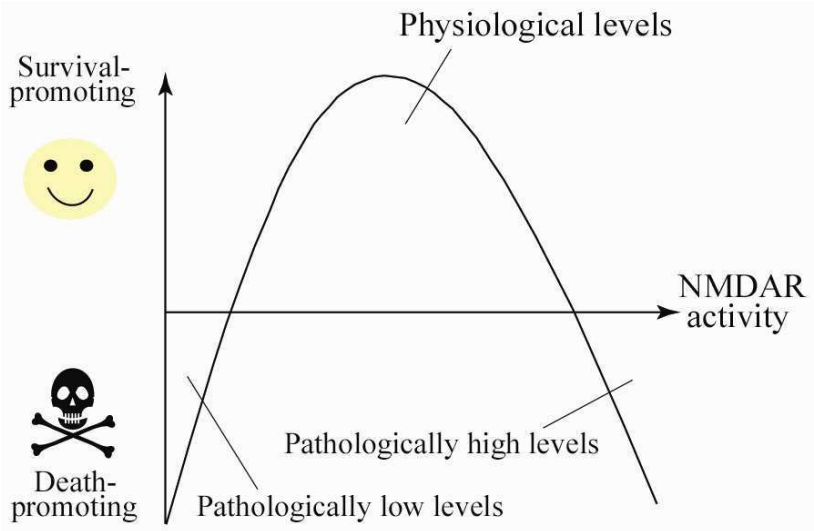

Figure 15. **Physiological levels of NMDAR activation are necessary for normal neuronal function**. *Normal level of NMDAR activity is required for normal survival of neurons. Excessive NMDAR activity leads to excitotoxic trauma and cell death. Different levels of NMDAR activity can make neurons more susceptible (''death-promoting'') or more resistant (''survival-promoting'') to subsequent trauma (taken and modified from Hardingham and Bading, 2003[216]).*

On the other hand, if the activation of the NMDAR is sustained, it can provoke cell death in many neuropathological conditions[218].

Upon activation of the NMDAR, Ca^{2+} that comes into the cell, through the receptor, is taken up by mitochondria[219,220]. Extremely high levels of NMDAR-

induced Ca^{2+} influx will likely cause an initial depolarization of the mitochondria and mitochondrial dysfunction, which subsequently leads to excitotoxic cell death[219,221].

Blockade of NMDAR activity *in vivo* promotes neuronal death associated with oxidative damage[222]. *In vitro*, NMDAR blockade also leads to neuronal vulnerability to oxidative insults through the weakening of antioxidant defenses[154,222]. Therefore, physiological levels of NMDAR activity generally promote neuronal survival, and a complete absence of NMDAR activity is, thus, deleterious to the cell[216].

3.5.2. Physiological roles of the NMDAR in peripheral cells and tissues

A wide spectrum of cellular functions in a variety of cell types is being controlled by the activity of ion channels. While the activity of calcium channels is important in the regulation of cell migration[174,223-225], calcium signaling is significant in mediating actin rearrangement[226,227] and organization of cadherins and catenins into intercellular junctions[228]. Indeed, NMDAR activation has been shown to induce changes in actin organization in cerebellar granule cells[213] and retinal neurons[229] and to inhibit cell migration in neuronal cells[223] and keratinocytes[174]. Numerous function have been ascribed to NMDAR such as proliferation[174,175], apoptosis[175,177], cell adhesion and migration[174,175,230], actin rearangament[213,231], cell growth and differentiation[174] in different non neuronal cells and tissues. Nahm et al. (2004) demonstrated that the Ca^{2+} entry through functional NMDAR in human keratinocytes had an influence on the cycle of keratinocyte proliferation, differentiation, and migration during epithelialization[174]. Moreover, the same authors suggested that NMDAR activation might play a role in contact-mediated inhibition of growth, a process that is absent during neoplastic pathology[174].

Importance of the NMDAR in the kidney and its functional role has emerged as an interesting research topic, although experimental data are scarce. Results from Deng et al.[179] showed the presence of NR1 subunit in the basolateral proximal tubules of the rat kidney and confirmed a role for renal NMDAR in the regulation of renal vasodilatation. Recently, this group demonstrated that renal NMDARs independently stimulate proximal tubular reabsorption and glomerular filtration[183]. It has been reported that NMDAR plays an important role in maintaining the stability of the glomerular filtration barrier, while derangements in glutamatergic signaling driven by podocytes may lead to proteinuric kidney disease[185]. Recent data from Anderson et al. (2011) suggested that, as in the brain, basal activation of NMDAR may be essential for normal podocyte and kidney function, but excessive activation may trigger a number of pathophysiological processes[184].

Recently, Sproul et al. (2011) have demonstrated the reno-protective role of NR3A subunit of the NMDAR in inner medullary collecting duct (IMCD) cells. NR3A knockdown IMCD cells exhibited consistent elevation of basal intracellular calcium concentration, reduced cell growth, higher rate of cell death and reduced water transport in response to the addition of vasopressin. Generally, these authors concluded that NR3A subunit of the NMDAR may have a protective role in collecting duct cells through regulation of the intracellular calcium levels which enables the principal cells of the collecting duct to reabsorb water and thereby increase medullary osmolality[186].

However, the function of NMDAR in tubular cells is not yet fully understood.

Objectives

The N-methyl-D-aspartate receptor (NMDAR) is a member of a heterogeneous family of ionotropic glutamate receptors, with a wide spectrum of functions in a variety of cell types and tissues. Importance of NMDAR in the kidney and its functional role has emerged as an interesting research topic, although the function of this receptor in tubular cells is not fully understood.

Taking into consideration knowledge of multiple characteristics of NMDAR in a variety of tissues, including renal itself, we sought to examine the role of this calcium receptor in the maintenance of normal proximal tubular epithelial cell's (PTEC) phenotype and its role in tubular EMT *in vitro*. Furthermore, we wished to examine its effect in a mouse model of tubulointerstitial fibrosis (TIF) induced by UUO.

The main objectives of this Doctoral Thesis are:

I. To investigate the role of basal NMDAR activation in the maintenance of the epithelial phenotype of human proximal tubular epithelial cells.

1. *To study the role of NMDAR activation in human proximal tubular epithelial cell migration.*
2. *To study the role of NMDAR activation in actin cytoskeleton distribution in human proximal tubular epithelial cells.*
3. *To determine if the absence of NMDAR1 subunit, therefore lack of glutamatergic signaling driven by the NMDA receptor, affects normal phenotype and functionality of proximal tubular epithelial cell.*

II. To investigate the role of NMDAR activation in modulation of tubular epithelial-mesenchymal transition (EMT) *in vitro*.

1. *To study the effects of NMDAR activation on important key steps of tubular EMT in vitro.*
2. *To study the role of NMDAR activation in TGF-β1-stimulated proximal tubular epithelial cell (PTEC) migration.*

3. *To study the molecular mechanisms that stand behind the effect of NMDA on tubular EMT in vitro.*
4. *To study the specific effects of Ca^{2+} entry through NMDA receptor on EMT modulation.*

III. To investigate the potential role of NMDAR activation in a mouse model of tubulointerstitial fibrosis induced by unilateral ureteral obstruction (UUO).

1. *To study the effects of NMDA administration on expression of important markers of renal fibrosis such as α-SMA, Collagen I and FSP1 in obstructed mouse kidney.*
2. *To study the effects of NMDAR activation on preservation of epithelial phenotype in vivo.*

Materials and Methods

MATERIALS

1. Reagents and cell culture material

COMPANY	PRODUCT
Applied Biosystems (New Jersey, USA)	TaqMan Universal PCR Master Mix, no AmpErase® UNG
BD Biosciences (Bedford, MA, USA)	growth-factor-free Matrigel™
Biological Industries (Israel)	EZ ECL Chemiluminescence Detection kit for HRP
BioRad Laboratories (CA, USA)	30% Acrylamide/Bis solution, 29:1 Colorimetric kit for detection of proteins
BIOTOOLS (B&M Labs, S.A., Spain)	DNA markers 100bp Ladder
Corning Life Sciences (Amsterdam, Netherlands)	500ml Vacuum Filter/Storage Bottle System, 0.22µm
Falcon (BD Labware, USA)	Plates 100x20 Serological pipet (different volumes) Transwell inserts (polyethylene terepthalate (PET) track-etched membrane-diameter 6,4 mm; 8 µm
Fermentas (Madrid, Spain)	Fermentas Gene Ruler 1kb DNA Ladder
Fisher Scientific (Madrid, Spain)	Centrifuge tubes (different volumes) Methanol
GE Healthcare (UK)	Amersham ECL Advance Western Blotting Detection Kit Glutathione Sepharose 4B beads ECL Advanced blocking agent
GIBCO-Invitrogen (NY, USA)	BenchMark Pre-Stained Protein Ladder Dulbecco's modified Eagle's medium (DMEM) EpiLife (Ca^{2+}-free medium) Fetal bovine serum (FBS) Ham's F-12 mixture HEPES Non-essential amino acids (NEAA) Sodium Pyruvate Streptavidin Alexa Fluor 594 SYBR Safe DNA gel stain Taq DNA polymerase Trypsin-EDTA
Fisher Scientific (Madrid, Spain)	Centrifuge tubes (different volumes) Methanol
Iwaki (Asahi Glass, Japan)	Microplates (6, 24, 48, 96 well plates)
Merck (Barcelona, Spain)	β-mercaptoethanol
Millipore (Bedford, MA)	Polyvinylidine fluoride (PVDF) membrane, Immobilon-P Syringe-driven filter unit MILLEX-OR 0.22µm
Takara Bio Inc (Japan)	Age I Bam HI
Thermo Scientific (MA, USA)	NE-PER Nuclear and Cytoplasmic Extraction kit
Roche (Germany)	First Strand cDNA Synthesis Kit for RT-PCR (AMV)

COMPANY	PRODUCT
R&D Systems (Minneapolis, MN, USA)	Human Transforming Growth Factor-β1 (TGF-β1)
Sigma Aldrich (Barcelona, Spain)	3,3′,5-Triiodo-L-thyronine sodium salt (T3) 3-[4,5-dimethylthiazol-2-yl]-2,5-diphenyltetrazolium bromide (MTT) Ammonium persulfate (APS) Aprotinin Bovine serum albumin (BSA) Bromphenol blue Citric acid Chromotrope 2R Collagen type I Crystal violet Dexamethasone D-Glucose Dimethyl sulfoxide (DMSO) Dodecyl sodium sulfate (SDS) DPX mounting medium Epidermal growth factor (EGF) Ethylenediaminetetraacetic acid (EDTA) Fibronectin Glycerol Glycine Hoechst (Bisbenzimide H) 33258 Hydrogen peroxide Igepal CA-630 Insulin Isopropyl-β-D-thiogalactopyranoside (IPTG) N,N,N′,N′-Tetramethylethylenediamine (TEMED) N-methyl-D-aspartic acid (NMDA) Penicillin Phenylmethanesulfonyl fluoride (PMSF) Polyethylenimine (PEI) Phosphatase substrate Protein inhibitor cocktail (PIC) Sodium azide (NaN3) Sodium chloride (NaCl) Sodium deoxycholate Sodium fluoride (NaF) Sodium orthovanadate (Na_3VO_4) Sodium pyrophosphate (NaPPi) Sodium selenite (Na2SeO3) Streptomycin Thapsigargin Transferrin Tris base Triton X-100 TRIzol reagent Tween-20 β-glycerophosphate
Tocris Bioscience (Bristol, UK)	(+)-MK-801 maleate
Pronadisa (Madrid, Spain)	Agarose MS-12
Nunc GmbH (Germany)	4-well plates Thermanox Plastic Coverslips
Knittel glass (Germany)	Microscopic slides

COMPANY	PRODUCT
Panreac (Barcelona, Spain)	Ethanol Formol Hydrochloric acid (HCl) Isopropanol NP-40 Xylene
Vector Laboratories (Burlingame, CA, USA)	Vector Vectastain Universal ABC kit PK-6200 Peroxidase substrate kit DAB SK-4100

All other reagents were from the best commercial grade available.

2. Antibodies

COMPANY	Antibody
Abcam (UK)	Rabbit anti-FSP-1 (S100A4) polyclonal Rabbit anti-Snail1 polyclonal
BD Biosciences (Bedford, MA, USA)	Mouse anti-β-Catenin monoclonal Mouse anti-E-cadherin monoclonal Mouse anti-NMDAR1 monoclonal Mouse anti-NMDAR2B monoclonal Mouse anti-Vimentin monoclonal
Cell Signaling Technology (UK)	Mouse anti-total Akt monoclonal Mouse anti-total Erk-1/2 monoclonal Rabbit anti-phospho-specific Akt (Ser 473) polyclonal Rabbit anti-phospho-specific Erk-1/2 (Thr 202, Tyr 204) polyclonal IgG, HRP linked Antibody
Invitrogen (NY, USA)	Goat-anti-mouse Alexa Fluor 488 Goat-anti-mouse Alexa Fluor 546 Rabbit-anti-mouse Alexa Fluor 488
Jackson Immunoresearch (UK)	Peroxidase-conjugated affiniPure Goat Anti-mouse IgG (H+L)
Molecular Probes (Eugene, OR, USA)	Alexa Fluor® 488 phalloidin Alexa Fluor® 568 phalloidin ProLong antifade reagent
Santa Cruz Biotech (UK)	Mouse anti-Histone 1 monoclonal Goat anti-phospho-Smad2/3 (Ser 423/425) polyclonal
Sigma (Barcelona, Spain)	Mouse anti-α-SMA monoclonal Mouse anti-α-Tubulin monoclonal
Upstate Biotechnology (Barcelona, Spain)	Mouse anti-Ras monoclonal

3. Primers

Gene	Species	forward	reverse
NMDAR1	human	5’-AGA CGT GGG TTC GGT ATC AG-3’	5’-AGG ACC CAT CAG TGT CCT TG-3’
NMDAR2A	human	5’-GTC CTT CTC CGA CTG TGA GC-3’	5’-ACT GCC CGT TGA TAG ACC AC-3’
NMDAR2B	human	5’-GCC TGA GCG ACA AAA AGT TC-3’	5’-CAT CTC CCC ATC TCC AAA GA-3’
NMDAR2C	human	5’-CGC TGG TCT TCA ACA ACT CA-3’	5’-GTC CTT GCC TGC CAT GTA GT-3’
NMDAR2D	human	5’-TTC ACC ATT GGG AAA TCC AT-3’	5’-GGA TAG TTG CTG CGG ATG TT-3’
GAPDH	human	5’-GAA GGT GAA GGT CGG AGT-3’	5’-GAA GAT GGT GAT GGG ATT TC-3’
NMDAR1	mouse	5’-CCA ATA CGC TTC AGC ACC TC-3’	5’-GTG GGA GTG AAG TGG TCG TT-3’
NMDAR2A	mouse	5’-TAC TCC AGC GCT GAA CAT TG-3’	5’-TCA GCT GGA CCT GTG TCT TG-3’
NMDAR2B	mouse	5’-AGA ACT GAA AGG GCA AGC AA-3’	5’-GAT CCT GCA GTC AAG CTT CC-3’
NMDAR2C	mouse	5’-GCA GAA CTT CCT GGA CTT GC-3’	5’-CTC TTC ACG GGA GCA GTA GG-3’
NMDR2D	mouse	5’-TTT TGA GGT GCT GGA GGA GT-3’	5’-GTC TCG GTT ATC CCA GGT GA-3’

Real time PCR gene-specific primers for mouse α-SMA, collagen I, GAPDH and human NMDAR1 and GAPDH, were purchased from Applied Biosystems.

METHODS

1. Cell culture

HK-2 cells (human renal proximal tubular epithelial cells immortalized by transduction with human papilloma virus (HPV) 16 E6/E7 genes[232] obtained from ATCC (USA), were maintained in Dulbecco's modified Eagle's medium with Ham's F-12 mixture (DMEM/F-12) supplemented with 2% FBS, Hepes buffer, insulin (5 µg/ml), transferrin (5 µg/ml), sodium selenite (60 nM), D-glucose (2.24 g/L), dexamethasone (5.10^{-8}M), EGF (5 ng/ml), T_3 (2.10^{-9}/L), penicillin (100 U/ml) and streptomycin (100 µg/ml). Cells were grown at 37°C in a humidified atmosphere under 5% CO_2 and 95% air. Fresh growth medium was changed every 2 to 3 days. At 80% of confluence, cells were growth-arrested in serum-free medium for 24 hours and then used for experiments (unless otherwise indicated). Experiments were done in serum-free medium; cells were treated separately with serum-free medium (control), TGFβ-1 (1.3 ng/ml), TGFβ-1 (1.3 ng/ml) plus N-methyl-D-aspartic acid (NMDA) (0.5 mM), TGF-β1 plus Thapsigargin (TG) (2 µM), TGF-β1 plus MK-801 (NMDAR antagonist; 0.1 mM), MK-801 or NMDA alone for indicated periods of time. For the experiments in Ca^{2+}-free conditions, adequate treatments were prepared in EpiLife (calcium free) medium.

1.1. Trypsinization of adherent cells

In order to facilitate subculture or harvesting, cells were trypsinized under the commonly used procedure for trypsinization of cells in monolayer culture. Briefly, after reaching an adequate confluence, cells were rinsed with warm phosphate buffered saline (PBS, pH 7.4, 37°C) to eliminate traces of serum from the medium and then incubated with 0.25% Trypsin/EDTA solution for 3-5 minutes at 37°C. Trypsinization was stopped by dilution with 2%FBS/DMEM/F-12 and resuspended cells were centrifuged at 1000 rpm, 5 minutes, RT. Supernatant was discarded and cell pellet was resuspended in 1ml of fresh medium. From this cell suspension, cells were counted and subsequently seeded in adequate dishes depending of the experimental design.

1.2. Freezing and thawing cultured cells

Cells were grown until approximately 80% of confluence and 24 hours before freezing, fresh growth medium was replaced. On the day of freezing, cells were trypsinized as previously described. After centrifugation, cell pellet was resuspended in special freezing medium composed of complete growth medium supplemented with 7.5% DMSO. Cell suspension was aseptically aliquoted into sterile cryovials which were placed in styrofoam container. Cells underwent process of gradual freezing (48 hours at -80ºC), to avoid formation of intracellular crystals and then were transferred to a liquid nitrogen freezer for long time storage. **Thawing** out cells was done in a 37°C water bath by gentle agitation for approximately 1-2 minutes. As soon as the content was thawed, cryovial was removed from the water bath and decontaminated by spraying with 70% ethanol. All the operations were carried out under strict aseptic

conditions. Vial content was transferred to a centrifuge tube containing 9 ml complete culture medium and centrifuged at 1000 rpm for 5 minutes. Cell pellet was resuspended with the complete medium and dispensed into a 100x20 mm culture dish for further propagation.

1.3. Viability assay

In order to determine the range of NMDA and MK-801 concentrations to be used, the MTT (3-[4,5-dimethylthiazol-2-yl]-2,5-diphenyltetrazolium bromide) assay was performed on treated and untreated HK-2 cells upon incubation for 24, 48, 72 hours with selected drugs, according to the method previously described[233]. Briefly, HK-2 cells were plated in 96-well plates at 10^4 cells/well in 200 µl of 2%FBS/DMEM/F-12 with different concentrations of NMDA and MK-801 for the indicated periods of time. After treatments, growth medium was aspirated and 100 µl/well of MTT (1mg/ml) in 0%FBS/DMEM/F-12 was added. After incubation for 2 hours at 37°C, medium was replaced by isopropanol (100 µl/well) and the plates were gently shaken for 10 minutes until complete dissolution of MTT formazan crystals. Active mitochondrial dehydrogenases of living cells convert the yellowish MTT to an insoluble purple formazan, a conversion that doesn't take place in dead cells. MTT conversion is therefore a good indicator of mitochondrial enzyme activity as well as viability and proliferation. Absorbance was measured at 570 nm using a microplate reader (Biorad Model 680).

2. Cell migration study

2.1. In vitro wound migration assay

Wound migration was assayed utilizing a monolayer wounding system as described previously[234]. Briefly, before plating the cells into 6-well plate, two parallel lines are drawn at the underside of each well of the 6-well plate with a marker, representing the wound areas to be analysed. HK-2 cells were grown until 100% of confluence and then were growth-arrested in serum-free medium for 24 hours. Cell monolayer was injured in a linear fashion with a sterile 200-µl pipette tip, gently washed with warm PBS and then incubated with 0%FBS/DMEM/F-12 alone (control), TGF-β1, TGF-β1 plus NMDA or NMDA alone. All treatments were made in serum-free medium. Cells were incubated for 24 and 48 hours. Closure of the denuded area was monitored using a LEICA Microsystems DFC 480 inverted microscope and digital images were obtained at 0, 24 and 48 hours (4 images per treatment). The width of the wounds was measured using LEICA Quantity Software IM50 Image Manager v. 4.0 (Cambridge, UK). The progression of migration was estimated by subtracting the width of the wound (at 24 or 48 hours) from the initial width of the wound (at 0 hour). The experiments were repeated 8 times and every treatment group was done in triplicate.

2.2. Transwell migration assay

Transwell inserts (polyethylene terepthalate (PET) track-etched membrane-diameter 6,4 mm; 8 µm porosity) were coated with 20 µL of growth-factor-free Matrigel (1:10 dilution) in 0%FBS/DMEM/F-12 and incubated at 37°C for 30

minutes. After 24 hours of deprivation in serum-free medium, HK-2 cells were seeded ($5x10^4$) in the upper wells of Matrigel coated transwell chambers in 200 µL of 0%FBS/DMEM/F-12 in the presence of TGF-β1, TGF-β1 plus NMDA or NMDA alone. The bottom compartments of transwell chambers were filed with 500µL of DMEM/F-12 with 10% FBS. Media in the upper and bottom chambers were supplemented with the same concentrations of corresponding treatments. Control group of cells were grown in medium without TGF-β1 or NMDA. After 24 hours of incubation, medium was removed, cells were washed with PBS and fixed with 4% paraformaldehyde for 10 minutes and 0,1% Triton X-100 for 5 minutes at RT. Cells remained on the upper side of the filter membranes were gently removed with a cotton swab. Membranes were cut out from the inserts with a scalpel blade and the cells from the bottom side of the membrane were stained with 1% Hoechst 33258 (cell nuclei) or 0.2% crystal violet (cell body; *not shown*) for 10 minutes at RT. After gentle washing, membranes were mounted on microscope slides using ProLong antifade reagent, with the lower surface facing up. Cells/nuclei were counted and analyzed using LEICA Microsystems DFC 480 fluorescent microscope. Fifty random fields were examined and the results were plotted as the percentage of control. The experiments were repeated 4 times and every treatment group was performed in triplicate.

2.3. Time-lapse phase-contrast imaging of cell migration

Time-lapse phase-contrast microscopy is a useful approach that affords an opportunity to observe dynamic processes such as cell migration. It allows us to analyze specific cell motion parameters such as average speed, persistence and

directionality, important information for many research and therapeutic applications such as drug development or wound healing.

2.3.1. ECM coating

For analysis of human proximal tubular cell motility, non-tissue culture treated polystyrene 48-well plates were prepared as described previously[235]. Briefly, plates were coated with different concentrations of fibronectin or collagen type I from calf skin and incubated overnight at 4°C. Next day, plates were washed 3 times with PBS and blocked with 1% heat denatured bovine serum albumin (BSA) in PBS for 30 minutes at 37 °C.

2.3.2. Live cell imaging

For the purpose of this experiment, HK-2 cells were trypsinized and seeded in fibronectin or collagen-coated or non-coated 48-well plates in an amount of $2.5x10^3$/well or $4x10^3$/well depending of the incubation time planned. Next day, medium was changed to serum-free medium and after 24 hours of deprivation, adequate treatments were added. Cells were treated separately with 0%FBS/DMEM/F-12 (control), TGF-β1, TGF-β1 plus NMDA or NMDA alone. Cells were incubated for 24 and 48 hours. Prior to imaging, wells were completely filled with adequate medium and the plate was sealed using silicon grease and a glass plate. Images were acquired using a 10×0.5 NA Plan objective lens and a 0.5 NA ELWD condenser with a Zeiss Axiocam camera on a Zeiss Axiovert 200 M microscope in climate-controlled incubator. A robotic stage (Zeiss MCU 28) with linear position feedback encoders was used to collect images at different stage positions over time. All electronic microscope

functions were controlled using Axiovision software (Zeiss). Phase-contrast images were taken in rapid succession at multiple positions (3 positions/well for each condition), evenly distributed over the chambers to exclude differences due to experimental variation, at 3 minutes intervals for 5 hours.

2.3.3. Analysis of cell migration in time-lapse movies

To analyse cell behaviour during migration, software was written in Matlab (Mathworks) by de Rooij J and G. Danuser[235] that automatically segments phase-contrast images based on pixel intensity and determines the presence of nuclei (centroids) based on phase-density, size and shape. Using nearest neighbour and gap-closing algorithms, it tracks the nuclei throughout time-lapse image series to determine cell velocity. Software was used to detect and track single cells in the time-lapse images of migrating cells and to determine their velocity and persistence throughout the process of migration. The velocity was calculated as the displacement (µm) over three consecutive frames, divided by the elapsed time (3 minutes). The persistence is defined as the ratio of the vectorial distance travelled to the total path length described by the cell. Detection fidelity in our experiments was over 80%, which was confirmed by eye for each individual time-lapse. To distinguish single cells from clustered cells in this program, areas occupied by the cells were determined by edge detection and overlaid with the detected nuclei to determine if one (single cell) or more (clustered cells) nuclei were present in a detected cell-area. Only cells that were faithfully tracked for at least six consecutive frames and stayed “single” during that period of time were taken in consideration.

3. Adhesion assay study

To assay cell adhesion, the appropriate ECM substrates were prepared (*as described in sections 2.2 and 2.3.1*) in 96-well polystyrene plates. HK-2 cells were trypsinized, washed once in DMEM containing 2% FBS, and allowed to recover surface proteins for 1 hour in suspension in DMEM containing 0.5% FBS, antibiotics, and 10 mM Hepes, pH 7.4, at 37°C with constant, gentle shaking. $2x10^4$ cells were plated per well, and adhesion was allowed to proceed for the indicated time at 37°C. Unbound cells were discarded by washing three times with PBS preheated to 37°C. Detection of total cellular protein per well was performed by acid phosphatase activity as previously described[235]. In brief, cells were lysed in the wells by adding 200 µl/well of assay buffer containing 0.4% Triton X-100, 50 mM sodium citrate, and 10 mg/ml phosphatase substrate. The reaction was incubated for 20 hours at 37°C and terminated by addition of 100 µl/well of 1 N NaOH. Absorbance was measured at 405 nm. Every condition was measured at least in triplicate.

4. Flow cytometry analysis of filamentous actin (F-actin)

To investigate possible effect of TGFβ-1 and NMDA on filamentous actin in HK-2 cells, flow cytometry analysis was employed. Cells were grown in 100x20 mm culture dishes in 2%FBS/DMEM/F-12. At 80% of confluence, cells were serum deprived for 24 hours and then incubated in 0%FBS/DMEM/F-12 with or without TGF-β1, TGF-β1 plus NMDA or NMDA alone for another 24 hours. After incubation, cells were washed in PBS and briefly exposed to Trypsin-EDTA (0.05%). Trypsinization was stopped by dilution with 2%FBS/DMEM/F-12 and suspended cells were centrifuged at 2000 rpm, 5 minutes, RT. Cell pellets were washed once in PBS

and again centrifuged at 2000 rpm, 5 minutes, RT. HK-2 were then stained for flow cytometry analysis. Briefly, cells were first fixed in 4% Paraformaldehyde for 10 minutes at RT, washed in PBS and then incubated with 0,1% Triton X-100/PBS for 5 minutes at RT. After subsequent washing in PBS and centrifugation at 2000 rpm for 5 minutes at RT, cells were incubated with 1%BSA/PBS for 30 minutes at RT (blocking of non-specific binding). HK-2 cells were stained with Alexa Fluor® 488 phalloidin (dilution 1/150 in 1%BSA/PBS) for 1 hour at RT in the dark. During incubation in the staining solution, content of the incubation tube was gently resuspended few times. Ten thousand HK-2 cells were aspirated into a flow cytometer (Epics XL flow cytometer). The cells were examined on fluorescence channel 1 (FL1) which measures excitation at 488 nm and emission at 530 nm. The resulting histogram is a measure of Phalloidin staining per cell, which is indicative of the amount of F-actin structure to which the fluorescent phallotoxin is bound.

5. Immunofluorescence microscopy

For immunofluorescence analysis, HK-2 cells were grown on glass cover slips in 4-well plates in already described conditions. After adequate incubation, culture medium was removed and cells were gently washed twice with cold PBS and fixed in ice-cold 100% Methanol for 10 minutes (vimentin staining) or 4% Formol for 4 minutes and subsequently in 100% Methanol for 2 minutes at RT (β-catenin staining). Blocking of non-specific binding was performed by incubation of cells in 1% BSA/PBS for 30 minutes. Cells were incubated with primary antibody against vimentin over night at 4°C or primary antibody aganst β-catenin for 2 hours at RT and then with corresponding fluorescently labeled secondary antibody for another 1 hour at

RT. Nuclear counterstaining was performed by 1% Hoechst 33258 for 10 minutes. Between each step, cells were washed with PBS. For examination of cytoskeleton organization, after described incubation treatments, cells were washed twice in PBS, fixed in 4% Paraformaldehyde/PBS for 8 minutes at RT and permeabilized with 0.1% Triton X-100/PBS for 5 minutes at RT. After fixation, cells were incubated in 1%BSA/PBS for 30 minutes and then with Alexa Fluor® 568 phalloidin diluted (1:40) in 1%BSA/PBS for another hour at RT. After washing in PBS, nuclear staining was performed by incubating cells with 1% Hoechst 33258 for 10 minutes at RT. Negative controls were performed routinely. Omission of the primary antibody or use of 1%BSA/PBS in place of a specific antibody or fluorescent dye resulted in complete absence of staining. Cover slips with stained cells were mounted on microscope slides using ProLong antifade reagent and were examined using a LEICA Microsystems DFC 480 fluorescent microscope with a Digital Camera System.

6. Measurements of cell volume

For cell volume measurements, HK-2 cells were cultured in 6-well plates in 2%FBS/DMEM/F-12 medium with or without NMDA (0.5 mM). After 2 and 24 hours of incubation, cells were washed with PBS, trypsinized and resuspended in the culture media. Cell volume was measured in Coulter Counter (Model Z2).

7. Determination of Ras activation

Ras activation was assessed by specific binding of Ras-GTP (activated form) to the Ras binding domain (RBD) of Raf-1[236] as described previously[237]. Ras binding domain (Raf-1 residue 1–149) was expressed as glutathione-S-transferase (GST) fusion protein.

7.1. Expression of fusion protein GST-RBD Raf1 in Escherichia coli

The plasmid pGEX-RBD, encoding the Ras binding domain of Raf-1 fused to glutathione-S-transferase (GST-RBD) (provided by Dr. P. Crespo from the University of Cantabria, Spain) was transfected into *E. coli* (DH5α) and the GST-RBD expression was induced by 1 mM isopropyl-β-D-thiogalactopyranoside (IPTG) for 3 hours at 37°C. Transformed *E. coli* were harvested and resuspended in a solution containing 25 mM Tris (pH 7.5), 150 mM NaCl, 1 mM EDTA, 2 mM PMSF and PIC (50 µl/ml). Cells were lysed in the same buffer containing 0.5% Triton X-100 by sonication and centrifuged at 10.000 rpm at 4°C for 10 minutes. Glutathione Sepharose 4B beads were washed thoroughly with PBS and incubated with the supernatant containing GST-RBD for 2 hours at 4°C. Beads coupled with GST-RBD were washed 3 times with PBS and resuspended in PBS (pH 7.4) buffer containing 20% glycerol and 0.5 mM PMSF (stored at -20°C). Adequate amount of bound GST-RBD was eluted by boiling in SDS sample buffer and subjected to SDS-PAGE electrophoresis and Coomassie blue staining. The band corresponding to the fusion protein was quantified by Quantity One software (Bio-Rad Laboratories) by comparing its intensity to the band intensities of known amounts of bovine serum albumin (BSA) run on the same gel.

7.2. Ras-GTP pull-down assay

For determination of Ras-GTP, HK-2 cells were treated separately with serum-free medium (control), TGF-β1, TGF-β1 plus NMDA and TGF-β1 plus TG. After treatments, cells were incubated with magnesium-containing lysis buffer (MLB: 25 mM HEPES (pH 7.5), 150 mM NaCl, 1% NP-40, 0.25% Na-deoxycholate, 10%

glycerol, 25 mM NaF, 10 mM $MgCl_2$, 1 mM EDTA, 1 mM Na_3VO_4, 2 mM PMSF and PIC (50µl/ml) for 10 minutes at 4°C. Cells were cold centrifuged for 10 minutes at 10.000 rpm and supernatant was collected. Following measurement of protein concentrations, 10 µg of lysate proteins were employed in the detection of total Ras after mixing with Laemmli sample buffer and boiling for 5 minutes. Amount of 70 µg of lysate proteins were incubated with 2 µg of GST-RBD pre-coupled with glutathione-Sepharose at 4°C for 2 hours. The sepharose conjugates were recovered by short centrifugation, washed 2 times with MLB buffer, resuspended in Laemmli sample buffer and boiled for 5 minutes. Sample supernatants were subjected to 15% SDS-PAGE and used in western blot detection of Ras-GTP.

8. Lentiviral-driven gene knockdown

8.1. Design of siRNAs

The human NMDAR1 subunit (GRIN1) sequence was obtained from GenBank (transcript variant accession numbers: NM_000832.5, NM_007327.2 or NM_021569.2). Candidate siRNA sequences were designed using the shRNA design tool (http://www.broad.mit.edu/genome_bio/trc/publicSearchForHairpinsForm.php) from the RNAi Consortium (TRC), Broad Institute. This computational tool implements several algorithms to identify siRNAs with a high probability of silencing the target gene. The program presents information about properties of the 21-mers, including the guanine cytosine base content and other features that may contribute to the effectiveness of a siRNA[238]. The 21-mer sequence to NMDAR1 was CGCCAACTACAGCATCATGAA and is predicted to be specific only for NMDAR1 as determined by basic local alignment search tool (BLAST) (National Center for

Biotechnology Information). The corresponding DNA sequence of each siRNA was converted into a short hairpin by the addition of a loop sequence *TTCAAGAGA*[239] and the end nucleotide overhangs that are compatible with the restriction enzymes AgeI and BamHI. The complementary oligonucleotide strands were purchased from Sigma Aldrich and annealed in buffer (150 mmol/L NaCl; 50 mmol/L Tris, pH 7.6) to produce the desired sequence. Each double-stranded sequence was then cloned into the AgeI-BamHI restriction site of FSVsi lentiviral vector for RNA interference-mediated gene silencing under the control of U6 promoter for expression of short hairpin shRNAs. Transduction efficiency was analyzed by detection of the green fluorescence protein (GFP) expression, whose coding sequence (Venus variant) is present in the FSVsi vector and is under the control of SV40 promoter. FSVsi vector and the virion packaging plasmids were kindly provided by Dr. M. Encinas (Cell Signaling and Apoptosis Group, University of Lleida, Spain).

8.2. Lentiviral production

Human embryonic kidney cell line (HEK293T) was used to produce infective lentiviral particles. HEK293T cells were grown in DMEM supplemented with 10% FBS, 1 mM sodium pyruvate, 10% non-essential amino acids (NEAA), 20 U/ml penicillin and 20 μg/ml streptomycin, at 37°C in a humidified atmosphere under 5% CO_2 and 95% air. One or two days before transfection, cells were seeded in 100x20 mm culture dishes at a density of $3x10^6$/dish. At approximately 70-80% of confluence, growth medium was replaced with DMEM without serum and antibiotics. 293T cells were cotransfected by the polyethylenimine (PEI) transfection method with the virion packaging plasmids (pMD2G encoding VSV-G virus envelope and psPAX2 encoding

viral packaging proteins) and the shRNA-producing vector (FSVsi-NMDAR1 or FSVsi as a control). Total amount of 40 µg of DNA were transfected according to the following scheme:

Plasmid	amount
Vector FSVsi/FSVsi-NMDAR1	20µg
psPAX2	13µg
pMD2G	7µg

DNA and PEI were diluted in 150 mM NaCl to an adequate concentration for transfection and mixed by adding PEI directly to the DNA solution. After 10 minutes of incubation at room temperature, prepared PEI-DNA mix was added drop by drop to a HEK293T cell monolayer. Cells were incubated for 3 hours and medium was replaced with complete growth medium to avoid cell toxicity. HEK293T cells were allowed to produce lentiviral particles during 48-60 hours. Culture medium was collected and centrifuged at 3000 rpm for 10 minutes. Collected supernatant was concentrated by centrifugation through Vivaspin 20 ultrafiltration spin columns (Sartorius) at 4000 rpm for 30 minutes and subsequently aliquoted in sterile vials for long term storage at -80°C. Virus titer was determined by infecting HK-2 cells with different amounts (µl) of concentrated lentiviruses.

8.3. Cell transduction

For lentiviral transduction, HK-2 cells were seeded in 24-well plates at a density of $2x10^4$/well in a complete growth medium. On the day of infection, fresh growth medium was replaced and 1-10 µl of the concentrated lentiviruses were added

to the medium and incubated overnight. Next day, fresh growth medium (DMEM/F12) supplemented with L-Glutamine (2 mM) and 5% FBS was replaced and the cells were grown for additional 3-4 days to allow endogenous gene knockdown. Western blot and real-time PCR were performed to check for gene knockdown.

9. Western blot analysis

After desired treatments, cells were rinsed twice in cold PBS and collected in adequate lysis buffer, depending of the experimental design.

9.1. Cell lysis and whole cell protein extraction

For the analysis of E-cadherin and α-SMA expression in HK-2 cells, total cell lysates were obtained by scraping the cell monolayer in lysis buffer containing 125 mM Tris (pH 6.8), 2% SDS, 2 mM PMSF and PIC (50 µl/ml). Lysates were sonicated 3 times for the interval of 6 seconds at 10% amplitude. Between two cycles of sonication lysates were placed on ice for 5 seconds. For the analysis of pAkt, pErk1/2, pSmad2/3 and Snail1 expression, after adequate treatments cells were collected in lysis buffer containing 20 mM Tris (pH 7.5), 120 mM NaCl, 0.5% NP-40, 100 mM NaF, 0.25% Na-deoxycholate, 1 mM EDTA, 10% glycerol, 1 mM Na_3VO_4, 2 mM PMSF and PIC (50µl/ml). Cell extracts were centrifuged at 12.000 rpm at 4°C for 10 minutes and concentration of proteins was measured from supernatants. Kidney tissue was homogenized in lysis buffer containing 20 mM Tris (pH 7.4), 120 mM NaCl, 0.5% NP-40, 100 mM NaF, 2 mM Na_3VO_4, 50 mM β-glycerophosphate, 10 mM NaPPi, 100 U/ml aprotinin, 2 mM PMSF and PIC (50 µl/ml) using a polytron homogenizer. Homogenized tissue was incubated 20 minutes on ice and the supernatant was collected after centrifugation at 12.500 rpm at 4°C for 10 minutes.

9.2. Nuclear protein extraction

HK-2 cells were serum deprived for 24 hours and subsequently incubated in serum-free medium (control), TGF-β1 and TGF-β1 plus NMDA for 120 minutes. After incubation, cells were washed in cold PBS and nuclear protein fraction was extracted using NE-PER Nuclear and Cytoplasmic Extraction kit.

9.3. Isolation of NMDAR1 subunit

For detection of the NMDAR1 subunit, HK-2 cells were grown in 100x20 mm culture dish in an adequate growth medium. At approximately 80% of confluence, cells were rinsed in PBS, trypsinized as previously described and centrifuged at 1000 rpm for 5 minutes. Supernatant was discarded and the cell pellet was resuspended in *Lysis buffer 1* (20 mM Tris (pH7.5), 120 mM NaCl, 0.5% Igepal CA-630, 100 mM NaF, 1 mM EDTA, 10% Glycerol, 1 mM Na_3VO_4, 2 mM PMSF and PIC (50 µl/ml)). After incubation in lysis buffer for 5 minutes on ice, cells were centrifuged at 13.000 rpm for 20 minutes at 4°C. Supernatant was transferred in a new tube and pellet was resuspended in *Lysis buffer 2* (125 mM Tris (pH 6.8), 2% SDS, 2 mM PMSF and PIC (50µl/ml)) and sonicated as described previously. Samples were vortexed and concentration of proteins was measured.

Protein concentration was determined using a DC protein assay kit (Bio Rad). 20 µg (or 80-100 µg for NMDAR1 detection) of proteins were electrophoresed on 8%, 10%, 12% or 15% SDS-PAGE gels, as appropriate, and transferred to PVDF membranes. Membranes were probed with primary antibodies against E-cadherin (1:2500), NMDAR1 (1µg/ml), Snail1 (1:1000), phospho-Smad2/3 (Ser 423/425)

(1:1000), Histone 1 (1:1000), α-SMA (1:24000), α-tubulin (1:5000), phospho-specific Akt (Ser 473) (1:2000) and total Akt (1:1000), phospho-specific Erk-1/2 (Thr 202, Tyr 204) (1:2000) and total Erk-1/2 (1:1000) or Ras (1:1000) over night at 4ºC. Horseradish peroxidase-conjugated secondary antibodies were used at 1:10000. The immunoreaction was visualized using EZ ECL or ECL Advanced Western Blotting Detection Kits. Images were digitally acquired by VersaDoc Imaging system Model 4000 (Bio-Rad). Positive immunoreactive bands were quantified by densitometry and compared with the expression of adequate loading control.

10. The polymerase chain reaction (PCR)

The polymerase chain reaction (PCR) is a rapid procedure for *in vitro* enzymatic amplification of a specific segment of DNA. In the present study, semi-quantitative and real-time PCR techniques were employed.

10.1. Isolation of RNA and cDNA synthesis

Total RNA was extracted from cultured cells or from whole kidney tissue using TRIzol reagent and the final concentration was determined by Nanodrop (ND-1000) spectrophotometer. Reverse transcription was performed using First Strand cDNA Synthesis Kit for RT-PCR (AMV). Both experimental procedures mentioned above were done according to the manufacturer's instructions.

10.2. Semi-quantitative PCR

For semi-quantitative PCR analysis of NMDAR subunits in HK-2 cells and mouse kidney, following oligonucleotide primers were used: human and mouse NMDAR1, NMDAR2A, NMDAR2B, NMDAR2C, NMDAR2D and GAPDH as an

internal control. Twenty microlitre (20 μL) reaction contained 10x reaction buffer (2 μL), $MgCl_2$ (50 mM, 0.6 μL), dNTP's (2 mM, 2 μL), sterile water (10.2 μL), Taq Polymerase (0.2 μL), adequate NMDAR subunit primer (forward and reverse; 10 μM, 1 μL each), GAPDH primer (forward and reverse; 5 μM, 1 μL each) and cDNA (1 μL). Reaction was run in a termocycler Techne TC-412. Forty cycles of PCR amplification included: denaturation at 95°C for 1 minute, annealing at 60°C (human NMDAR primers) or 62ºC (mouse NMDAR primers) for 1 minute and extension at 72°C for 1 minute. Equal volumes of PCR product (10μl) taken at PCR cycle 40 were loaded and electrophoresed in a SYBR Safe-stained 2% agarose gel. The images of agarose gels were taken using Kodak EDAS 290 imaging system with Kodak 1D 3.6 software. Experiments were performed in triplicates and representative images were presented.

10.3. Real time PCR

Real time PCR amplification with gene-specific primers for human NMDAR1, mouse α-SMA and collagen I was performed with an ABI Prism 7000 Sequence Detection System (Applied Biosystems) using TaqMan Universal PCR Master Mix. This detection system determines the absolute quantity of a target nucleic acid sequence in a test sample by analyzing the cycle-to-cycle change in fluorescent signal as a result of amplification during PCR. Forty cycles at 95°C for 15 seconds and 60ºC for 1 minute were performed. The results are obtained in the form of a value Ct (*cycle threshold*) which represents the cycle of PCR where the exponential growth of PCR product starts. Therefore, the higher expression of the gene in the sample is detected - the lower value of Ct will be obtained as a result. The relative quantity of mRNA for

every gene was calculated in the following manner: ΔCt = Ct of the target gene – Ct of GAPDH gene; Δ(ΔCt) = ΔCt of the sample – ΔCt of the control. Relative mRNA levels were calculated and expressed as fold induction over contralateral controls (value=1.0) following the formula $2^{-\Delta(\Delta Ct)}$. Every experiment was carried out three times, all samples were amplified in triplicate and data were normalized using GAPDH as an endogenous control.

11. *In vivo* animal study

11.1. Animal housing and experimental groups

In vivo animal study was performed on female mice (B6CBJ) weighing 18 to 22 g, obtained from Charles River (Barcelona, Spain). Mice were housed and maintained in a barrier facility and pathogen-free procedures were employed in all mouse rooms. Animals were kept in a 12-hour light/dark cycle at 22°C with *ad libitum* access to food (standard chow) and water. Mice were randomly assigned to two groups.

(1) UUO group (n=7). These mice underwent left ureteral obstruction. They received injections of the vehicle (0.9% saline solution, intraperitoneally). Parameters of renal fibrosis of the post-obstructed left kidney were compared with the healthy non-obstructed right kidney of the same animal. Therefore, contralateral right kidneys of UUO group acted as a control group.

(2) UUO+NMDA group (n=7). These mice underwent left ureteral obstruction and received NMDA treatment 3 days prior and every day after the surgery

(20 mg/kg body weight per day dissolved in 0.9% saline solution (vehicle), intraperitoneally).

All efforts were made to minimize both animal suffering and the number of animals used throughout the experiment. All procedures performed in this study followed the National Institute of Health Guide for the Care and Use of Laboratory Animals.

11.2. Unilateral ureteral obstruction (UUO)

Mice were subjected to a left unilateral ureteral obstruction (UUO) using an established procedure[240,241]. Briefly, under general anesthesia with isoflurane and oxygen, ureteral obstruction was performed by double ligation of the left ureter using 2.0 silk after a lateral abdominal incision. At the end of the operation, the incision was closed in layers under sterile conditions. The animals were allowed to recover from anesthesia and returned to their cages. At 5 and 15 days after the surgery, both obstructed and contralateral kidneys were removed under general anesthesia. Kidneys were perfused in PBS and cross section of each kidney were fixed over night in 4% paraformaldehyde/PBS and embedded in paraffin. Four μm sections were cut and mounted for histological examinations. The remaining portion of each kidney was snap-frozen in liquid nitrogen and stored at -80ºC for protein and mRNA extraction.

11.3. Histological and histochemical analysis of kidney tissue

11.3.1. Immunohistochemistry of paraffin-embedded tissue sections

Immunostaining was carried out on 4 μm thick tissue sections that were first baked at 60ºC for 1 hour and then taken through xylene and graded ethanols (100%,

95%, 90% and 70%) into distilled water. For α-SMA staining, antigen retrieval was done by incubating tissue sections with trypsin for 30 minutes at 37ºC and for E-cadherin and FSP1 staining, antigen retrieval was performed by boiling the slides in 10 mM citrate buffer (pH 6) for 10 minutes. Endogenous peroxidase quenching was done by 30 minutes incubation in 0.66% (v/v) H_2O_2/PBS which was followed by blocking of non-specific binding with 4% BSA/PBS (α-SMA staining) or normal horse blocking serum from Vector Vectastain Universal ABC kit (E-cadherin and FSP1 staining) for 1 hour at RT. All primary antibodies in single immunostaining experiments were incubated overnight at 4ºC. After washing in PBS, slides were treated with universal biotinylated secondary antibody (30 minutes, RT) which was followed by the avidin-biotin-peroxidase complex (30 minutes, RT) and 3, 3'-diaminobenzidine (DAB) as chromogen (10 minutes, RT). Sections were counterstained with Hematoxylin to visualize the nuclei. In addition, double fluorescent immunostaining experiments were performed. After deparaffinization, rehydratation, antigen retrieval and blocking of non-specific binding as previously explained, sections were incubated with primary rabbit anti-FSP1 antibody (1/500) over night at 4°C. After washing in PBS, slides were incubated with universal biotinylated secondary antibody for 30 minutes at RT, then with Streptavidin Alexa Fluor 594 (1/2000) for 1 hour, in the dark. Between steps, sections were washed 3 times in PBS. After the first cycle of immunohistochemistry, slides were incubated with primary mouse anti-E-cadherin antibody (1/200) over night at 4°C. The corresponding secondary anti-mouse-Alexa 488 (1/500) antibody was applied for 1 hour in the dark. After washing in PBS, nuclear staining was performed by incubating slides with 1% Hoechst 33258 for 10 minutes. Negative controls were performed

routinely. Omission of the primary antibody or use of non-immune serum in place of a specific antibody resulted in complete absence of staining. After immunostaining, all slides except ones stained with double-fluorescent immunostaining technique, were dehydrated, cleared in xylene and mounted with DPX permanent mounting medium. Double stained slides were mounted using ProLong antifade reagent. Tissue sections were examined using a Nikon Eclipse 80i microscope with a Nikon automatic camera system. The images were taken using NIS-Elements F2.20 (Build 232) or Isis FISH imaging system v.5 software.

11.3.1.1. Immunohistochemical evaluation

Immunoreactivity of tubular cells for E-cadherin and FSP1 was independently evaluated by semiquantitative method. Kidney sections stained with anti-E-cadherin antibody were scored for the staining intensity as well as for the percent of tubular cells stained. For the staining intensity of tubular proximal cells, samples were scored as follows: 0 for no reactivity, 1 for the presence of both negative and trace positive cells, 2 for weak, 3 for moderate, and 4 for strong staining. The percent of E-cadherin stained tubular cells was scored as follows: 0 for no positive cells, 1 for 1-20% cells positive, 2 for 21-50% cells positive, 3 for 51-80%, and 4 for 81-100% positive cells. Samples were considered positive when both scores were ≥2. The sum of the two scores gave a final score between 0 and 8. Semiquantitative analysis of immunohistochemical staining for FSP1 positive interstitial fibroblasts in non-obstructed mouse kidney was done by counting the positive fibroblasts in 15 optical fields per section.

11.3.2. Morphometric analysis of interstitial fibrosis

For histological examination of interstitial collagen deposition, paraffin-embedded kidney sections were stained with Masson's Trichrome and Sirius Red.

11.3.2.1. Masson's Trichrome staining

Masson's Trichrome is a multi-step technique used for the detection of collagen fibers in different tissues on formalin-fixed, paraffin-embedded and frozen sections. Following this procedure, collagen fibers will be stained green, nuclei will be stained black and cytoplasm, muscle, and erythrocytes will be stained red.

After deparaffinization and rehydratation as previously described, tissue samples underwent process of fixation in Bouin's reagent for 1 hour at 56°C. Slides were washed in running tap water to remove yellow color from sections and incubated in Weigert's Iron Hematoxylin solution for 5 minutes. After washing in running tap water, samples were incubated in *Trichrome solution* (0.6% Chromotrope 2R, 0.3% Light green, 1% glacial acetic acid, 0.8% phosphotungstic acid) for 15 minutes which was followed by one minute incubation in 2% Light green solution. Samples were quickly washed in water and subsequently in 100% ethanol. Slides were dehydrated, cleared in xylene and mounted with DPX permanent mounting medium. Tissue sections were examined using a Nikon ECLIPSE 80i microscope with an Nikon automatic camera system. The representative images were taken using NIS-Elements F2.20 (Build 232) software.

11.3.2.2. Sirius Red staining

For Sirius red staining, slides were baked at 60°C for 1 hour and then taken through xylene and graded ethanols (100%, 95%, 90%, and 70%) into distilled water. Slides were then incubated in Picrosirius Red solution (1% Sirius red in saturated picric acid) for 30 minutes at RT. Slides were dehydrated in absolute ethanol, cleared and mounted with DPX permanent mounting medium. After staining, the connective tissue fibers, except elastin, were brightly red stained and the remaining tissue showed light yellow color. Samples from each animal were examined in a blind manner. Quantification of collagen content was done by determining the % of staining area in 20 randomly chosen fields (x40) using computerized image analyzer and Image-Pro Plus software. Data are expressed as positive stained area vs. total analyzed area.

12. Statistical analysis

Statistical significance was evaluated by Student's t-test or by one-way ANOVA followed by a Tukeys´s posthoc test (SPSS Inc., Chicago, IL), as appropriate. Values of $P<0.05$ was considered statistically significant. All data examined are expressed as mean ± standard error of the mean (SEM).

Results

Objective 1

I. Basal activation of NMDA receptor is essential for the preservation of the epithelial phenotype of PTECs

1. Expression of NMDA receptor in human PTECs

Expression of NMDA receptor in human proximal tubular epithelial cells (PTECs) was first studied by a semi-quantitative PCR analysis of mRNA purified from HK-2 cells using specific PCR primer pairs detected against human NR1 and NR2 (A-D) subunits (*Section 3 in Material & Methods*).

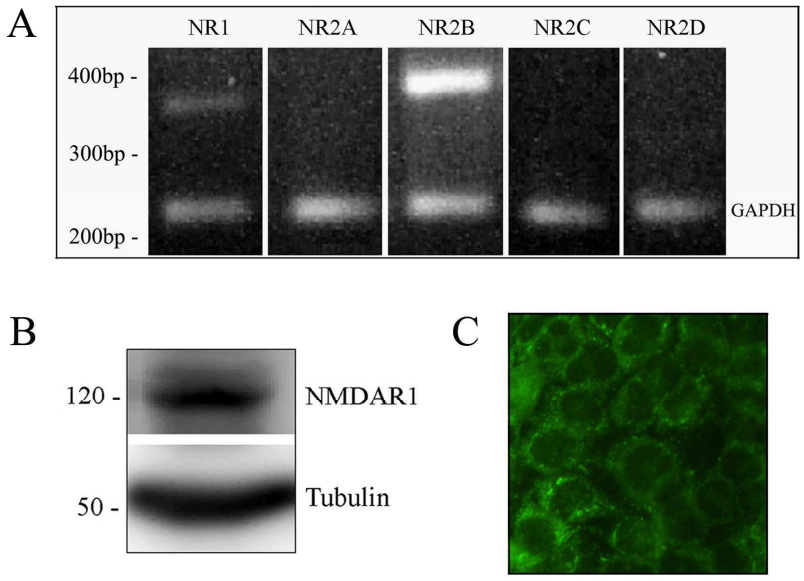

Figure 16. **Expression of NMDA receptor subunits in HK-2 cells.** *(**A**) Total RNA was submitted to RT with an oligo dT reverse primer followed by PCR with different set of primers for NMDAR subunits and GAPDH as an internal control. Representative image after agarose gel electrophoresis shows differential expression of investigated receptor subunits (NMDA R1~370 bp; R2A~300 bp; R2B~376 bp; R2C~397 bp; R2D~280 bp). (**B**) Representative Western blot demonstrates the expression of NMDAR1 protein (120 kDa) in HK-2 cells. The same samples were reprobed with tubulin to ensure equal loading. (**C**) Immunofluorescence staining was performed on permeabilized HK-2 cells using specific anti-NR1 monoclonal antibody. Original magnification x40.*

The results demonstrate that HK-2 cells express mRNA encoding NR1, an NMDAR subunit essential for receptor functioning. In addition, transcript for NR2B subunit was the main NR2 subunit expressed in this cell line, as indicated by the presence of amplicon of appropriate size (Figure 16 A). The expression of NR1 subunit was further investigated at the protein level by Western blot analysis and immunofluorescence. Immunoblotting studies revealed presence of NR1 subunit protein (120 kDa) in human proximal tubular cell line (Figure 16 B). Immunofluorescence microscopy showed diffuse cell membrane and cytoplasmic staining in HK-2 cells incubated with anti-NR1 antibody (Figure 16 C) and absence of staining in the negative control (*not shown*). Therefore, a functional NMDA receptor was expected to be present in HK-2 cell line.

2. Effects of NMDAR agonist and antagonist on viability of PTECs

Viability of HK-2 cells upon treatment with different concentrations of NMDA and MK-801 was estimated using MTT assay, as described in Material and Methods. We first assessed "24-hour drug concentration screening" by evaluating cell population's response upon 24-hour-incubation with increasing concentrations of NMDAR agonist (NMDA; 5-1000 μM) and a specific uncompetitive antagonist ((+)-MK-801; 5-1000 μM). Results show that none of the concentrations tested had statistically significant effect on cell viability after 1 day of incubation, except 1 mM dose of MK-801 ($P<0.01$) (Figure 17 A). Afterwards, we tested the viability of cell population with selected doses of NMDA (0.1-1 mM) for time points (24, 48, 72 hours) we considered important to investigate in further experiments. As shown in Figure 17 B, NMDA treatment did not affect significantly cell viability in any treated

group of cells compared with control. Only very high dose of NMDA (10 mM) reduced cell viability down to 66% of the control (P<0.01) after 72 hours of incubation (Figure 17 C).

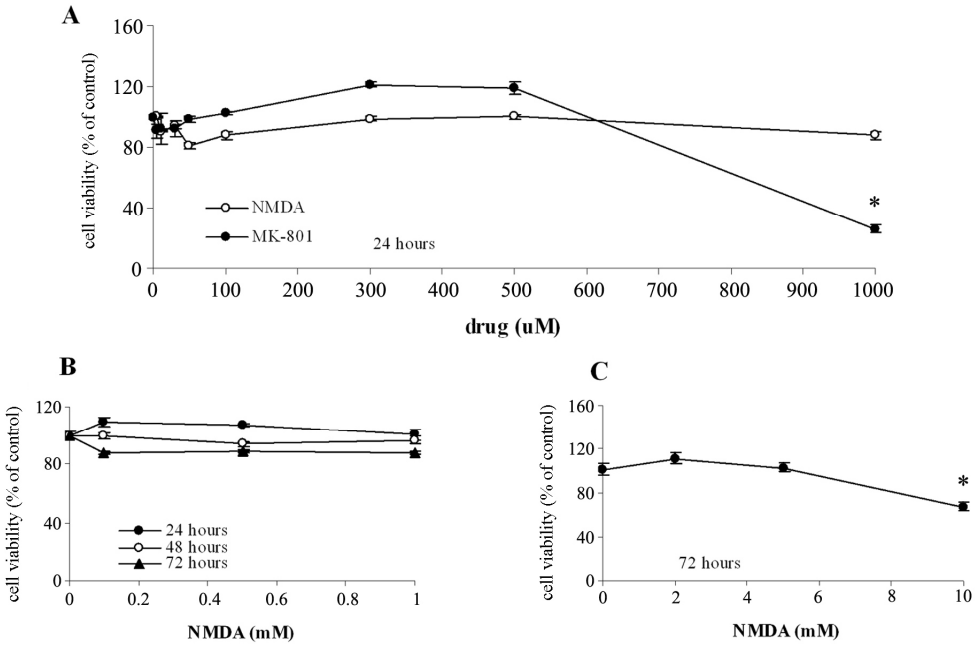

Figure 17. **Concentration-response curves of the effects of NMDA receptor agonist (NMDA) and antagonist (MK-801) on HK-2 cell viability.** *HK-2 cells were treated with increasing concentrations of either NMDA (5-1000 μM and 2-10 mM) or (+)-MK-801 (5-1000 μM). Cell viability was measured by MTT colorimetric assay after 24 hours (**A**, **B**), 48 hours (**B**), or 72 hours (**B**, **C**) of drug treatment. Data are presented as a percentage of control. Values are means ± SEM of at least 3 experiments, run as six replicates per treatment. None of the concentrations tested had statistically significant effect on cell viability except very high concentration of 10 mM NMDA (**C**) and 1 mM MK-801 (**A**) *P<0.01 vs. control.*

According to the results obtained, we decided to use NMDA at the concentration of 0.5 mM and MK-801 at 0.1 mM for our further experiments.

3. NMDAR activation alters human PTEC's migration *in vitro*

Migration of kidney proximal tubular cells is an important physiological and pathophysiological process in renal tissue. PTEC's migration is critical during embryogenesis for tubule formation but after reaching an adult stage of the kidney, tubular cells do not normally migrate[242]. Evidence suggests that upon injury tubular cells do migrate and this migratory behaviour is common for both tubular repair and epithelial-mesenchymal transition[243]. Taking into consideration the fact that NMDAR plays an important role in modulating cytoskeletal migration machinery in many different cell types thus regulating optimal cell locomotion, we sought to examine the role of NMDAR in basal migration of PTECs.

3.1. NMDA inhibits basal cell migration in wound-healing and transwell migration assay

The role of NMDAR in human proximal tubular cell migration was studied using *in vitro* wound-healing and transwell migration assays. Figure 18 shows wound closure in control and NMDA treated group of cells after making a wound in confluent monolayer. After 24 hours of incubation, NMDA inhibited cell migration, by 30% at 0.1 mM (*not shown*) and 0.5 mM (Figure 18 B, E, H), compared with the control. Similarly, after 48 hours of incubation, cell migration was decreased by 30% with NMDA (0.5 mM) compared with the control (Figure 18 C, F, H). To obtain more quantitative estimation of cell motility, we assessed the ability of HK-2 cells to

migrate through a matrix barrier, in a modified Boyden chamber assay, in the absence or presence of NMDA (Figure 18 G, I).

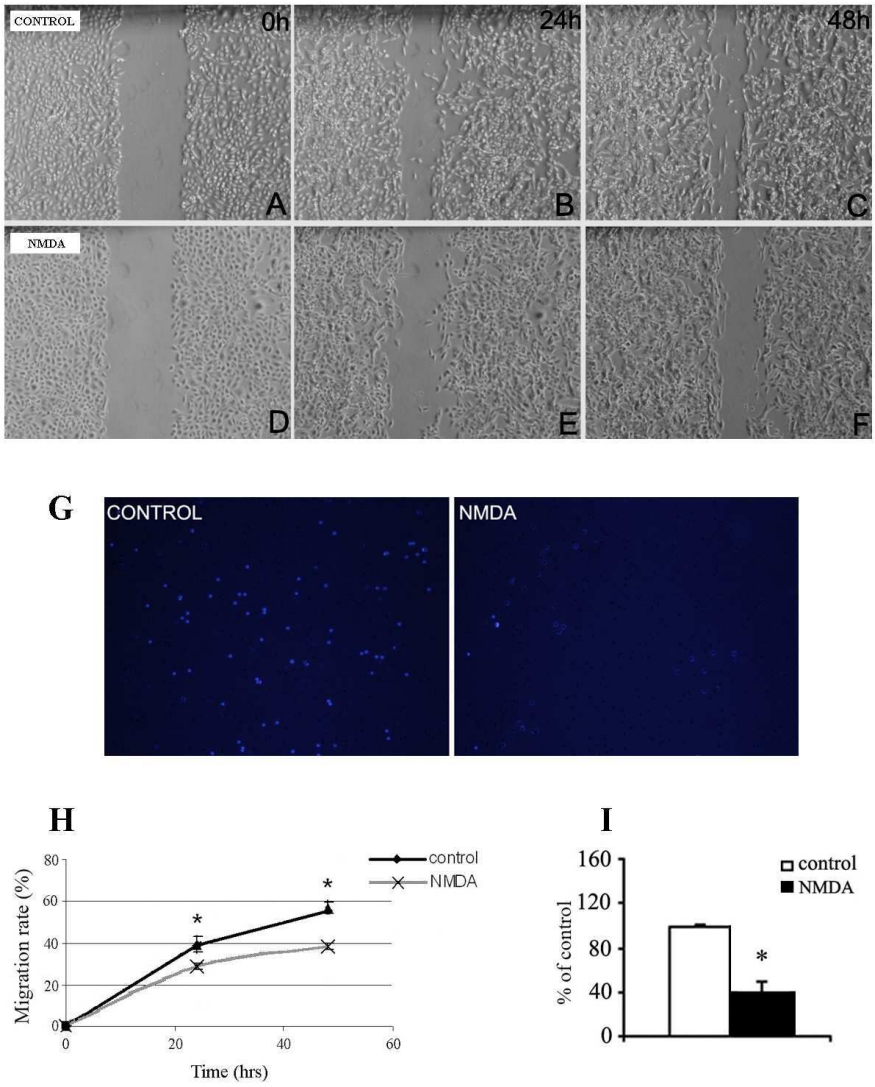

Figure 18. **NMDA inhibits basal cell migration in wound-healing and transwell migration assay.** ***(A-F)*** *Wound-healing assay. Contrast phase micrographs of HK-2 cells migrating into the denuded area of the scratch wound at various times after monolayer wounding. One representative experiment is shown to illustrate the wound closure after 24 (**B**, **E**) and 48 hours (**C**, **F**) in control conditions (**B**, **C**) and NMDA*

*(**E**, **F**) compared with the corresponding wounds at the point 0 hour for the control (**A**) and NMDA (**D**) Magnification x4. (**G**) Transwell migration assay. Representative photos show parts of transwell inserts for control and NMDA treated group of cells after 24 hours of incubation. Nuclei were stained with Hoechst. Magnification x20. Quantification of cell migration in wound-healing assay after 24 and 48 hours (**H**) and transwell migration assay after 24 hours (**I**). Data are presented as means ± SEM (wound-healing assay) or percentage of control (means values ± SEM; transwell migration assay) of 5 independent experiments assayed in triplicate for each time point and condition. (**H**) *P<0.05 vs. control at both time points. (**I**) *P<0.05 vs. control.*

As shown in Figure 18, treatment with NMDA reduced cell migration down to 60% of the control, after 24 hours of incubation (Figure 18 I). Immunofluorescence microscopy of randomly chosen fields of the insert membrane shows occupied pores after transwell migration assay (Figure 18 G). As tested previously in MTT assay, viability of HK-2 cells was not significantly affected after 24 and 48 hours of incubation with NMDA (Figure 17 B), indicating that the detected decrease in migration was not due to reduced cell viability.

Here, we demonstrate by two independent methods that the activation of NMDA receptor has an inhibitory effect on HK-2 cell migration which supports its important role in regulation of human proximal tubular cell migration.

3.2. NMDA modulates basal cell velocity and persistence

Taking into consideration the fact that during migration cells use different migrational modes to move with varying degrees of speed and directionality[244], we wished to examine the effect of NMDA on cell velocity and persistence. We performed several migration assays on different matrices where we measured cell

velocity and persistence using time-lapse phase contrast microscopy. Matlab analysis of image sequences allowed us to quantitatively estimate differences in persistence and velocity between treated and untreated cultures. Incubation with NMDA for 24 hours on non-coated plates did not cause significant differences in cell persistence (Figure 19 A) compared with control.

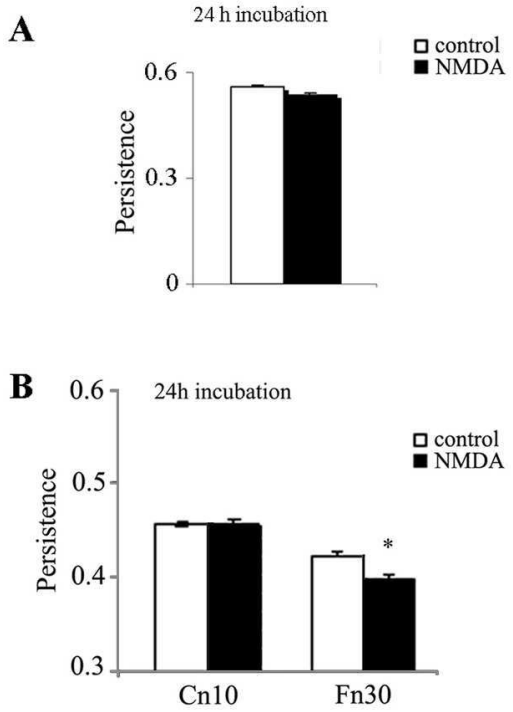

Figure 19. **NMDAR activation modulates basal cell directionality of human proximal tubular cells.** *HK-2 cells were seeded in non-coated (**A**), fibronectin (30 µg/ml) and collagen I-coated (10 µg/ml) (**B**) 48-well plates and incubated with or without NMDA (0.5 mM). Cell's migratory behavior was recorded by time-lapse video microscopy during a 5 hour period (3 min frame interval) after 24 or 48 hours of treatment. Migrational persistence of each cell population was quantified using Matlab software. Persistence is defined as the ratio of the vectorial distance traveled to the total path length described by the cell. Cell densities of both populations were*

*equivalent (not shown). Histograms represent the average persistence during 0-300 minute's period after 24 hours (**A**, **B**) of treatment. Values are average cell persistence (averaging values from all time-points during 0-300 minutes) ± SEM.*

All tested cell populations showed analogous migrational persistence with values under 0.6 which is generally considered as not very directional. Cells grown on type I collagen and fibronectin showed comparable random migration behavior as ones grown on non-coated plates (directionality under 0.6) but with statistically significant difference between control and NMDA when grown on fibronectin coated surface (Figure 19 B).

In order to get more insights into the nature of proximal tubular cell migration, we analyzed migrational velocity in the settings of already described treatments. NMDA incubation caused statistically significant reduction in cell velocity of HK-2 cells grown on non-coated plates for 24 hours compared with non-treated controls (Figure 20 A, B). Taking into account that the cell migration is modulated in a great deal by the extracellular matrix (ECM) composition[245], we wished to assess the cell velocity on different matrices. Consistent with the results on non-coated plates, HK-2 cells grown on collagen I (Cn, 10 µg/ml) and fibronectin (Fn, 30 µg/ml) coated surfaces showed statistically significant reductions of cell velocity when treated with NMDA for 24 hours (Figure 20 C).

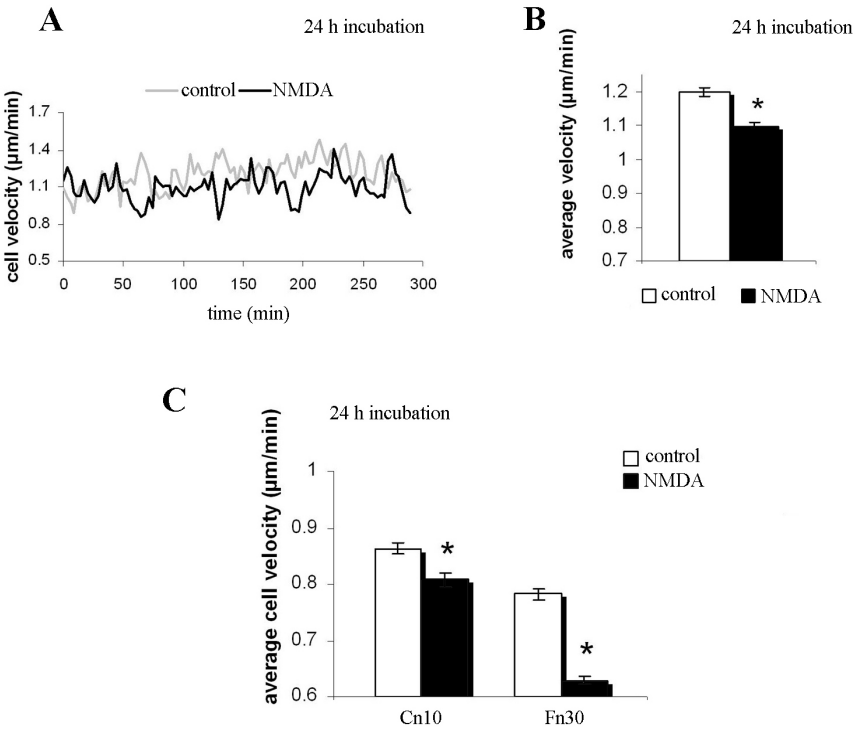

Figure 20. **NMDAR activation modulates basal cell velocity of human proximal tubular cells.** *HK-2 cells, plated in non-coated plates (**A**, **B**) or plates coated with collagen I (Cn) (10 µg/ml) and fibronectin (Fn) (30 µg/ml) (**C**) were incubated with or without NMDA (0.5 mM). Cell behavior was recorded by time-lapse video microscopy during a 5 hours period (3 minutes frame interval) after 24 hours of treatment. (**A**) Velocity time-course by tracking of approximately 50 cells of each group from 3 independent time-lapse image series quantified using Matlab software. (**B**) Average cell velocities (averaging values from all time-points during the period of 0-300 minutes (± SD) from each of the velocity time-courses in A. *P<0.0001 vs. control. Cell densities of both populations were equivalent (not shown). (**C**) Average velocities of cells (avg. values ± SEM) grown on Collagen I (10 µg/ml) and Fibronectin (30 µg/ml) followed over the 0-300 minutes period after 24 hours of treatment. *P<0.0001 vs. control.*

Velocity data represent a valuable contribution to wound and transwell migration results and confirm that NMDA receptor is important in regulation of human proximal tubular cell's migration *in vitro*.

4. NMDAR activation does not alter cell-ECM adhesion

For cells to migrate efficiently, both cell–cell adhesions and cell-extracellular matrix (ECM) interactions need to be regulated and tension within the actomyosin cytoskeleton needs to be induced[27,246,247]. Adhesion to extracellular matrix components, such as fibronectin and laminin, is primarily mediated by the integrin family of heterodimeric receptors[248]. Therefore, we wished to investigate if the reduction of cell migration as well as migrational velocity of HK-2 cells on different matrices could be due to alterations in cell-ECM adhesion.

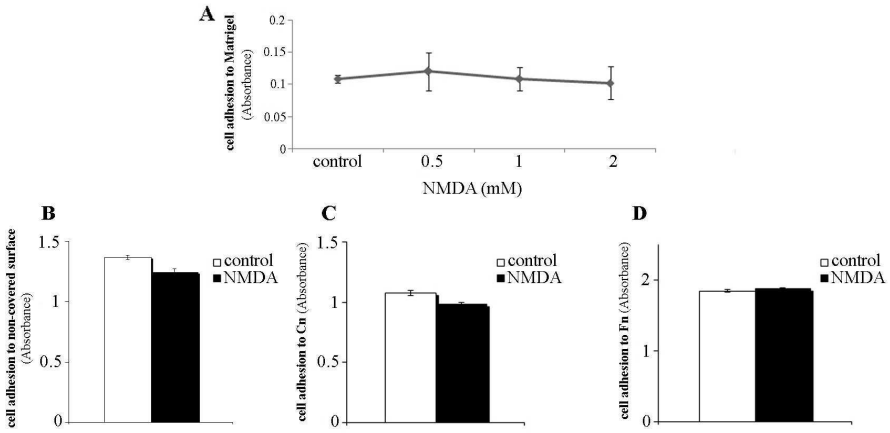

Figure 21. **NMDA treatment does not have influence on cell adhesion to different extracellular matrices.** *HK-2 cells plated on Matrigel (**A**), non-covered surface (**B**), collagen I (Cn; 10 µg/ml) (**C**) and fibronectin (Fn; 30 µg/ml) (**D**) were allowed to adhere for 2 hours in the presence or absence of NMDA at 0.5, 1 and 2 mM (**A**) or*

*only 0.5 mM (**B**, **C**, **D**). Unbound cells were removed and bound cells were quantified by measuring acid phosphatase activity. Histograms show means values of absorbance ± SEM of 3 independent experiments assayed in 6 replicates for every condition.*

Treatment of HK-2 cells with NMDA did not significantly alter cell adhesion to non-covered surface (Figure 21 B), compared with control. Cell adhesion to different matrices followed the same pattern. After measuring acid phosphatase activity in cell-ECM attachment assay, no significant differences in cell adhesion to collagen I, fibronectin or matrigel (mixture of ECM proteins such as laminin and collagen IV) were found, suggesting that reduced migration and migrational velocity of cells treated with NMDA were not due to altered integrin-dependent adhesion (Figure 21 A, C, D)[249-251].

5. NMDAR activation causes a decrease in cellular F-actin

Actin cytoskeleton plays an important role in cell morphology and migration, while actin reorganization is one of the most important characteristics of tubular epithelial-mesenchymal transition. Being aware of the existence of biochemical and functional interactions between NMDAR subunits and cytoskeleton proteins[231], we sought to examine the role of NMDAR activation in the distribution of filamentous actin in HK-2 cells. Changes in F-actin distribution were investigated using immunofluorescence staining and for better quantitative analysis, flow cytometry was employed. To determine whether cellular F-actin was altered by NMDA treatment, HK-2 cells were stained with Phalloidin 568, which binds specifically to F-actin structure. As shown in Figure 22 A, NMDA treatment at concentration of 0.5 mM

induced significant decrease of cellular F-actin which was visible after fluorescent staining.

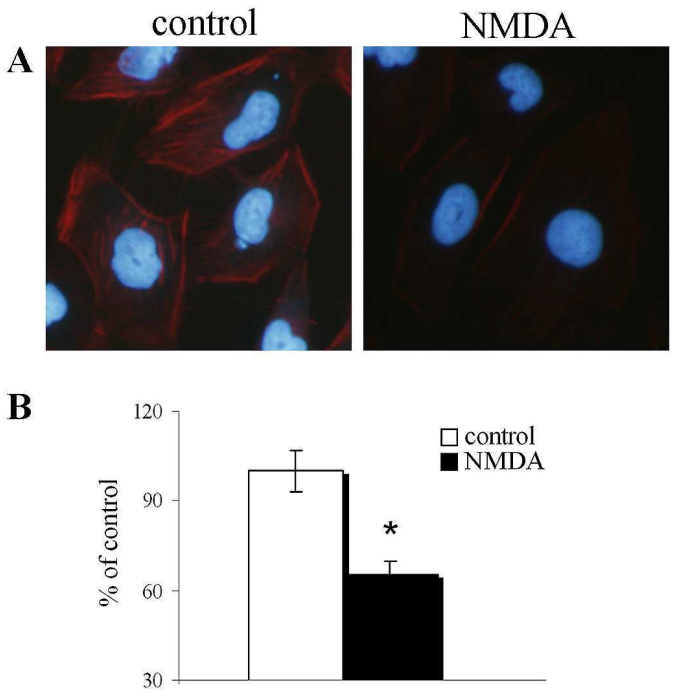

Figure 22. **NMDA treatment decreases the amount of F-actin in HK-2 cells.** *(**A**) Direct Phalloidin immunofluorescence. HK-2 cells grown on glass coverslips were treated with or without NMDA (0.5 mM) for 24 hours. Cells were fixed and stained with Phalloidin 568 and visualized by fluorescent microscopy. Nuclei were stained with Hoechst. Representative images from an experiment that was repeated 3 times with identical results are shown. Original magnification x40. (**B**) HK-2 cells treated with or without NMDA (0.5 mM) for 24 hours were examined by flow cytometry using Phalloidin fluorescence detected on FL1 (as described in Material and Methods). Values are given as percentage of the control (means ± SEM) of 3 independent experiments assayed in triplicate for every condition. *P<0.05 vs. control.*

To provide better quantitative analysis of the alterations of filamentous actin, after maintaining the cultures in the described treatments, cells were stained with Phalloidin 488 and the fluorescence was measured by flow cytometry analysis. The majority of HK-2 cells in the control group possessed high amounts of F-actin while NMDA treatment (0.5 mM; 24 hours) decreased the amount of filamentous actin, seen as a marked reduction in the number of cells with high Phalloidin fluorescence (down to 60% ± 4.7% of control) (Figure 22 B).

Cell volume changes have been reported to be in close relation to F-actin disturbance in epithelial cells[252]. To rule out the possibility that the changes in F-actin distribution were due to changes in cell volume in NMDA treated group of cells, cell volume was measured using Coulter Z2. Figure 23 shows that NMDA treatment did not induce changes in cell volume of HK-2 cells and that the detected decrease in cellular F-actin was not an artifact but the direct consequence of NMDA treatment.

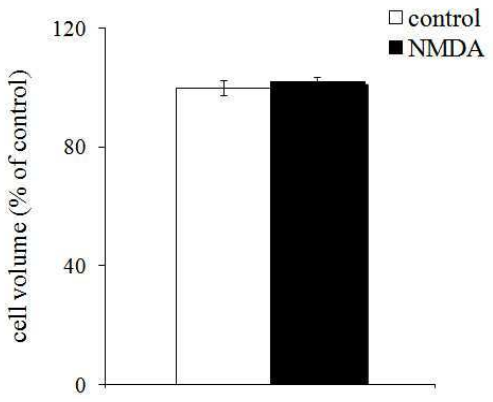

Figure 23. **NMDA treatment does not have an influence on cell volume of HK-2 cells.** *HK-2 cells were treated with or without NMDA (0.5 mM) for 2 hours and cell volume was measured by Coulter Z2. NMDA treatment does not have effect on HK-2*

cell's volume. Values are given as percentage of the control (means values ± SEM) of 3 independent experiments assayed in triplicate for every condition.

6. Knockdown of NMDAR1 influences PTEC's phenotype

The NR1 subunit is the main and an essential subunit for the functional NMDA receptor in a variety of cell types[143,151,179,253]. It has been reported that the basal level of NMDA receptor activation is essential for normal neuronal[154] and glomerular function[185] and tubular reabsorption[183] . In order to assess the function of the NMDAR in HK-2 cells in basal conditions, we designed NR1 shRNA vector for lentiviral infection and the expression of the NMDAR1 subunit was disrupted by short hairpin RNA. SQ PCR and real time PCR demonstrate an evident decrease in NMDAR1 expression at mRNA level (54.9% ± 7%) in HK-2 cells infected with FSVsi-NMDAR1 (shNR1) compared with control (FSVsi) (Figure 24 A, B). Quantification of Western blots of HK-2 cells expressing NR1 shRNA indicates a decrease of NR1 subunit protein levels of 28% (± 10%) down to control (FSVsi) (Figure 24 C, D). Transduction efficiency was analyzed by detection of the green fluorescence protein (GFP) expression (driven by the lentiviral vector) (Figure 24 E).

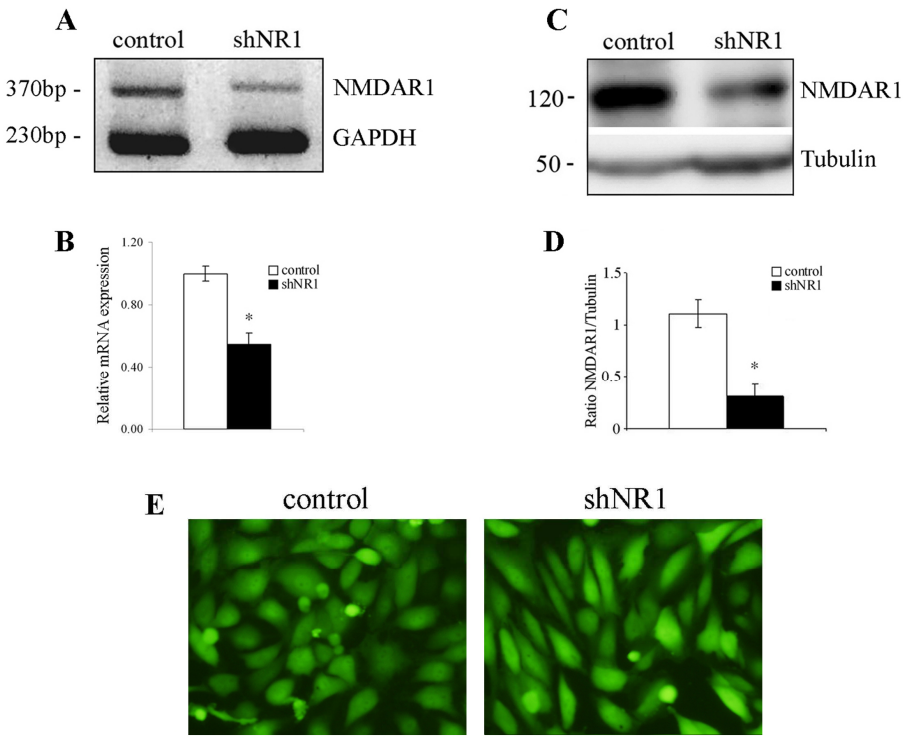

Figure 24. **NMDAR1 gene knockdown in human PTECs.** *Expression of NMDAR1 subunit in HK-2 cells was disrupted by short hairpin RNA and subsequently was tested by semi-quantitative PCR, real time PCR and western blot analysis. (**A**) SQ PCR. Total RNA was submitted to RT with an oligo dT reverse primer followed by PCR with specific set of primers for NMDAR1 subunit and GAPDH as an internal control. Representative image after agarose gel electrophoresis shows downregulation of NMDAR1 subunit (NMDA R1~370 bp). (**B**) Real time PCR analysis confirmed downregulation of NR1 subunit in HK-2 cells. Relative mRNA levels were calculated and expressed as fold induction over controls (FSVsi) (value = 1.0) after normalizing with GAPDH. *P<0.05 vs. control (FSVsi). Representative Western blot (**C**) and quantitative analysis (**D**) demonstrate decrease in NMDAR1 protein expression in HK-2 cells infected with FSVsi-NMDAR1 (shNR1) compared with control (FSVsi); *P<0.05 vs. control (FSVsi). (**E**) Representative photomicrographs show GFP-positive cells (GFP expression driven by the lentiviral vector) in FSVsi and shNR1 group of cells. Original magnification x10.*

After performing a successful knockdown of the NR1 subunit of the NMDAR in HK-2 cells, we further proceeded in analyzing the expression of E-cadherin, a calcium dependent cell-cell adhesion protein and a marker of epithelial phenotype, as well as α-smooth muscle actin (α-SMA), a marker of mesenchymal phenotype. Stunningly, downregulation of NMDAR1 subunit in human proximal tubular epithelial cells induced remarkable changes in epithelial phenotype (Figure 25).

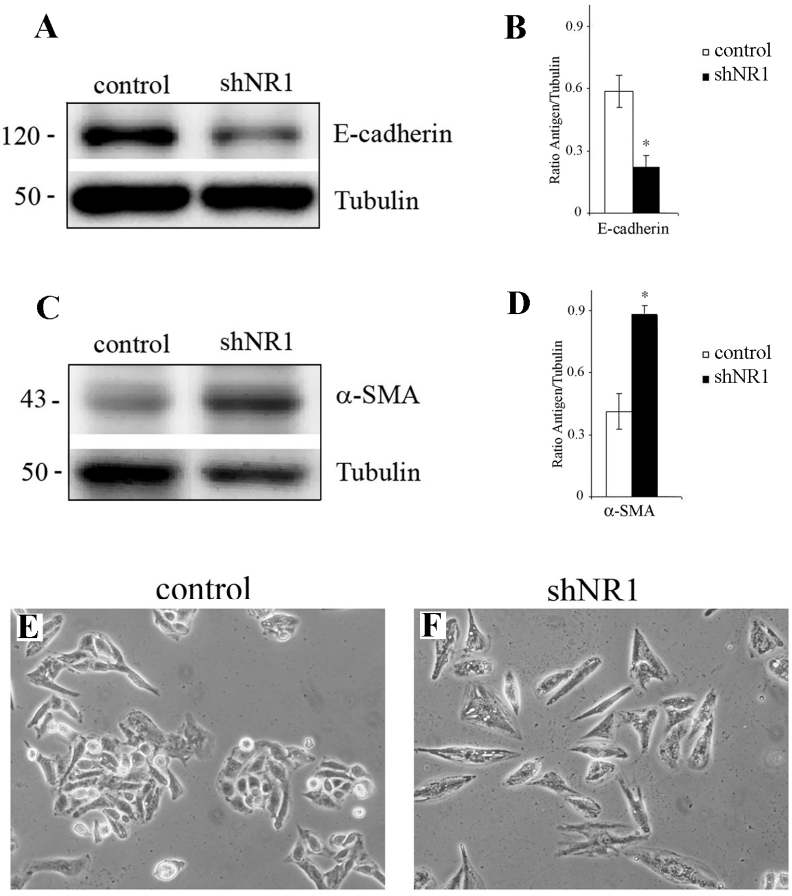

Figure 25. **NMDAR1 gene knockdown originates loss of epithelial phenotype in PTECs.** *HK-2 cells were infected with lentiviral driven FSVsi or NR1 shRNA and grown in DMEM/F12 medium for the maintenance of proximal tubular cell culture.*

*Whole cell lysates were immunoblotted with antibodies against E-cadherin and α-SMA. The same samples were reprobed with tubulin to ensure equal loading. Representative western blots and quantitative analysis demonstrate changes in epithelial phenotype evident as a decrease of E-cadherin (**A**, **B**) and an increase of α-SMA (**C**, **D**) expression in shNR1 group of cells compared with control (FSVsi) (n≥3 experiments). (**B**, **D**) *P<0.05 vs. control. (**E**, **F**) Representative photomicrographs show morphological changes in shNR1 group of cells (**F**) compared with the control (FSVsi) (**E**) Magnification x20.*

Quantification of Western blots of HK-2 cells expressing NR1 shRNA indicates a decrease of E-cadherin (37.8% ± 9%) (Figure 25 A, B) and an increase of α-SMA (214% ± 10%) (Figure 25 C, D) protein expression compared with HK-2 cells expressing empty FSVsi vector (control). Furthermore, knockdown of the NR1 subunit induced significant alterations in cell morphology seen as a loss of cobble-stoned shape and the acquisition of spindle-like form of loosely interconnected cells (Figure 25 E, F).

Lentiviral-driven knockdown of NMDAR1 provides a proof that the basal activation of NMDAR is essential for the maintenance of the epithelial phenotype of human proximal tubular epithelial cells.

Objective 2

II. NMDAR activation attenuates epithelial-mesenchymal transition *in vitro* (pathologic condition)

1. NMDAR activation modulates important key steps of tubular EMT *in vitro*

Once determined that basal NMDAR activation had a role in preserving the epithelial phenotype of human proximal tubular epithelial cells, we sought to assess if the activation of the channel could be a possible strategy in attenuating the phenotypic changes induced by transforming growth factor-β1 (TGF-β1), a cytokine known to be critical in regulation of proximal tubular epithelial cell phenotype.

1.1. NMDAR activation restores expression of E-cadherin, α-SMA, Snail1 and pSmad2/3 altered by TGF-β1

To investigate the possible influence of NMDA receptor on tubular epithelial-mesenchymal transition (EMT), we used human proximal tubular cell line (HK-2) induced to undergo EMT by transforming growth factor-β1 (TGF-β1), a well known inducer of EMT in diverse experimental models. Compared with control, TGF-β1-treated cells started to lose epithelial E-cadherin and gained mesenchymal marker α-SMA (Figure 26 A, B). Co-incubation with NMDA reduced expression of α-SMA and restored downregulation of E-cadherin close to control levels (Figure 26 A, B). Treatment with TGF-β1 caused upregulation of Snail1 in HK-2 cells within 6 hours (Figure 26 C, D) and phosphorylation of Smad2/3 and its translocation into the nucleus within 120 minutes (Figure 26 E, F) after stimulation, which was blunted by co-treatment with NMDA. In order to confirm that the described changes were NMDA channel specific, HK-2 cells were treated with an antagonist of NMDA receptor. Pharmacological blockade using an antagonist of NMDAR (MK-801) in cells treated

with TGF-β1 and NMDA abolished the downregulation of Snail1 induced by NMDA, showing that the effect of NMDA was achieved through the activation of the NMDA receptor (Figure 26 G).

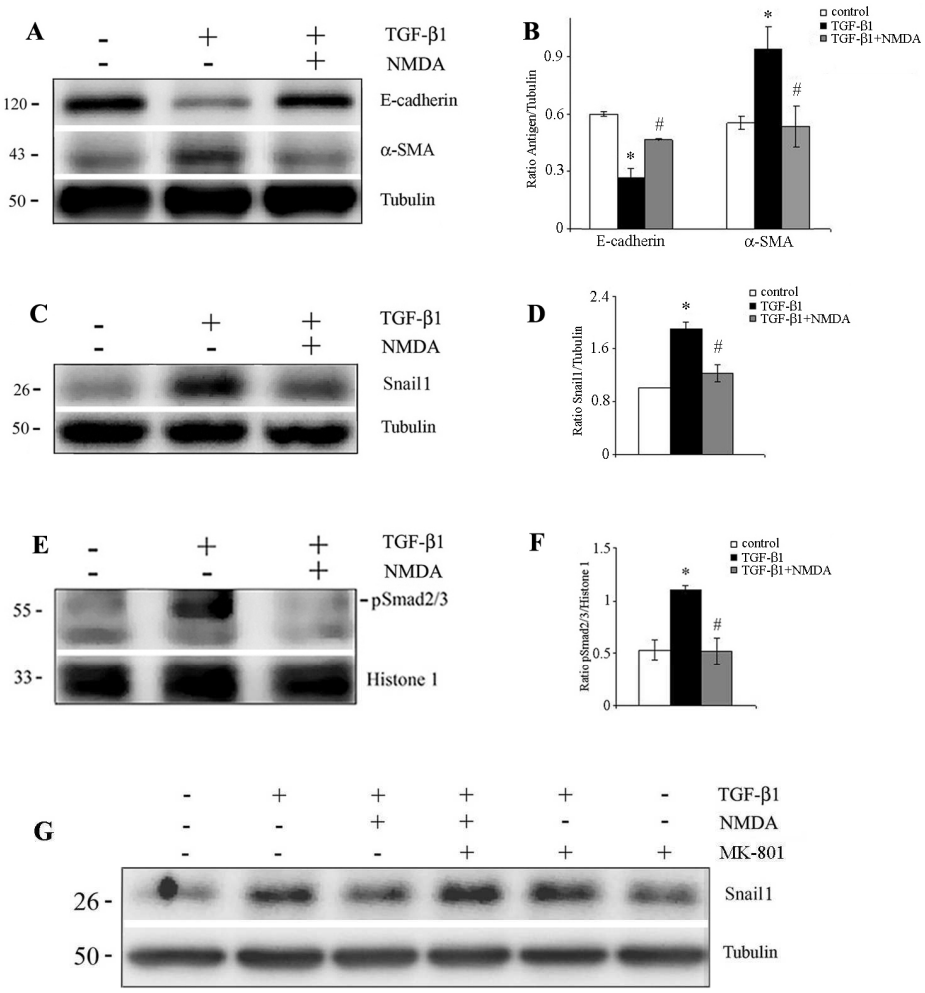

Figure 26. **NMDAR activation restores expression of E-cadherin, α-SMA, Snail1 and pSmad2/3 altered by TGF-β1.** *HK-2 cells were incubated in serum free medium (control), TGF-β1 or TGF-β1+NMDA for 72 hours (E-cadherin, α-SMA), 6 hours (Snail1) or 120 minutes (pSmad2/3). Whole cell lysates were immunoblotted with antibodies against E-cadherin, α-SMA and Snail1. The same samples were reprobed*

*with tubulin to ensure equal loading. Representative Western blots and quantitative analysis demonstrate decrease in E-cadherin (**A**, **B**) and increase in α-SMA (**A**, **B**) and Snail 1 (**C**, **D**) expression induced by TGF-β1. Co-treatment with NMDA restored expression of these molecules close to the control levels. (**E**, **F**) NMDA managed to reduce TGF-β1-induced translocation of pSmad2/3 into the nucleus after 120 minutes (nuclear extracts). Histone 1 was used as a loading control for pSmad2/3 expression. (**B**, **D**, **F**) *P<0.05 vs. control, #P<0.05 vs. TGF-β1. (**G**) Co-incubation of cells with MK-801 abolished the inhibitory effect of NMDA on TGF-β-1-induced overexpression of Snail1. HK-2 cells were incubated for 6 hours in serum-free medium (control), TGF-β1, TGF-β1+NMDA, TGF-β1+NMDA+MK-801, TGF-β1+MK-801 and MK-801 alone. Whole cell lysates were immunoblotted with antibody against Snail1. The samples were reprobed with antibody against tubulin to ensure equal loading.*

1.2. NMDAR activation restores expression of vimentin and β-catenin and preserves the cytoskeletal architecture altered by TGF-β1

Stability of proximal tubular cell-cell adhesions is important in modulation of cell migration and the loss of cell-cell contacts represents an important early characteristic of EMT. Tightness of adherens junctions is dependable of cadherin-catenin complexes linked to the actin cytoskeleton and is altered in TGF-β1 induced EMT. Therefore, we set out to investigate the influence of NMDAR on β-catenin distribution as well as F-actin reorganization in the settings of already described treatment. Changes in F-actin distribution induced by TGF-β1 treatment were analyzed using flow cytometry analysis. Treatment of HK-2 cells with TGF-β1 induced significant changes in F-actin organization seen as a strong increase in Phalloidin fluorescence (Figure 27 A) and spindly stress fibers (detectable by immunofluorescence) (*not shown*).

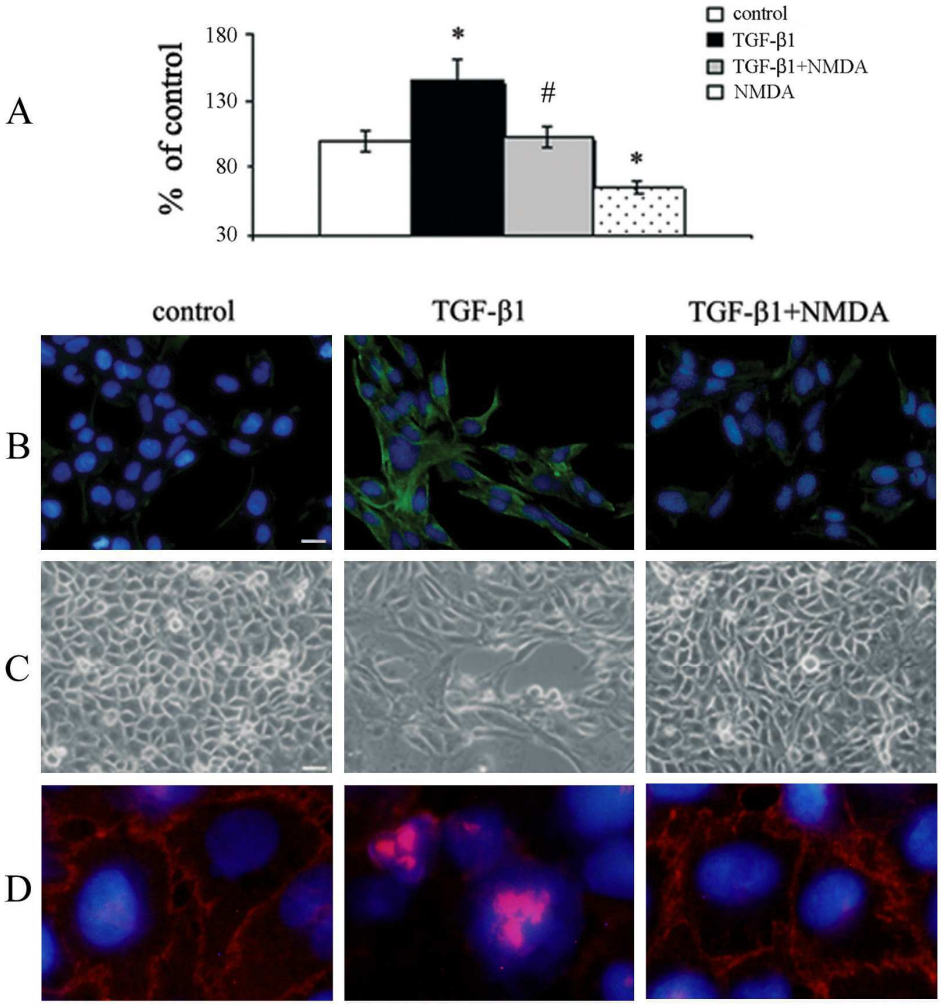

Figure 27. **NMDAR activation modulates important key steps in tubular EMT *in vitro*.** ***(A)*** *Activation of NMDAR decreases basal actin polymerization state and TGF-β1-induced actin reorganization in HK-2 cells. Cells were grown in control conditions, TGF-β1, TGF-β1+NMDA and NMDA for 24 hours and examined by flow cytometry using Phalloidin fluorescence detected on FL1 (as described in Methods). Values are given as percentage of the control (means ± SEM) of 3 independent experiments assayed in triplicate for every condition.* ***(A)*** **P<0.05 vs control; #P<0.05 vs.TGF-β1. Immunofluorescence staining for the distribution of vimentin* ***(B)*** *and β-catenin* ***(D)*** *in HK-2 cells after incubation with TGF-β1 or TGF-β1+NMDA.*

*TGF-β1 induced de novo expression of vimentin (72 hours) and translocation of β-catenin (24 hours) into the nucleus. Co-treatment with NMDA reduced vimentin expression and restored β-catenin to the cell periphery. (**C**) Light microscopy shows morphological changes caused by TGF-β1 and NMDA treatment. Scale bar (**B**) 10 µm; (**C**) 20 µm. (**D**) Original magnification x40.*

Co-treatment with NMDA managed to inhibit described changes induced by TGF-β1 down to control levels (Figure 27 A). Treatment with TGF-β1 induced significant alterations in cell morphology seen as loss of cobble-stoned morphology and acquisition of spindle-like shape, while co-treatment with NMDA restored the epithelial phenotype of HK-2 cells (Figure 27 C).

Immunofluorescence staining revealed strong upregulation of vimentin in TGF-β1-treated cells (72 hours, Figure 27 B) as well as translocation of β-catenin into the nucleus (24 hours, Figure 27 D). Co-treatment with NMDA managed to decrease expression of vimentin and restore β-catenin to its original localization at the cell periphery (Figures 27 B and 27 D, respectively).

1.3. Calcium influx through NMDAR is responsible for the attenuation of TGF-β1-induced tubular EMT

1.3.1. Thapsigargin does not restore expression of E-cadherin, α-SMA nor vimentin altered by TGF-β1

In order to demonstrate that the NMDAR's inhibitory effect on tubular EMT described above is triggered by the entry of calcium ions exclusively through the NMDA receptor, we used thapsigargin (TG), a non-competitive inhibitor of smooth

endoplasmic reticulum Ca^{2+}-ATPase (SERCAs) that has been previously shown to rise intracellular calcium concentrations in proximal tubular cells in culture[254]. Co-incubation with thapsigargin did not restore the expression of E-cadherin altered by TGF-β1 and failed to decrease α-SMA expression induced by this cytokine in HK-2 cells (Figure 28 A, B).

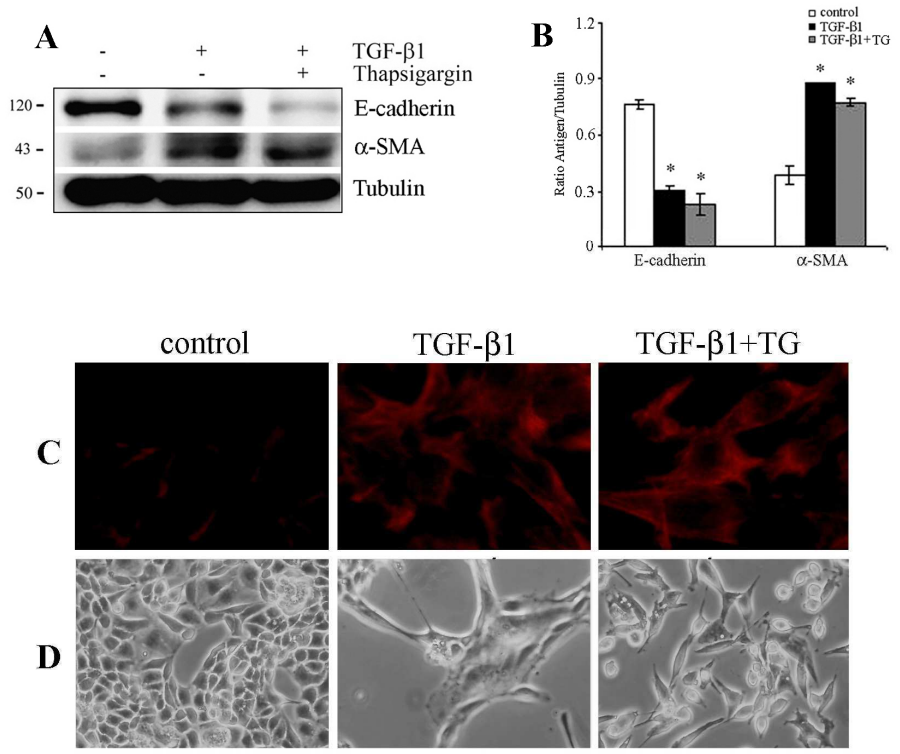

Figure 28. **Thapsigargin does not lead to the recovery of the expression of E-cadherin, α-SMA nor vimentin altered by TGF-β1**. *HK-2 cells were incubated in serum-free medium (control), TGF-β1 or TGF-β1+Thapsigargin for 72 hours. (**A**) Whole cell lysates were immunoblotted with antibodies against E-cadherin and α-SMA. The same samples were reprobed with tubulin to ensure equal loading. Representative Western blot (**A**) and quantitative analysis (**B**) demonstrate decrease in E-cadherin and increase in α-SMA expression induced by TGF-β1. Co-incubation*

*with TG for 72 hours did not result in restoration of E-cadherin and α-SMA expression in HK-2 cells (**A**, **B**). (**B**) *P<0.05 vs. control. (**C**) Immunofluorescence staining for the distribution of vimentin in HK-2 cells after incubation with TGF-β1 or TGF-β1+TG. Co-treatment with TG did not reduced de novo expression of vimentin induced by TGF-β1 in HK-2 cells. (**D**) Light microscopy shows morphological changes caused by TGF-β1 and TG treatment. Original magnification x40 (**C**) or x10 (**D**).*

Cells co-treated with TGF-β1+TG maintained the same expression levels of E-cadherin and α-SMA as ones treated with TGF-β1 alone. Moreover, d*e novo* expression of vimentin (Figure 28 C) induced by TGF-β1 in tubular cells was not attenuated after co-treatment with TG, showing that calcium released from intracellular stores failed to decrease expression of vimentin induced by this cytokine. Additionally, co-incubation with TG did not restore alterations in cell morphology seen as a loss of cobble-stoned shape and the acquisition of spindle-like cell form induced by TGF-β1 after 72 hours of incubation (Figure 28 D).

Results demonstrated here confirm that calcium ions derived from other sources than NMDAR did not have influence on preservation of epithelial phenotype of human proximal tubular epithelial cells.

1.3.2. NMDAR activation failed to ameliorate TGF-β1-induced alterations in HK-2 cells in the absence of calcium in the culture medium

In order to confirm that the influx of Ca^{2+} exclusively through the activated NMDAR is the one responsible for the preservation of the epithelial phenotype, we performed experiments in Ca^{2+}-free medium.

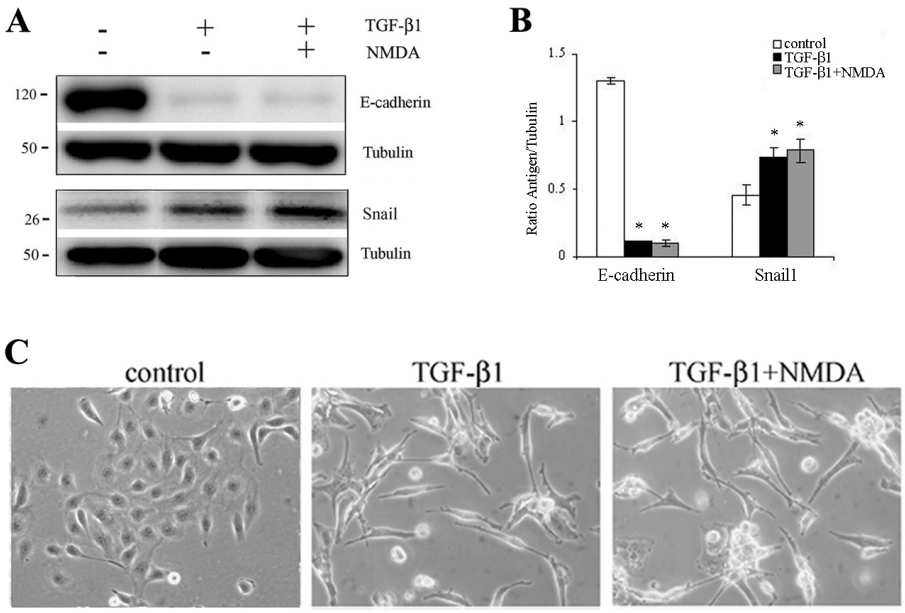

Figure 29. **NMDAR activation failed to ameliorate TGF-β1-induced upregulation of E-cadherin and Snail1 in HK-2 cells in the absence of calcium in the medium**. *HK-2 cells were incubated in serum free medium (control), TGF-β1 or TGF-β1+NMDA (in serum free EpiLife (Ca2+ free) medium) for 72 hours (E-cadherin) and 6 hours (Snail). Representative Western blots (**A**) and quantitative analysis (**B**) demonstrate decrease in E-cadherin and an increase in Snail 1 expression induced by TGF-β1. Co-treatment with NMDA in Ca^{2+}-free medium shows no benefits in reversing the expression of investigated molecules. (**B**) *P<0.05 vs. control. (**C**) Light microscopy shows morphological changes caused by TGF-β1 and NMDA treatment in Ca^{2+}-free medium. Magnification x20.*

As expected, in the absence of Ca^{2+} in the culture medium, NMDAR activation failed to ameliorate TGF-β1-induced downregulation of epithelial cell marker E-cadherin and the upregulation of a key regulator of EMT, Snail1 in HK-2 cells (Figure 29 A, B). Furthermore, co-treatment with NMDA in Ca^{2+}-free medium did not manage to preserve characteristic cobble-stoned morphology of tubular epithelial cells (Figure

29 C), pointing again to an increase in extracellular Ca^{2+} flux as the responsible for NMDA effect.

2. NMDAR activation inhibits TGF-β1-stimulated PTEC's cell migration

In the light of the previously gained results and the fact that one of the hallmarks of EMT is increased cell migration, we wished to test if NMDA receptor activation plays a role in modulating cell migration stimulated by TGF-β1, a well known inducer of epithelial cell migration.

2.1. NMDA inhibits TGF-β1-stimulated PTEC's cell migration in wound-healing and transwell migration assay

The role of NMDA receptor in cell migration stimulated by TGF-β1 was studied using *in vitro* wound-healing and transwell migration assays. Figure 30 shows wound closure in different treatment groups after making a wound in confluent monolayer. Incubation of HK-2 cells with TGF-β1 for 24 and 48 hours caused a significant increase in cell migration in wound-healing assay (Figure 30 A-F, J), while co-treatment with NMDA reduced migration of HK-2 cells down to the control level (Figure 30 A-F, J). To obtain more quantitative estimation of cell motility, we assessed the ability of HK-2 cells to migrate through a Matrigel covered filters in modified Boyden chamber in already described treatments. Transwell migration assay followed the same pattern as wound-migration assay. After 24 hours of incubation, TGF-β1 augmented cell migration of HK-2 cells for 35% of control, which was inhibited by addition of NMDA down to 62% compared with the control (Figure 30 I, K).

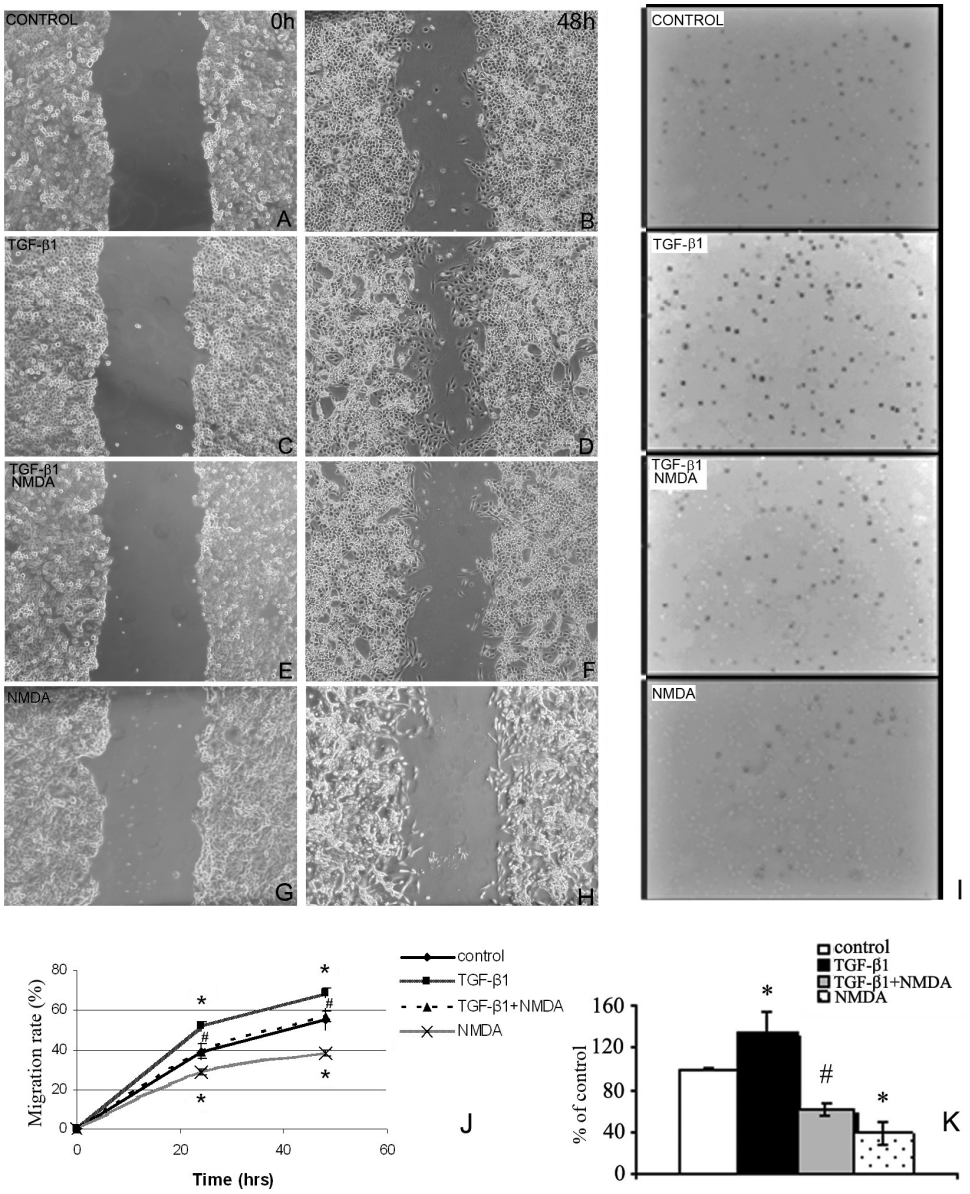

Figure 30. **NMDA inhibits TGF-β1-stimulated cell migration in wound-healing and transwell migration assay.** ***(A-H)*** *Wound-healing assay. Contrast phase micrographs of HK-2 cells migrating into the denuded area of the scratch wound at various times after monolayer wounding. One representative experiment is shown to illustrate the wound closure after 48 hours in control conditions (**B**), TGF-β1 (**D**), TGF-β1+NMDA (**F**) and NMDA (**H**) compared with the corresponding wounds at the point 0 hour for the control (**A**), TGF-β1 (**C**), TGF-β1+NMDA (**E**) and NMDA (**G**).*

*(**A**-**H**) Original magnification x4. (**I**) Transwell migration assay. Representative photos show parts of transwell inserts for control, TGF-β1, TGF-β1+NMDA and NMDA treated group of cells after 24 hours of incubation. Nuclei were stained with Hoechst. Original magnification x20. Quantification of cell migration in wound-healing assay after 24 and 48 hours (**J**) and transwell migration assay after 24 hours (**K**). Data are presented as means ± SEM (wound-healing assay) or percentage of control (means values ± SEM; transwell migration assay) of 3 independent experiments assayed in triplicate for each time point and condition. (**J**) *P<0.05 vs. control at both time points and #P<0.05 vs. TGF-β1 at both time points. (**K**) *P<0.05 vs. control; #P<0.05 vs. TGF-β1.*

As already mentioned in the Result section, NMDA did not significantly modify cell viability (Figure 17 B), indicating that the detected decrease in cell migration was not due to a reduced cell viability.

2.2. NMDA reduces TGF-β1-stimulated cell velocity and persistence on different matrices

Incubation of HK-2 cells with TGF-β1 for 24 hours caused an increase in cell directionality of cells grown on collagen I and fibronectin (Figure 31 A) compared with non-treated control. Co-incubation with NMDA reduced TGF-β1-induced increase in cell persistence on both tested matrices (Figure 31 A). In spite of detected statistical significance in migrational directionality among tested groups, average cell persistence in every tested cell population was still under 0.6 (as already shown for NMDA treatment in the *section I 3.2. of Results).*

In order to get more insights into the nature of TGF-β1-stimulated PTEC's migration, we further analyzed cell velocity in the settings of already described

conditions. TGF-β1 treatment induced high increase in cell velocity of HK-2 cells grown on collagen I and fibronectin after 24 hours (Figure 31 B) compared with control. Co-incubation with NMDA caused statistically significant reduction of TGF-β1-induced increase of cell velocity on both tested matrices (Figure 31 B).

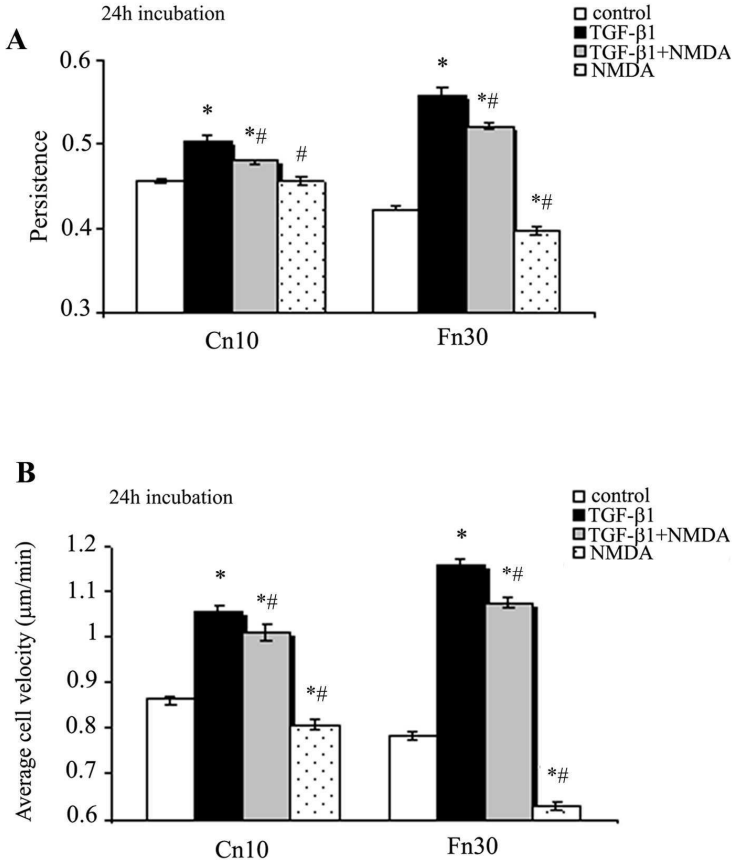

Figure 31. **NMDA reduced TGF-β1-stimulated cell velocity and persistence on different matrices.** *HK-2 cells were plated on Collagen I (Cn) or Fibronectin (Fn)-coated 48-well plates and incubated with different treatments as described in Methods. Cell's migratory behavior was recorded by time-lapse video microscopy during a 5 hours period (3 minutes frame interval) after 24 hours of treatment. Cell persistence and velocity were quantified using Matlab software. Persistence is defined as the ratio*

*of the vectorial distance traveled to the total path length described by the cell. Cell densities of all populations were equivalent (not shown). (**A**) Histograms represent the average persistence during 0-300 minutes period after 24 hours of treatment. Values are average cell persistence (averaging values from all time-points during 0-300 minutes) ± SEM. (**B**) Average cell velocities of cells (avg. values ± SEM) grown on Coll I and Fn followed over the 0-300 minutes period after 24 hours of treatment. (**A**, **B**) *P<0.05 vs. control; #P<0.05 vs.TGF-β1.*

3. NMDAR antagonizes TGF-β1's actions through inactivation of Ras and Ras signaling effectors Erk1/2 and Akt

It has been demonstrated that the activation of Ras signaling effectors Erk1/2 and Akt represent important signaling events responsible for TGF-β1-induced EMT in different epithelial cell types[67,69,82]. Furthermore, it has been shown that Akt activation caused EMT characterized by downregulation of E-cadherin, upregulation of vimentin, reduced cell-cell adhesion and increased cell motility on fibronectin-coated surfaces[82]. Therefore, we set out to investigate the mechanism that stands behind the effect of NMDA on tubular epithelial-mesenchymal transition.

3.1. NMDAR activation reduces phosphorylation of Erk1/2 and Akt and blocks activation of Ras induced by TGF-β1

Treatment of HK-2 with TGF-β1 resulted in a rapid increase in phosphorylation of Akt (Figure 32 A, B) and Erk1/2 (Figure 32 C, D) within 60 and 30 minutes after stimulation, respectively. Co-treatment with NMDA reduced phosphorylation of investigated molecules induced by TGF-β1 (Figure 32).

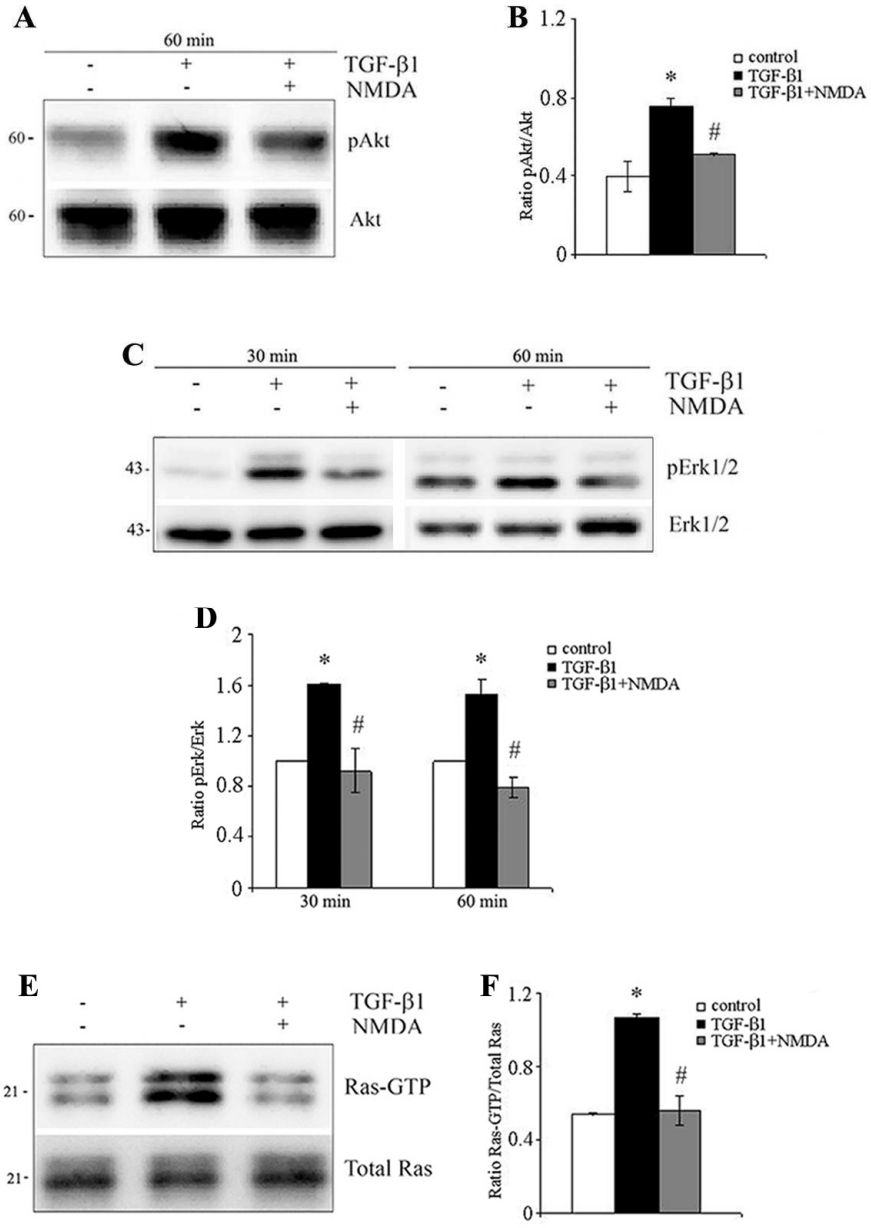

Figure 32. **NMDAR activation reduces phosphorylation of Erk and Akt as well as activation of Ras induced by TGF-β1 treatment.** *HK-2 cells were incubated in serum free medium (control), TGF-β1 or TGF-β1+NMDA for 30 and 60 minutes (pErk, pAkt) and 10 minutes (Ras-GTP). Representative Western blots (**A**, **C**, **E**) and quantitative analysis (**B**, **D**, **F**) show alterations in protein expression induced by*

*TGF-β1 in HK-2 cells. NMDA treatment reduced phosphorylation of Akt (**A**, **B**) and Erk (**C**, **D**) induced by TGF-β1 in HK-2 cells. After incubation with different treatments, whole cell lysates were immunoblotted with either phospho-Akt or total-Akt and phospho-Erk or total-Erk. (**E**, **F**) NMDA reduced TGF-β1-induced activation of Ras. Total cell extracts were prepared and incubated with GST-RBD to measure the amount of Ras-GTP (upper panel). Aliquots of total cell lysates (10 μg) were run in parallel for detection of total Ras protein (lower panel). (**B**, **D**, **F**) *P<0.05 vs. control, #P<0.05 vs. TGF-β1.*

As shown in Figure 32 E, F, TGF-β1 caused rapid activation of Ras within 10 minutes after stimulation, while co-treatment with NMDA managed to reduce Ras-GTP down to control levels. Therefore, NMDAR activation blocks important key steps of EMT in proximal tubular cells by blocking TGF-β1-induced activation of Ras suggesting that the mechanism that stands behind the effect of NMDA on tubular EMT is related to the regulation of the activation of the Ras pathway.

3.2. Calcium influx through NMDAR is responsible for the attenuation of TGF-β1-induced phosphorylation of Erk1/2 and Akt as well as activation of Ras

3.2.1. Thapsigargin does not reduce phosphorylation of Erk1/2 nor prevents activation of Ras induced by TGF-β1

In order to demonstrate that the effect of NMDAR activation on expression levels of pErk1/2 and Ras-GTP is a direct consequence of an influx of Ca^{2+} ions exclusively through NMDA channel, we set out to investigate the levels of phosphorylation of these molecules in the settings of thapsigargin (TG) treatment. HK-

2 cells treated with TGF-β1 and TGF-β1+TG for the indicated periods of time showed high levels of both phosphorylated Erk1/2 (Figure 33 A, B) and activated Ras (Figure 33 C, D).

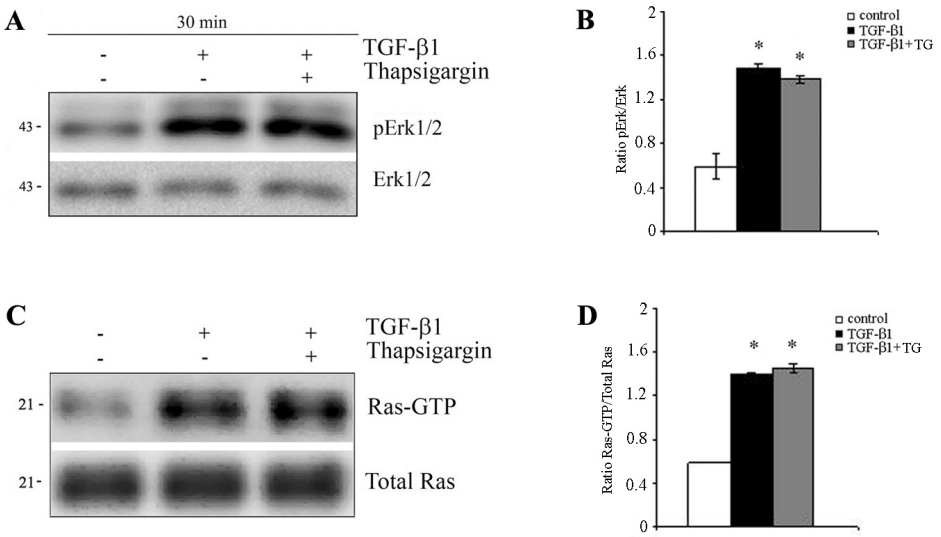

Figure 33. **Thapsigargin does not reduce phosphorylation of Erk1/2 nor prevents activation of Ras induced by TGF-β1.** *HK-2 cells were incubated in serum-free medium (control), TGF-β1 or TGF-β1+Thapsigargin for 30 min (pErk) and 10 min (Ras-GTP). (**A**) After incubation with different treatments, whole cell lysates were immunoblotted with phospho-Erk or total-Erk. Representative Western blot (**A**) and quantitative analysis (**B**) demonstrate that the co-incubation of HK-2 with TGF-β1 and TG did not induce a decrease in phosporylation of Erk1/2 (**A**, **B**) as NMDA treatment did. (**C**) Total cell extracts were prepared and incubated with GST-RBD to measure the amount of Ras-GTP (upper panel). Aliquots of total cell lysates (10 μg) were run in parallel for detection of total Ras protein (lower panel). Co-incubation of TG and TGF-β1 did not induce deactivation of Ras. (**B, D**) *P<0.05 vs. control.*

Results indicate that Ca^{2+} released from intracellular stores had no effect on dephosphorylation of pErk1/2 and failed to result in deactivation of Ras-GTP, pointing

to a specific effects of Ca^{2+} entry through NMDA receptor as the responsible for NMDA effect.

3.2.2. NMDAR activation failed to reduce phosphorylation of Erk1/2 and Akt induced by TGF-β1 in the absence of calcium in the culture medium

In order to confirm that the inhibition of the phosphorylation of Ras signaling effectors Erk1/2 and Akt, caused by the NMDAR activation, could be attributed to the influx of calcium ions through NMDA receptor, we performed experiments in Ca^{2+}-free culture medium. Treatment of HK-2 cells with TGF-β1 for 30 minutes induced strong increase in the phosphorylation of Erk1/2 and Akt (Figure 34 A, B).

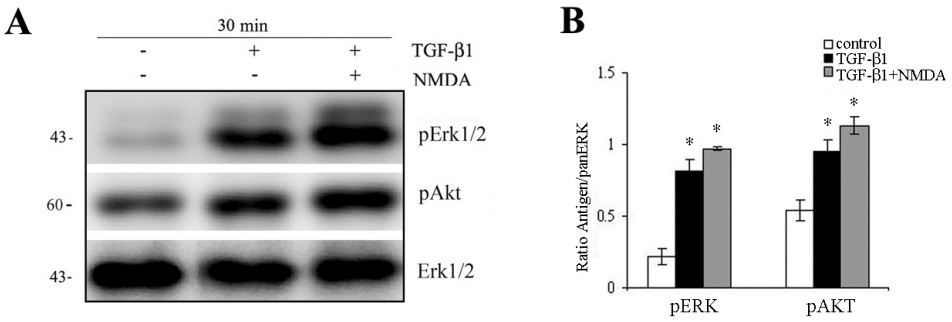

Figure 34. **NMDAR activation failed to reduce TGF-β1-induced phosphorylation of Erk1/2 and Akt in the absence of calcium in the medium.** *HK-2 cells were incubated in serum free medium (control), TGF-β1 or TGF-β1+NMDA (in serum free EpiLife (Ca2+ free) medium) for 30 minutes. Representative Western blots (**A**) and quantitative analysis (**B**) demonstrate phosphorylation of Erk and Akt induced by TGF-β1. Co-treatment with NMDA in Ca^{2+}-free medium shows no benefits in reversing the expression of investigated molecules. (**B**) *P<0.05 vs. control.*

On the other hand, simultaneous incubation of HK-2 cells with TGF-β1 and NMDA in the calcium free culture medium for the indicated period of time failed to reduce phosphorylation of these Ras signaling effectors (Figure 34 A, B). Results obtained point again to a specific role of Ca^{2+} entry through the activated NMDAR as the responsible for NMDA effect.

4. TGF-β1 treatment does not alter the expression pattern of NR1 and NR2B subunits in HK-2 cells

It has already been reported that different growth factors could alter expression of NMDAR subunits in neuronal cells thus modulating their activity and function[255-258]. Therefore, we wished to investigate the expression levels of NMDAR1 and NMDAR2B subunits in HK-2 cells during/after the treatment with TGF-β1.

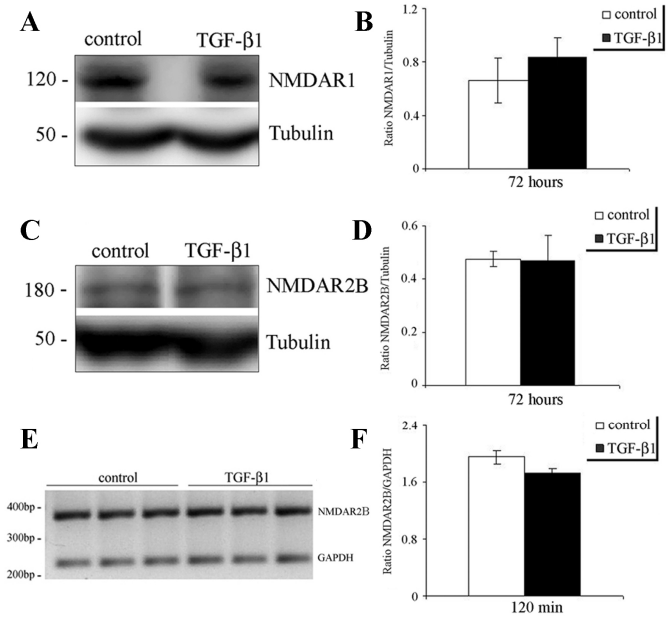

Figure 35. **TGF-β1 treatment does not alter the expression pattern of NR1 and NR2B subunits in HK-2 cells.** *HK-2 cells were incubated with or without TGF-β1 for 72 hours (**A**, **C**) or 120 minutes (**E**). Representative Western blots demonstrate the expression of NMDAR1 protein (120 kDa) (**A**) and NMDAR2B protein (180 kDa) (**C**) in HK-2 cells. The same samples were reprobed with tubulin to ensure equal loading. (**B**, **D**) Quantitative densitometric analysis shows no differences in expression levels of investigated receptor subunits. (**E**) Total RNA was submitted to RT with an oligo dT reverse primer followed by PCR with different set of primers for NMDAR1 subunit and GAPDH as an internal control. Representative image after agarose gel electrophoresis shows expression of investigated NR1 subunit (NMDA R1~370 bp). (**F**) Quantitative densitometric analysis shows no difference in expression of NMDAR2B subunit after 120 minutes of treatment with TGF-β1.*

SQ PCR analysis shows no changes in expression of mRNA encoding NR2B subunit in HK-2 cells 120 minutes after TGF-β1 treatment (Figure 35 E, F). Western blot (Figure 35 A, C) and quantitative densitometric analysis (Figure 35 B, D) show no significant changes in expression levels of NR1 and NR2B subunits after 72 hours of treatment with TGF-β1.

Objective 3

III. NMDAR activation preserves epithelial phenotype and attenuates renal fibrosis *in vivo*

1. Expression of NMDA receptor subunits in mouse kidney cortex

To study the expression of NMDA receptor subunit genes in the mouse kidney, we performed a PCR analysis of mRNA purified from the mouse renal cortex by using specific PCR primer pairs detected against mouse NR1 and NR2 (A-D) subunits (*Section 3 in Mat & Meth*). The results demonstrate the presence of NMDA R1, R2B, R2C and R2D in the mouse kidney cortex (Figure 36).

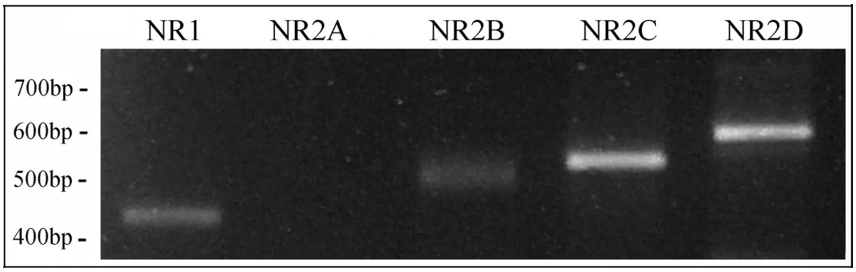

Figure 36. **Expression of NMDA receptor subunits in mouse kidney cortex.** *Total RNA from mouse renal cortex was submitted to RT with an oligo dT reverse primer followed by PCR with different set of primers for either NR1 or NR2 (A-D) subunits. Representative image after agarose gel electrophoresis shows presence of NMDA R1 (471 bp), R2B (532 bp), R2C (541 bp) and R2D (595 bp) subunits in the mouse kidney.*

The expression pattern of NMDAR subunits in mouse kidney cortex is similar to one detected in human proximal tubular epithelial cell line (HK-2).

2. Activation of NMDAR in the mouse kidney affected by fibrosis preserves epithelial phenotype and attenuates renal fibrosis

2.1. NMDA administration inhibits α-SMA and Collagen I expression in the obstructed mouse kidney

In order to study if the effects of NMDA administration *in vitr*o could have a role in an *in vivo* model of renal fibrosis, mice underwent unilateral ureteral obstruction (UUO) and were treated with NMDA. We first examined mRNA expression of mesenchymal marker α-SMA and the major interstitial matrix component, type I collagen in different groups of mice by real time PCR technique. UUO induced marked upregulation of α-SMA and type I collagen at 5 and 15 day after surgery compared with contralateral controls (Figure 37 A, B). Administration of NMDA significantly decreased α-SMA mRNA expression in obstructed mouse kidneys at both time points (Figure 37 A, B). Additionally, NMDA treatment showed a tendency to reduce Collagen I mRNA 5 days after UUO (Figure 37 A), while at day 15 post-UUO, NMDA managed to significantly diminish expression of Collagen I in obstructed kidneys (Figure 37 B), compared with contralateral controls. We further evaluated expression of α-SMA at the protein level in different groups of mice by Western blot analysis. As shown in Figure 37 D, E, F, significant increase of α-SMA protein levels was found in the obstructed kidneys at days 5 and 15 post-UUO, compared with contralateral controls. In accordance with the mRNA data, NMDA treatment significantly inhibited α-SMA at the protein level. Similar results were obtained by immunohistochemistry of kidney sections from paraffin-embedded tissue using antibodies against α-SMA (Figure 37 B).

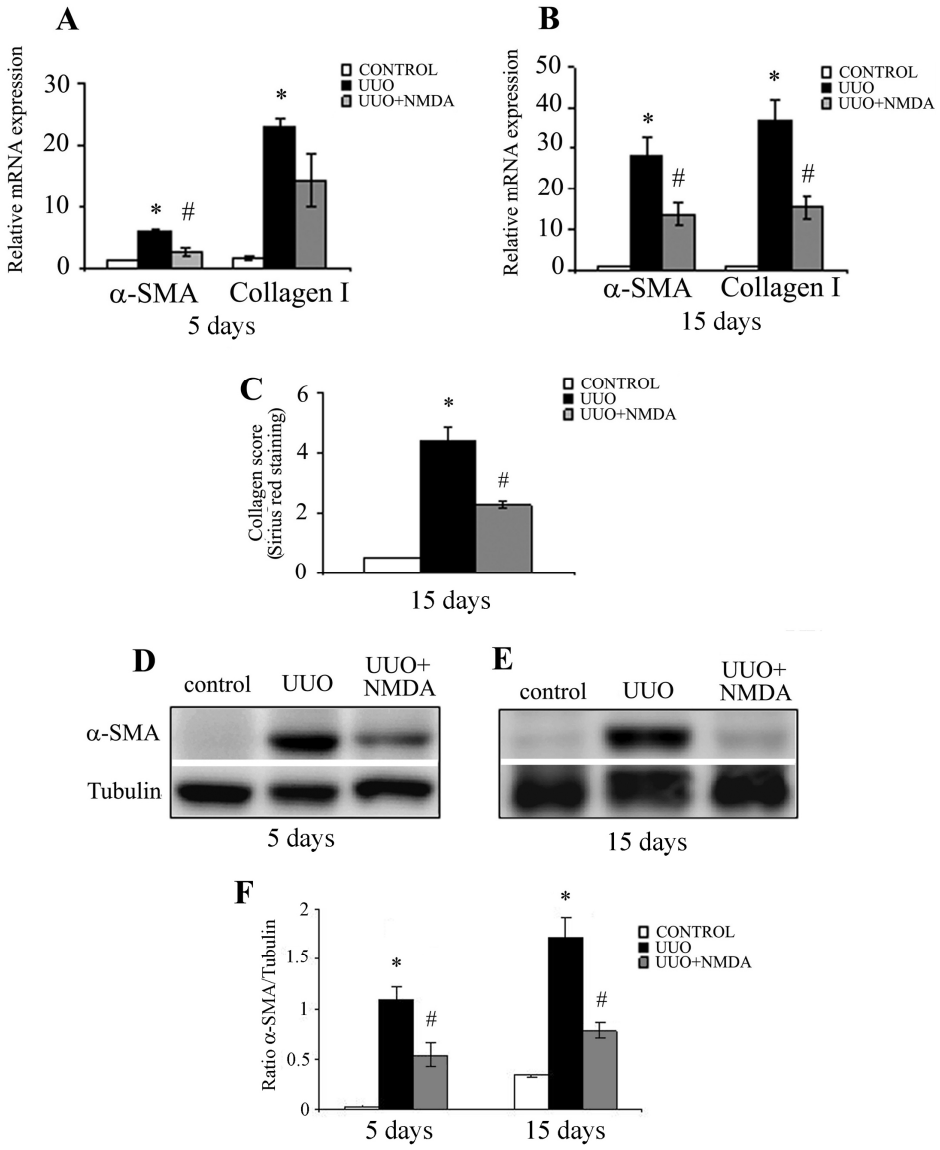

Figure 37. **NMDA treatment reduced α-SMA and collagen I expression in the obstructed mouse kidney.** ***(A, B)*** *Real time PCR analysis demonstrates downregulation of α-SMA and collagen I mRNA expression in obstructed mouse kidney after NMDA treatment at different time points (5 and 15 days). Relative mRNA levels were calculated and expressed as fold induction over contralateral controls (value = 1.0) after normalizing with GAPDH. *P<0.05 vs. control; #P<0.05 vs. UUO.* ***(C)*** *Quantification of collagen content after Sirius Red staining. Data are means ±*

*SEM of seven animals per group (n=7) *P<0.05 vs. control; #P<0.05 vs. UUO. (**D**, **E**) Western blot demonstrates increased expression of α-SMA in the obstructed kidneys at 5 and 15 days after UUO and inhibition of α-SMA in UUO+NMDA group of mice. Whole kidney lysates were processed for protein analysis at day 5 (**D**, **F**) and 15 (**E**, **F**) after UUO and were immunoblotted with antibodies against α-SMA and tubulin, respectively. (**F**) *P<0.05 vs. control; #P<0.05 vs. UUO.*

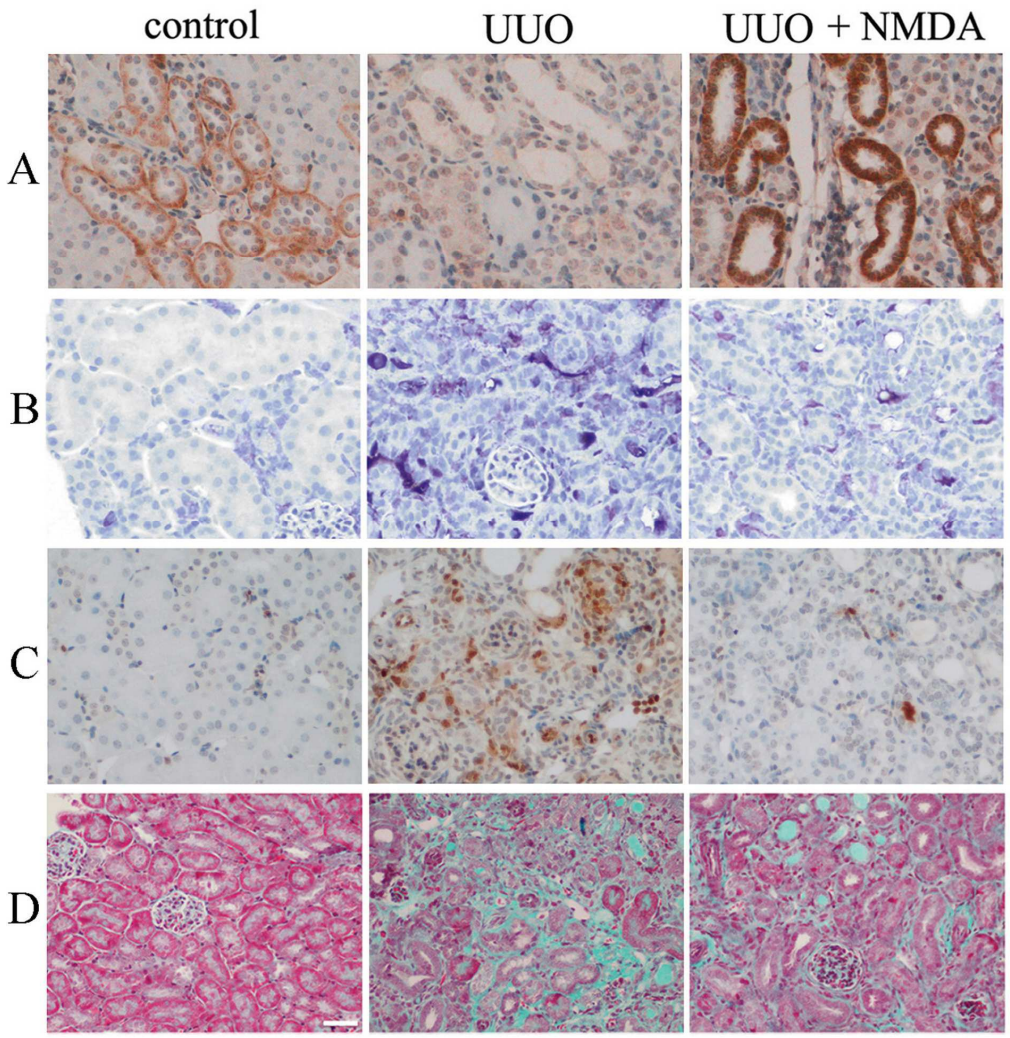

Figure 38. **NMDA administration attenuates renal fibrosis induced by UUO.** *Administration of NMDA reduced the loss of E-cadherin (**A**) and decreased α-SMA (**B**), FSP1 (**C**) and collagen I (**D**) expression in the obstructed mouse kidney 15 days*

*after UUO. Paraffin-embedded tissue sections were stained with antibodies against E-cadherin (**A**), α-SMA (**B**), FSP1 (**C**) and with Masson-Trichrome staining (**D**). Representative photomicrographs of kidney sections from 3 investigated groups of mice are presented. (**A**, **B**, **C**) Original magnification x20, (**D**) Scale bar, 20µm.*

These results indicate that administration of NMDA significantly reduced α-SMA expression in obstructed mouse kidney at day 15 after surgery. We further proceeded in measuring the interstitial collagen deposition by Sirius red staining. All kidneys at day 15 after UUO showed significant increase in interstitial collagen deposition compared with contralateral intact kidneys (Figure 37 C). An increasing accumulation of interstitial collagen in obstructed mouse kidneys at day 15 after UUO was also evident after Masson-Trichrome staining (Figure 38 D). In contrast, NMDA-treated mice showed significant decrease in interstitial collagen fibers in obstructed kidneys by 52% down when compared with UUO kidneys, as measured by Sirius red (Figure 37 C). Masson-Trichrome staining confirmed decreasing amount of collagen fibers in 15-days obstructed kidneys of mice treated with NMDA (Figure 38 D).

2.2. NMDA administration restores E-cadherin and attenuates FSP1 expression in obstructed mouse kidney

To investigate the potential role of NMDAR activation in preservation of tubular epithelial phenotype in a mouse model of TIF induced by UUO, we assessed the expression of epithelial cell marker E-cadherin by immunohistochemistry. Of interest, immunohistochemical staining revealed an evident decrease of E-cadherin in atrophic tubules (Figure 38 A and Figure 39) and an increase in immunostaining for FSP1 (Figure 38 C) in the obstructed kidneys at day 15 post-UUO. Administration of

NMDA managed to inhibit the reduction of E-cadherin (Figure 38 A and Figure 39) and an increase in FSP1 immunostaining induced by UUO, preserving the epithelial phenotype (Figure 38 C).

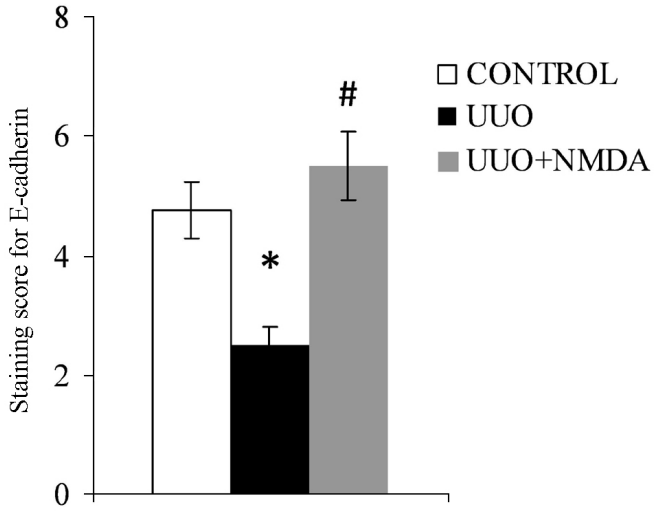

Figure 39. **Semiquantitative analysis of immunohistochemical staining for E-cadherin**. *Kidney sections from various groups of mice were stained and evaluated as described in Material & Methods. Data are presented as mean ± SEM from 7 animals per group (n = 7). *P<0.01 vs. control; #P<0.01 vs. UUO.*

Immunofluorescence staining also demonstrated that NMDA administration reversed an alteration of the expression of E-cadherin and FSP1 in proximal tubules of UUO+NMDA group of mice (Figure 40). The increase in the number of dual-stained E-cadherin and FSP1-positive tubular cells in UUO group of mice was ameliorated by NMDA treatment in UUO+NMDA group of animals (Figure 40).

These results provide evidence that NMDA administration may attenuate renal fibrosis induced by UUO by preserving the epithelial phenotype, as shown by the inhibition of the reduction of E-cadherin induced by UUO. Furthermore, in the

obstructed kidneys of NMDA-treated mice, markers of mesenchymal phenotype (FSP1 and α-SMA) were reduced, together with the collagen deposition, pointing to NMDAR as a possible therapeutic target to slow down the progression of renal fibrosis.

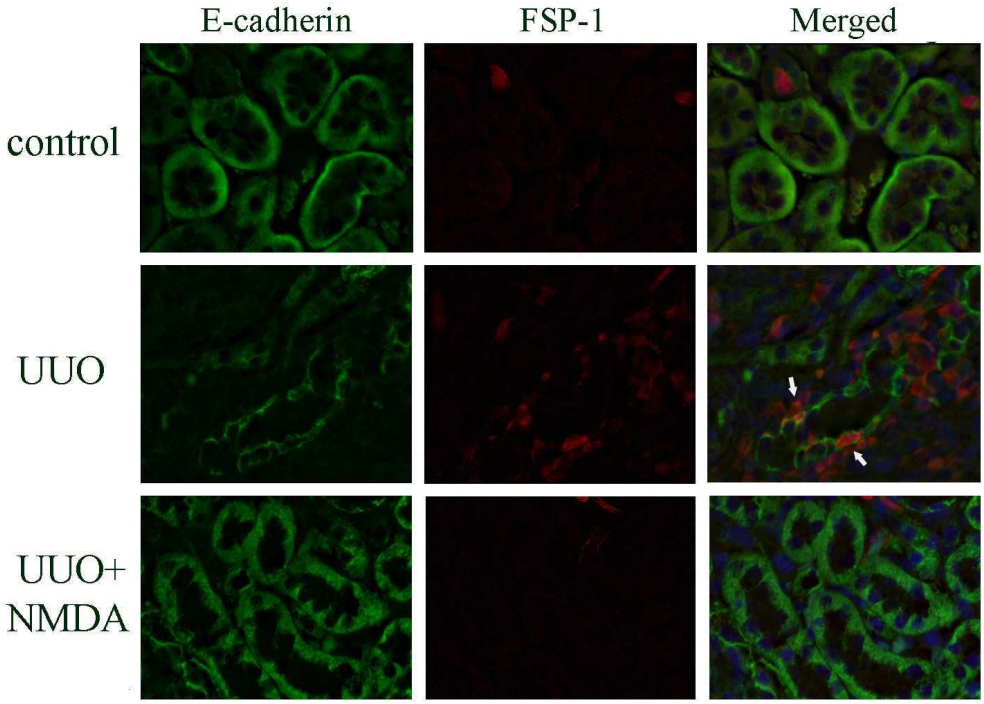

Figure 40. **Effect of NMDA administration on E-cadherin and FSP1 immunostaining in the obstructed mouse kidney.** *Immunofluorescence microscopy of kidney sections stained for E-cadherin (green) and FSP1 (red) with nuclear counterstain (blue, Hoechst) demonstrates an increase in dual-stained E-cadherin and FSP1-positive proximal tubular cells (arrow) in UUO group of mice with a decrease in E-cadherin and an increase in FSP1 expression. UUO+NMDA group of mice showed a decrease of double stained tubular cells. Original magnification x40.*

2.3. NMDA does not have direct effect on interstitial fibroblasts

To test whether NMDA administration has no direct effects on interstitial fibroblasts, we performed immunohistochemical staining of kidney sections for fibroblast specific protein, FSP1. Figure 41 A, B shows representative photomicrographs of paraffin embedded sections from non-obstructed kidneys of mice treated with vehicle or NMDA for 15 days. As shown by semiquantitative analysis of immunohistochemical staining, NMDA administration did not have significant effect on the expression of FSP1 by interstitial fibroblasts (Figure 41 C).

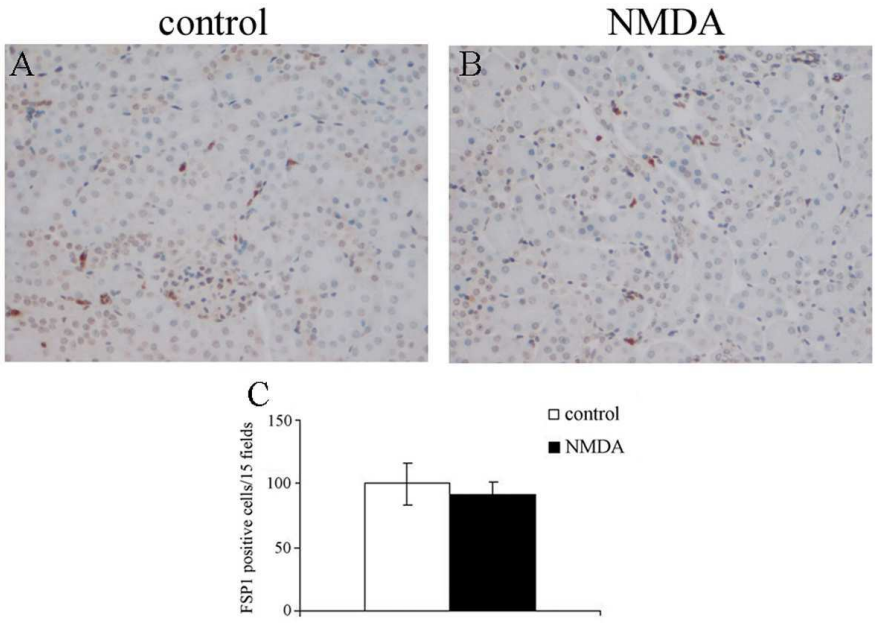

Figure 41. **Effect of NMDA treatment on interstitial fibroblasts.** (**A, B**) *Representative photomicrographs of right non-obstructed mouse kidneys. Kidney sections were stained with FSP1 to detect interstitial fibroblasts in vehicle-treated mice (**A**) and NMDA-treated mice (**B**) at day 15 after NMDA administration. Magnification x20. (**C**) Semiquantitative analysis of immunohistochemical staining for*

FSP1 positive interstitial fibroblasts. Fifteen fields were analyzed. Data are mean ± SEM. NMDA administration did not have significant effect on interstitial fibroblasts stained with FSP1 compared with the control kidneys.

Results gained confirm that the effect of NMDA administration toward the attenuation of fibrosis in the obstructed mouse kidney was due to the inhibition of tubular EMT and not the inhibition of residual fibroblasts activated in the kidney after unilateral ureteral obstruction.

Discussion

The human renal tubule is a complex epithelial system with high metabolic activity that plays a critical role in the maintenance of kidney homeostasis[259]. Injury of the renal tubule, therefore the alteration of the epithelial integrity, is the most common cause of acute dysfunction of the kidneys. Whereas the normal response to renal injury is migration and proliferation of renal proximal tubular cells to reestablish an intact epithelial lining, the persistent and repetitive injury could culminate in progressive tubular fibrosis which can lead to the scarring of the kidney and disruption of renal function. As a major players in renal fibrosis have been considered not only resident fibroblasts, but also epithelial cells of the proximal tubule through a process known as epithelial-mesenchymal transition[25]. EMT represents a dynamic course of events and has been described as one of the key mechanisms in the pathogenesis of renal fibrosis[32] where fibroblast activation represents an important pathway for the progression of chronic kidney disease[33]. Destabilization of the integrity of renal epithelium followed by the loss of cell-cell adhesive properties, changes in cell morphology and actin distribution, as well as acquisition of migratory mesenchymal phenotype represents the main set of events associated with EMT[5].

Proximal tubular cells form a polarized epithelial monolayer whose integrity is maintained by the physical interactions of neighboring cells through intercellular junctional complexes[250]. Formation and maintenance of intercellular contacts is a vital prerequisite for the structural coherence of renal epithelium where an important role is attributed to intracellular calcium[260,261]. It has been reported that the intracellular calcium and its signaling has an important role in the regulation of cell migration[174,223-225], actin cytoskeleton dynamic[226,227] and organization of cadherins and catenins into intercellular junctions[228].

The N-methyl-D-aspartate receptor (NMDAR) is a member of a heterogeneous family of ionotropic glutamate receptors widely investigated in the central nervous system[118], where it plays an important role in synaptic plasticity during development[154,215], learning and memory[138,154]. NMDAR is a heteromeric protein complex composed of an essential NR1 subunit combined with one or more NR2 subunits[144] which form a channel highly permeable to Ca^{2+}. Activation of NMDAR requires simultaneous binding of glutamate and glycine, leading to the channel opening and Ca^{2+} influx. NMDA, a non-metabolic agonist of NMDAR, mimics the action of glutamate, thus regulating only this receptor. Activation of the NMDAR followed by an influx of calcium ions could elicit a range of Ca^{2+}-mediated intracellular events through which this channel performs its important physiological roles[193] in processes such as neuronal differentiation and migration, synaptogenesis, structural remodelling, synaptic plasticity and higher cognitive functions[262]. Appart of being widely distributed in the brain, functional NMDAR is also expressed in a variety of non-neuronal cells and tissues such as human keratinocytes[173,174], lymphocytes[175], bone cells[176,177], rat heart, lung, thymus, stomach[151], parathyroid gland[178] and the kidney[151,179]. Presence of NMDAR and its potential significance in the kidney has become an interesting research topic recently. The NR1 subunit of the NMDAR has been reported to be present in the proximal tubules of the rat kidney[179] where it perfomes an important role in the maintenance of normal renal function by stimulating proximal tubular reabsorption and glomerular filtration[183]. Previous study of our research group showed that activation of the NMDAR in human proximal tubular cells induced an increase of intracellular Ca^{2+}, showing that the NMDAR in proximal tubular cells (HK-2) is fully functional and its activation induces a fast and transient

increase in intracellular Ca^{2+}[263]. Presence of the NMDAR has also been demonstrated in podocytes, visceral epithelial cells of the kidney glomerulus, where it could have a role in the maintenance of the integrity of glomerular filtration barrier[185]. Furthermore, it has been recently suggested by Anderson et al.[184] that basal activation of NMDAR could be an important prerequisite for normal podocyte and kidney function. It has been also reported that physiological levels of synaptic NMDAR activity are very important for the survival of many types of neurons[216], while the sustained activation of the NMDA receptor can provoke cell death in many neuropathological conditions[218]. The basal activation of NMDAR in human proximal tubular epithelial cells is indispensable in the maintenance of the normal tubular epithelial phenotype. On the one hand, knockdown of NMDAR1 expression in HK-2 cells using shRNA, induced changes in epithelial phenotype, evident as a decrease of E-cadherin and increase of α-SMA, alongside with the changes in cell morphology toward mesenchymal phenotype. On the other hand, activation of the channel in normal HK-2 cells led to a decrease in basal cell motility and F-actin content, two key steps in EMT which are modulated by Ca^{2+} levels[224-226]. Taken together, these results point to an indispensable role of basal NMDA receptor activity in the preservation of the epithelial phenotype of human proximal tubular epithelial cells.

Tightness of adherens junctions, and thus stability of the epithelial phenotype, relies on cadherin-catenin complexes linked to the actin cytoskeleton. These complexes are disrupted in EMT caused by TGF-β1, a potent inducer of fibrosis[5,264]. Number of factors has been stated as potential inducers of tubular EMT in different experimental models[37,38,48], among which transforming growth factor-β1 (TGF-β1) is

able to initiate and complete the whole process of EMT[45]. In our model, after addition of TGF-β1, proximal tubular epithelial cells started disassociating from neighboring cells, acquired spindle-shaped morphology which was accompanied by the reorganization of the actin cytoskeleton and elevated cell migration and migrational velocity. Furthermore, cells lost epithelial marker E-cadherin, had translocated β-catenin from the cell periphery into the nucleus and acquired myofibroblast markers such as α-SMA and vimentin. Treatment with NMDA blunted all changes induced by TGF-β1, demonstrating that the activation of NMDAR was able to preserve the epithelial phenotype in cells undergoing EMT, as evidenced by the restoration of E-cadherin, inhibition of α-SMA and vimentin, as well as attenuation of TGF-β1-induced cell migration and F-actin reorganization. It has already been reported that in normal kidney epithelial cells TGF-β1 induces β-catenin dissociation from cell-cell contacts and its translocation to the nucleus[5,264]. During human epithelial cell migration, accumulation of a cytoplasmic β-catenin[265,266] is implicated in activation of important genes involved in EMT[5], such as vimentin[267] and α-smooth muscle actin[264]. Therefore, preservation of E-cadherin and restoration of β-catenin to its localization on cell periphery by NMDA treatment could be an important step in the attenuation of tubular EMT, *in vitro*.

Acquisition of migratory phenotype and reorganization of actin cytoskeleton are prerequisites for effective migration of transformed cells through the basement membrane toward the interstitium and they are considered to be common for both tubular repair process and epithelial-mesenchymal transition. Being aware of the existence of biochemical and functional interactions between NMDAR subunits and

cytoskeletal proteins[216,268], as well as the fact that NMDAR plays a vital role in modulation of migratory behavior of different cell types[174,223,269,270], we sought to examine the influence of NMDAR activation on migration and F-actin distribution in HK-2 cells. In this work, it was demonstrated by two independent *in vitro* migration assays that the activation of NMDAR has an inhibitory effect on cell migration. In wound migration assay, NMDA treatment (0.5 mM) reduced basal as well as TGF-β1-stimulated cell migration after 24 and 48 hours of incubation. Transwell migration assay followed the same pattern with NMDA reducing basal cell migration as well as TGF-β1-stimulated motility after 24 hours. In order to confirm that the decrease in migration was not due to the reduced cell viability, MTT assay was performed showing that NMDA did not modify cell viability at any concentration used.

During migration cells use different migrational modes to move with varying degrees of speed and directionality[244]. Patterns of migratory behaviour are dictated by characteristics that are genuine to particular cell type and they could variate depending of the physiological or pathophysiological process in which cells are participating. During processes such as wound healing, certain types of cells migrate directionally and with high persistence (i.e., tendency to continue travelling in the same direction without turning)[244]. Knowing that the speed and directionality of cell migration are foundational regulators of cell motility, we wished to gain more mechanistic insight into cell migration by examining the effect of NMDA on cell velocity and persistence. Several migration assays were done on different matrices where cell velocity and persistence were measured using time-lapse phase contrast microscopy. After 24 hours, NMDA (0.5 mM) treatment reduced basal level of cell persistence on fibronectin coated plates, as well as TGF-β1-induced increase in cell persistence on

both tested matrices. Wishing to get more insights into the nature of PTEC's migration, the migrational velocity of HK-2 cells was further analyzed. Twenty four hours of treatment with NMDA caused statistically significant reduction of basal and TGF-β1-induced migrational velocity on collagen and fibronectin coated surfaces. Cell velocity data support the wound and transwell migration results and confirm the role of NMDAR in the regulation of human proximal tubular cell's migration *in vitro.*

In addition, activation of NMDAR (NMDA 0.5 mM, 24 h) significantly decreased basal actin polymerization state and TGF-β1-induced actin reorganization in HK-2 cells, as demonstrated by immunofluorescence and flow cytometry analysis. Changes in F-actin distribution in epithelial cells have been reported to be in close relation with the alterations in cell volume[252]. By measuring the size of the cells we wanted to exclude the possibility that the changes in F-actin distribution in NMDA treated group of cells were due to changes in cell volume. Results showed that NMDA treatment did not affect the size of HK-2 cells implicating that the detected decrease in cellular F-actin was a direct consequence of NMDA treatment and not an artefact.

Regulation of cell-extracellular matrix (ECM) interactions and cell–cell adhesions, as well as coordinative actomyosin cytoskeleton dynamic are all necessary prerequisites for effective cell migration[27,246,247]. Adhesion to extracellular matrix components, such as fibronectin and laminin, is generally mediated by the integrin family of heterodimeric receptors[248]. For that reason, cell adhesion assay was done to determine if the decline of *in vitro* cell migration as well as migrational velocity of HK-2 cells on different matrices could be due to differences in cell-ECM adhesion. Treatment of HK-2 cells with NMDA did not significantly changed cell adhesion to collagen I, fibronectin or matrigel, as well as to non-covered surfaces, suggesting that

reduced migration and migrational velocity of cells treated with NMDA were not due to altered integrin-dependent adhesion[249-251].

The effect of NMDAR activation and Ca^{2+} on cell migration[174,223,269-271] and actin organization[213,229] has previously been reported in different cell types. The activity of the NMDAR has been shown to regulate the migration of granule cells in slice preparations of the developing mouse cerebellum[269]. Namba et al.[270] reported that the NMDAR-mediated signaling in brain is essential for the proper migration and that the blockade of the NMDAR induced an overextended migration of newborn neurons. Kihara et al.[223] reported that stimulation of NMDAR inhibited neuronal migration in embryonic rat cerebral cortex. Hahm et al.[174] demonstrated that in keratinocytes Ca^{2+} entry through activated NMDAR inhibited cell outgrowth and migration. Furthermore, Cristofanilli et al[229] showed that the NMDAR activation and influx of Ca^{2+} caused a reduction of F-actin in retinal neurons of salamander, while NMDAR activation in rat cerebellar granule cells rapidly shifted F/G-actin equilibrium in favor of depolymerization[213].

The role of NMDAR in preservation of tubular epithelial phenotype was further confirmed in *in vivo* studies, in a mouse model of TIF induced by unilateral ureteral obstruction. UUO is the most widely used and well-established model of renal interstitial fibrosis. UUO is induced by the ligation of a ureter of one kidney, while the contralateral kidney serves as a normal control. As early as 3 days after surgery, it is possible to detect interstitial fibrosis with all characteristic signs. Consistent with the *in vitro* results, significant changes in cell phenotype were seen in renal tubules in the obstructed kidneys such as downregulation of E-cadherin, increase in α-SMA expression and FSP1 immunostaining, and interstitial collagen deposition. These

results provide evidence that NMDA treatment may attenuate renal fibrosis induced by UUO by preserving the epithelial phenotype, as shown by the inhibition of the decrease in E-cadherin induced by UUO. Furthermore, in obstructed kidneys of NMDA-treated mice, markers of mesenchymal phenotype (FSP1 and α-SMA) were reduced, together with the collagen deposition, pointing to NMDAR as a possible therapeutic target to slow down the progression of renal fibrosis. In order to assess whether NMDA administration has no direct effects on interstitial fibroblasts, paraffin embedded sections from non-obstructed kidneys of mice treated with vehicle or NMDA for 15 days were stained with FSP-1. Our results showed that NMDA treatment did not induce statistically significant changes in expression of FSP-1 in two investigated groups of mice. Results gained here provide evidence that the effect of NMDA administration toward the attenuation of fibrosis in the obstructed kidneys was due to the inhibition of tubular EMT and not the inhibition of residual fibroblast population activated in the kidney after UUO.

The mechanism behind the effect of NMDA on tubular EMT seems to be related with the regulation of the activation of Ras pathway. Ras is one of the most common pathways leading to the activation of Erk and Akt, which represent important signaling events responsible for TGF-β1-induced EMT in different epithelial cell types[67,69,82]. A growing body of evidence describes the role of TGF-β1 in activation of Ras pathway[83-85]. Furthermore, it has been shown that Akt activation caused EMT characterized by downregulation of E-cadherin, upregulation of vimentin, reduced cell-cell adhesion and increased cell motility on fibronectin-coated surfaces[82]. Therefore, we set out to investigate the mechanism that stands behind the effect of NMDA on tubular epithelial-mesenchymal transition. In our own hands, TGF-β1

treatment induced rapid activation of Ras in HK-2 cells within 10 minutes after stimulation, which was blunted by co-treatment with NMDA. Treatment of HK-2 with TGF-β1 resulted in a rapid increase in phosphorylation of Akt and Erk1/2 within 60 and 30 minutes after stimulation, respectively, while co-treatment with NMDA reduced phosphorylation of investigated molecules. Therefore, NMDAR activation blocks important key steps of EMT in proximal tubular cells by blocking TGF-β1-induced activation of Ras suggesting that the mechanism that stands behind the effect of NMDA on tubular EMT is related to the regulation of the activation of the Ras pathway.

This effect of NMDA inhibiting the Ras pathway has previously been reported. Chandler et al[117] described that different levels of Ca^{2+} influx through NMDAR could activate opposing stimulatory and inhibitory pathways that regulate Erk activation and suggested the presence of a Ca^{2+}-activated inhibitory pathway that can attenuate Ras/Erk signaling. Ivanov et al[272] and Sutton et al[273] showed that NMDAR-dependent activating/inactivating pathways are spatially separated in neurons and that extrasynaptic NMDARs, containing NR2B subunit, mediate Erk inactivation. Finally, Kim et al[274] demonstrated that NMDAR activation could have differential effects on Ras/Erk pathway in neurons depending of the receptor subunit composition showing that NR2B subunit is coupled to the inhibition rather than the activation of the Ras/Erk pathway[274]. Our results revealed that in HK-2, NR2B subunit was the main NR2 subunit expressed. Downregulation of Ras pathway by NMDA supports the subunit-regulatory hypothesis and suggests that Ca^{2+} influx through NR2B-NMDAR in HK-2 cells could be responsible for the inactivation of Ras and subsequently Erk and Akt pathways.

Being aware of the fact that different growth factors could alter expression pattern of NMDA receptor subunits, therefore modulating their activity and function[255-258], we assessed the expression of NR1 and NR2B subunits in the setting of TGF-β1 treatment. Results proved that TGF-β1 treatment did not have effect on the expression of neither, an essential NR1 subunit of the NMDAR nor NR2B subunit, the main NR2 subunit expressed in HK-2 cells.

It is well known that Snail1 acts as a key regulator of EMT by suppressing E-cadherin transcription and modulating tight junction protein expression[95,275,276] and it is crucial in initiation and progression of EMT[45,95]. Moreover, it has been demonstrated that Smad3 is necessary for TGF-β1-induced Snail1 gene expression in a study using Smad3-null mice[63]. Our results show upregulation of Snail1 and translocation of pSmad2/3 into the nucleus after treatment with TGF-β1, which was blunted by co-treatment with NMDA, providing one more proof of the inhibitory effect of NMDA on EMT of PTECs. Additionally, pharmacological blockade using an antagonist of NMDAR (MK-801) in cells treated with TGF-β1 and NMDA eliminated downregulation of Snail1 induced by NMDA, showing that the above described effects are NMDAR specific. These results could also be explained by the inhibition of Ras activation with NMDA. It has been shown that the inhibition of Erk phosphorylation decreases TGF-β1-induced Smad phosphorylation[71,277]. Furthermore, it has also been shown that Ras activation is necessary to increase Snail expression induced by TGF-β1[278]. Thus, a decrease in Ras activation could explain both, the decrease in the activation of the Erk pathway and the Smad pathway.

In order to demonstrate that the described changes are the consequence of Ca^{2+} influx exclusively through NMDAR, we used Thapsigargin which has been previously shown to rise intracellular Ca^{2+} concentrations in proximal tubular cells in culture[254]. Co-treatment with TG did not lead to the recovery of E-cadherin and α-SMA expression modified by TGF-β1. Moreover, d*e novo* expression of vimentin and changes in cell morphology induced by TGF-β1 in tubular cells were not attenuated after co-treatment with TG. Simultaneous incubation of HK-2 with TGF-β1 and TG did not prevent the activation of Ras and induced strong phosphorylation of Erk1/2, showing that Ca^{2+} derived from other sources did not have the same effect on preservation of epithelial phenotype as Ca^{2+} influx through NMDAR. In order to confirm that the influx of Ca^{2+} exclusively through the activated NMDAR is the one responsible for the preservation of the epithelial phenotype, we performed experiments in Ca^{2+}-free medium. In the absence of Ca^{2+} in the medium, NMDA treatment failed to ameliorate TGF-β1-induced downregulation of E-cadherin and the upregulation of Snail in HK-2 cells. Additionally, simultaneous incubation of HK-2 cells with TGF-β1 and NMDA in the calcium free medium failed to reduce phosphorylation of pErk1/2 and pAkt. These results point to a specific role of Ca^{2+} entry through the activated NMDAR in maintaining the epithelial phenotype of PTECs.

In conclusion, basal NMDAR activation is essential for the maintenance of the epithelial phenotype of PTECs. Furthermore, activation of tubular NMDAR attenuates EMT by blunting the TGF-β1-induced activation of Ras and the following cascades. The results obtained in this study identify a new therapeutic target for the inhibition of EMT and treatment of related diseases.

Conclusions

1. Downregulation of NMDAR1 subunit in HK-2 cells induces changes in the epithelial phenotype, evident as a decrease of E-cadherin and an increase of α-SMA expression, alongside with the changes in cell morphology.

2. NMDAR activation restores the expression of important markers of tubular epithelial-mesenchymal transition such as: E-cadherin, α-SMA, vimentin, β-catenin, Snail1 and pSmad2/3 altered by TGF-β1.

3. NMDAR activation inhibits TGF-β1-stimulated proximal tubular cell migration in wound-healing and transwell migration assay and preserves the cytoskeleton architecture and cell morphology altered by this cytokine.

4. Calcium influx through NMDAR is responsible for the preservation of epithelial phenotype of human proximal tubular epithelial cells.

5. NMDA receptor antagonizes TGF-β1's actions through inactivation of Ras and Ras signaling effectors Erk1/2 and Akt, suggesting that the mechanism that stands behind the effect of NMDA on tubular EMT is related to the regulation of the activation of the Ras pathway.

6. Calcium influx through NMDAR is responsible for the attenuation of TGF-β1-induced phosphorylation of Erk1/2 and Akt as well as the activation of Ras.

7. NMDA administration may attenuate renal fibrosis induced by UUO by preserving the epithelial phenotype, as shown by the inhibition of the reduction of E-cadherin induced by UUO.

8. NMDA administration downregulates the expression of markers of mesenchymal phenotype (FSP1 and α-SMA) and reduces collagen deposition in the obstructed mouse kidney, pointing to NMDAR as a possible therapeutic target to slow down the progression of renal fibrosis.

References

1. Vainio S, Lin Y: Coordinating early kidney development: lessons from gene targeting. *Nat Rev Genet* 3:533-543, 2002

2. Guyton AC, Hall JE: Textbook of Medical Physiology. Philadelphia: Elsevier Saunders, 2006, p pp.310

3. Yang J, Liu Y: Dissection of key events in tubular epithelial to myofibroblast transition and its implications in renal interstitial fibrosis. *Am J Pathol* 159:1465-1475, 2001

4. Wagner MC, Molitoris BA: Renal epithelial polarity in health and disease. *Pediatr Nephrol* 13:163-170, 1999

5. Tian YC, Phillips AO: Interaction between the transforming growth factor-beta type II receptor/Smad pathway and beta-catenin during transforming growth factor-beta1-mediated adherens junction disassembly. *Am J Pathol* 160:1619-1628, 2002

6. Patel SD, Chen CP, Bahna F, Honig B, Shapiro L: Cadherin-mediated cell-cell adhesion: sticking together as a family. *Curr Opin Struct Biol* 13:690-698, 2003

7. Pappas DJ, Rimm DL: Direct interaction of the C-terminal domain of alpha-catenin and F-actin is necessary for stabilized cell-cell adhesion. *Cell Commun Adhes* 13:151-170, 2006

8. Gailit J, Colflesh D, Rabiner I, Simone J, Goligorsky MS: Redistribution and dysfunction of integrins in cultured renal epithelial cells exposed to oxidative stress. *Am J Physiol* 264:F149-F157, 1993

9. Zuk A, Bonventre JV, Brown D, Matlin KS: Polarity, integrin, and extracellular matrix dynamics in the postischemic rat kidney. *Am J Physiol* 275:C711-C731, 1998

10. Radisky DC: Epithelial-mesenchymal transition. *J Cell Sci* 118:4325-4326, 2005

11. Hay ED: The mesenchymal cell, its role in the embryo, and the remarkable signaling mechanisms that create it. *Dev Dyn* 233:706-720, 2005

12. Zhang QL, Rothenbacher D: Prevalence of chronic kidney disease in population-based studies: systematic review. *BMC Public Health* 8:117, 2008

13. Burns WC, Kantharidis P, Thomas MC: The role of tubular epithelial-mesenchymal transition in progressive kidney disease. *Cells Tissues Organs* 185:222-231, 2007

14. James MT, Hemmelgarn BR, Tonelli M: Early recognition and prevention of chronic kidney disease. *Lancet* 375:1296-1309, 2010

15. Anderson J, Glynn LG: Definition of chronic kidney disease and measurement of kidney function in original research papers: a review of the literature. *Nephrol Dial Transplant* 0:1-6, 2011

16. Cho MH: Renal fibrosis. *Korean J Pediatr* 53:735-740, 2010

17. Liu Y: Renal fibrosis: new insights into the pathogenesis and therapeutics. *Kidney Int* 69:213-217, 2006

18. Campbell RC, Ruggenenti P, Remuzzi G: Halting the progression of chronic nephropathy. *J Am Soc Nephrol* 13 Suppl 3:S190-S195, 2002

19. Boor P, Ostendorf T, Floege J: Renal fibrosis: novel insights into mechanisms and therapeutic targets. *Nat Rev Nephrol* 6:643-656, 2010

20. Liu Y: New insights into epithelial-mesenchymal transition in kidney fibrosis. *J Am Soc Nephrol* 21:212-222, 2010

21. Kalluri R, Neilson EG: Epithelial-mesenchymal transition and its implications for fibrosis. *J Clin Invest* 112:1776-1784, 2003

22. Wynn TA: Cellular and molecular mechanisms of fibrosis. *J Pathol* 214:199-210, 2008

23. Waller JR, Nicholson ML: Molecular mechanisms of renal allograft fibrosis. *Br J Surg* 88:1429-1441, 2001

24. Grgic I, Duffield JS, Humphreys BD: The origin of interstitial myofibroblasts in chronic kidney disease. *Pediatr Nephrol* 2011

25. Iwano M, Plieth D, Danoff TM, Xue C, Okada H, Neilson EG: Evidence that fibroblasts derive from epithelium during tissue fibrosis. *J Clin Invest* 110:341-350, 2002

26. Wada T, Sakai N, Matsushima K, Kaneko S: Fibrocytes: a new insight into kidney fibrosis. *Kidney Int* 72:269-273, 2007

27. Thiery JP: Epithelial-mesenchymal transitions in tumour progression. *Nat Rev Cancer* 2:442-454, 2002

28. Zeisberg M, Duffield JS: Resolved: EMT produces fibroblasts in the kidney. *J Am Soc Nephrol* 21:1247-1253, 2010

29. Kalluri R: EMT: when epithelial cells decide to become mesenchymal-like cells. *J Clin Invest* 119:1417-1419, 2009

30. Kalluri R, Weinberg RA: The basics of epithelial-mesenchymal transition. *J Clin Invest* 119:1420-1428, 2009

31. Zeisberg M, Neilson EG: Biomarkers for epithelial-mesenchymal transitions. *J Clin Invest* 119:1429-1437, 2009

32. Zeisberg M, Kalluri R: The role of epithelial-to-mesenchymal transition in renal fibrosis. *J Mol Med* 82:175-181, 2004

33. Stahl PJ, Felsen D: Transforming growth factor-beta, basement membrane, and epithelial-mesenchymal transdifferentiation: implications for fibrosis in kidney disease. *Am J Pathol* 159:1187-1192, 2001

34. Zeisberg M, Maeshima Y, Mosterman B, Kalluri R: Renal fibrosis. Extracellular matrix microenvironment regulates migratory behavior of activated tubular epithelial cells. *Am J Pathol* 160:2001-2008, 2002

35. Savagner P, Yamada KM, Thiery JP: The zinc-finger protein slug causes desmosome dissociation, an initial and necessary step for growth factor-induced epithelial-mesenchymal transition. *J Cell Biol* 137:1403-1419, 1997

36. Docherty NG, O'Sullivan OE, Healy DA, Murphy M, O'neill AJ, Fitzpatrick JM, Watson RW: TGF-beta1-induced EMT can occur independently of its proapoptotic effects and is aided by EGF receptor activation. *Am J Physiol Renal Physiol* 290:F1202-F1212, 2006

37. Okada H, Danoff TM, Kalluri R, Neilson EG: Early role of Fsp1 in epithelial-mesenchymal transformation. *Am J Physiol* 273:F563-F574, 1997

38. Fan JM, Huang XR, Ng YY, Nikolic-Paterson DJ, Mu W, Atkins RC, Lan HY: Interleukin-1 induces tubular epithelial-myofibroblast transdifferentiation through a transforming growth factor-beta1-dependent mechanism in vitro. *Am J Kidney Dis* 37:820-831, 2001

39. Yang J, Liu Y: Blockage of tubular epithelial to myofibroblast transition by hepatocyte growth factor prevents renal interstitial fibrosis. *J Am Soc Nephrol* 13:96-107, 2002

40. Bascands JL, Schanstra JP: Obstructive nephropathy: insights from genetically engineered animals. *Kidney Int* 68:925-937, 2005

41. Song W, Majka SM, McGuire PG: Hepatocyte growth factor expression in the developing myocardium: evidence for a role in the regulation of the

mesenchymal cell phenotype and urokinase expression. *Dev Dyn* 214:92-100, 1999

42. Thery C, Sharpe MJ, Batley SJ, Stern CD, Gherardi E: Expression of HGF/SF, HGF1/MSP, and c-met suggests new functions during early chick development. *Dev Genet* 17:90-101, 1995

43. Mizuno S, Kurosawa T, Matsumoto K, Mizuno-Horikawa Y, Okamoto M, Nakamura T: Hepatocyte growth factor prevents renal fibrosis and dysfunction in a mouse model of chronic renal disease. *J Clin Invest* 101:1827-1834, 1998

44. Cheng S, Lovett DH: Gelatinase A (MMP-2) is necessary and sufficient for renal tubular cell epithelial-mesenchymal transformation. *Am J Pathol* 162:1937-1949, 2003

45. Liu Y: Epithelial to mesenchymal transition in renal fibrogenesis: pathologic significance, molecular mechanism, and therapeutic intervention. *J Am Soc Nephrol* 15:1-12, 2004

46. Fan JM, Ng YY, Hill PA, Nikolic-Paterson DJ, Mu W, Atkins RC, Lan HY: Transforming growth factor-beta regulates tubular epithelial-myofibroblast transdifferentiation in vitro. *Kidney Int* 56:1455-1467, 1999

47. Zeisberg M, Bonner G, Maeshima Y, Colorado P, Muller GA, Strutz F, Kalluri R: Renal fibrosis: collagen composition and assembly regulates epithelial-mesenchymal transdifferentiation. *Am J Pathol* 159:1313-1321, 2001

48. Lan HY: Tubular epithelial-myofibroblast transdifferentiation mechanisms in proximal tubule cells. *Curr Opin Nephrol Hypertens* 12:25-29, 2003

49. Zavadil J, Bottinger EP: TGF-beta and epithelial-to-mesenchymal transitions. *Oncogene* 24:5764-5774, 2005

50. Willis BC, Borok Z: TGF-beta-induced EMT: mechanisms and implications for fibrotic lung disease. *Am J Physiol Lung Cell Mol Physiol* 293:L525-L534, 2007

51. Massague J, Wotton D: Transcriptional control by the TGF-beta/Smad signaling system. *EMBO J* 19:1745-1754, 2000

52. Branton MH, Kopp JB: TGF-beta and fibrosis. *Microbes Infect* 1:1349-1365, 1999

53. Sutaria PM, Ohebshalom M, McCaffrey TA, Vaughan ED, Jr., Felsen D: Transforming growth factor-beta receptor types I and II are expressed in renal

tubules and are increased after chronic unilateral ureteral obstruction. *Life Sci* 62:1965-1972, 1998

54. Bottinger EP, Bitzer M: TGF-beta signaling in renal disease. *J Am Soc Nephrol* 13:2600-2610, 2002

55. Boor P, Floege J: Special Series: Chronic Kidney Disease Growth Factors in Renal Fibrosis. *Clin Exp Pharmacol Physiol* 2011

56. Massague J, Blain SW, Lo RS: TGFbeta signaling in growth control, cancer, and heritable disorders. *Cell* 103:295-309, 2000

57. Massague J, Chen YG: Controlling TGF-beta signaling. *Genes Dev* 14:627-644, 2000

58. Cheng J, Grande JP: Transforming growth factor-beta signal transduction and progressive renal disease. *Exp Biol Med (Maywood)* 227:943-956, 2002

59. Schnaper HW, Hayashida T, Hubchak SC, Poncelet AC: TGF-beta signal transduction and mesangial cell fibrogenesis. *Am J Physiol Renal Physiol* 284:F243-F252, 2003

60. Li Y, Yang J, Dai C, Wu C, Liu Y: Role for integrin-linked kinase in mediating tubular epithelial to mesenchymal transition and renal interstitial fibrogenesis. *J Clin Invest* 112:503-516, 2003

61. Li Y, Yang J, Luo JH, Dedhar S, Liu Y: Tubular epithelial cell dedifferentiation is driven by the helix-loop-helix transcriptional inhibitor Id1. *J Am Soc Nephrol* 18:449-460, 2007

62. Phanish MK, Wahab NA, Colville-Nash P, Hendry BM, Dockrell ME: The differential role of Smad2 and Smad3 in the regulation of pro-fibrotic TGFbeta1 responses in human proximal-tubule epithelial cells. *Biochem J* 393:601-607, 2006

63. Sato M, Muragaki Y, Saika S, Roberts AB, Ooshima A: Targeted disruption of TGF-beta1/Smad3 signaling protects against renal tubulointerstitial fibrosis induced by unilateral ureteral obstruction. *J Clin Invest* 112:1486-1494, 2003

64. Zavadil J, Cermak L, Soto-Nieves N, Bottinger EP: Integration of TGF-beta/Smad and Jagged1/Notch signalling in epithelial-to-mesenchymal transition. *EMBO J* 23:1155-1165, 2004

65. Massague J: How cells read TGF-beta signals. *Nat Rev Mol Cell Biol* 1:169-178, 2000

66. Derynck R, Zhang YE: Smad-dependent and Smad-independent pathways in TGF-beta family signalling. *Nature* 425:577-584, 2003

67. Xie L, Law BK, Chytil AM, Brown KA, Aakre ME, Moses HL: Activation of the Erk pathway is required for TGF-beta1-induced EMT in vitro. *Neoplasia* 6:603-610, 2004

68. Kattla JJ, Carew RM, Heljic M, Godson C, Brazil DP: Protein kinase B/Akt activity is involved in renal TGF-beta1-driven epithelial-mesenchymal transition in vitro and in vivo. *Am J Physiol Renal Physiol* 295:F215-F225, 2008

69. Bakin AV, Tomlinson AK, Bhowmick NA, Moses HL, Arteaga CL: Phosphatidylinositol 3-kinase function is required for transforming growth factor beta-mediated epithelial to mesenchymal transition and cell migration. *J Biol Chem* 275:36803-36810, 2000

70. Bhowmick NA, Ghiassi M, Bakin A, Aakre M, Lundquist CA, Engel ME, Arteaga CL, Moses HL: Transforming growth factor-beta1 mediates epithelial to mesenchymal transdifferentiation through a RhoA-dependent mechanism. *Mol Biol Cell* 12:27-36, 2001

71. Rhyu DY, Yang Y, Ha H, Lee GT, Song JS, Uh ST, Lee HB: Role of reactive oxygen species in TGF-beta1-induced mitogen-activated protein kinase activation and epithelial-mesenchymal transition in renal tubular epithelial cells. *J Am Soc Nephrol* 16:667-675, 2005

72. Roux PP, Blenis J: ERK and p38 MAPK-activated protein kinases: a family of protein kinases with diverse biological functions. *Microbiol Mol Biol Rev* 68:320-344, 2004

73. Zhang M, Fraser D, Phillips A: ERK, p38, and Smad signaling pathways differentially regulate transforming growth factor-beta1 autoinduction in proximal tubular epithelial cells. *Am J Pathol* 169:1282-1293, 2006

74. Masaki T, Stambe C, Hill PA, Dowling J, Atkins RC, Nikolic-Paterson DJ: Activation of the extracellular-signal regulated protein kinase pathway in human glomerulopathies. *J Am Soc Nephrol* 15:1835-1843, 2004

75. Stratton R, Rajkumar V, Ponticos M, Nichols B, Shiwen X, Black CM, Abraham DJ, Leask A: Prostacyclin derivatives prevent the fibrotic response to TGF-beta by inhibiting the Ras/MEK/ERK pathway. *FASEB J* 16:1949-1951, 2002

76. Zavadil J, Bitzer M, Liang D, Yang YC, Massimi A, Kneitz S, Piek E, Bottinger EP: Genetic programs of epithelial cell plasticity directed by

transforming growth factor-beta. *Proc Natl Acad Sci U S A* 98:6686-6691, 2001

77. Yamaguchi K, Shirakabe K, Shibuya H, Irie K, Oishi I, Ueno N, Taniguchi T, Nishida E, Matsumoto K: Identification of a member of the MAPKKK family as a potential mediator of TGF-beta signal transduction. *Science* 270:2008-2011, 1995

78. Yue J, Mulder KM: Activation of the mitogen-activated protein kinase pathway by transforming growth factor-beta. *Methods Mol Biol* 142:125-131, 2000

79. Mor A, Philips MR: Compartmentalized Ras/MAPK signaling. *Annu Rev Immunol* 24:771-800, 2006

80. Vinals F, Pouyssegur J: Transforming growth factor beta1 (TGF-beta1) promotes endothelial cell survival during in vitro angiogenesis via an autocrine mechanism implicating TGF-alpha signaling. *Mol Cell Biol* 21:7218-7230, 2001

81. Santibanez JF, Iglesias M, Frontelo P, Martinez J, Quintanilla M: Involvement of the Ras/MAPK signaling pathway in the modulation of urokinase production and cellular invasiveness by transforming growth factor-beta(1) in transformed keratinocytes. *Biochem Biophys Res Commun* 273:521-527, 2000

82. Grille SJ, Bellacosa A, Upson J, Klein-Szanto AJ, van Roy F, Lee-Kwon W, Donowitz M, Tsichlis PN, Larue L: The protein kinase Akt induces epithelial mesenchymal transition and promotes enhanced motility and invasiveness of squamous cell carcinoma lines. *Cancer Res* 63:2172-2178, 2003

83. Reimann T, Hempel U, Krautwald S, Axmann A, Scheibe R, Seidel D, Wenzel KW: Transforming growth factor-beta1 induces activation of Ras, Raf-1, MEK and MAPK in rat hepatic stellate cells. *FEBS Lett* 403:57-60, 1997

84. Yue J, Frey RS, Mulder KM: Cross-talk between the Smad1 and Ras/MEK signaling pathways for TGFbeta. *Oncogene* 18:2033-2037, 1999

85. Santibanez JF, Guerrero J, Quintanilla M, Fabra A, Martinez J: Transforming growth factor-beta1 modulates matrix metalloproteinase-9 production through the Ras/MAPK signaling pathway in transformed keratinocytes. *Biochem Biophys Res Commun* 296:267-273, 2002

86. Hartsough MT, Frey RS, Zipfel PA, Buard A, Cook SJ, McCormick F, Mulder KM: Altered transforming growth factor signaling in epithelial cells when ras activation is blocked. *J Biol Chem* 271:22368-22375, 1996

87. Mulder KM, Morris SL: Activation of p21ras by transforming growth factor beta in epithelial cells. *J Biol Chem* 267:5029-5031, 1992

88. Martinez-Salgado C, Rodriguez-Pena AB, Lopez-Novoa JM: Involvement of small Ras GTPases and their effectors in chronic renal disease. *Cell Mol Life Sci* 65:477-492, 2008

89. Avruch J, Khokhlatchev A, Kyriakis JM, Luo Z, Tzivion G, Vavvas D, Zhang XF: Ras activation of the Raf kinase: tyrosine kinase recruitment of the MAP kinase cascade. *Recent Prog Horm Res* 56:127-155, 2001

90. Katz ME, McCormick F: Signal transduction from multiple Ras effectors. *Curr Opin Genet Dev* 7:75-79, 1997

91. Yu L, Hebert MC, Zhang YE: TGF-beta receptor-activated p38 MAP kinase mediates Smad-independent TGF-beta responses. *EMBO J* 21:3749-3759, 2002

92. Bakin AV, Rinehart C, Tomlinson AK, Arteaga CL: p38 mitogen-activated protein kinase is required for TGFbeta-mediated fibroblastic transdifferentiation and cell migration. *J Cell Sci* 115:3193-3206, 2002

93. Edlund S, Landstrom M, Heldin CH, Aspenstrom P: Transforming growth factor-beta-induced mobilization of actin cytoskeleton requires signaling by small GTPases Cdc42 and RhoA. *Mol Biol Cell* 13:902-914, 2002

94. Shen X, Li J, Hu PP, Waddell D, Zhang J, Wang XF: The activity of guanine exchange factor NET1 is essential for transforming growth factor-beta-mediated stress fiber formation. *J Biol Chem* 276:15362-15368, 2001

95. Lee JM, Dedhar S, Kalluri R, Thompson EW: The epithelial-mesenchymal transition: new insights in signaling, development, and disease. *J Cell Biol* 172:973-981, 2006

96. Strutz F, Okada H, Lo CW, Danoff T, Carone RL, Tomaszewski JE, Neilson EG: Identification and characterization of a fibroblast marker: FSP1. *J Cell Biol* 130:393-405, 1995

97. Okada H, Ban S, Nagao S, Takahashi H, Suzuki H, Neilson EG: Progressive renal fibrosis in murine polycystic kidney disease: an immunohistochemical observation. *Kidney Int* 58:587-597, 2000

98. Franke WW, Schmid E, Osborn M, Weber K: Different intermediate-sized filaments distinguished by immunofluorescence microscopy. *Proc Natl Acad Sci U S A* 75:5034-5038, 1978

99. Dellagi K, Vainchenker W, Vinci G, Paulin D, Brouet JC: Alteration of vimentin intermediate filament expression during differentiation of human hemopoietic cells. *EMBO J* 2:1509-1514, 1983

100. Bienz M: beta-Catenin: a pivot between cell adhesion and Wnt signalling. *Curr Biol* 15:R64-R67, 2005

101. Kalluri R, Danoff TM, Okada H, Neilson EG: Susceptibility to anti-glomerular basement membrane disease and Goodpasture syndrome is linked to MHC class II genes and the emergence of T cell-mediated immunity in mice. *J Clin Invest* 100:2263-2275, 1997

102. Cosgrove D, Meehan DT, Grunkemeyer JA, Kornak JM, Sayers R, Hunter WJ, Samuelson GC: Collagen COL4A3 knockout: a mouse model for autosomal Alport syndrome. *Genes Dev* 10:2981-2992, 1996

103. Zeisberg M, Soubasakos MA, Kalluri R: Animal models of renal fibrosis. *Methods Mol Med* 117:261-272, 2005

104. Janssen U, Phillips AO, Floege J: Rodent models of nephropathy associated with type II diabetes. *J Nephrol* 12:159-172, 1999

105. Sung SA, Jo SK, Cho WY, Won NH, Kim HK: Reduction of renal fibrosis as a result of liposome encapsulated clodronate induced macrophage depletion after unilateral ureteral obstruction in rats. *Nephron Exp Nephrol* 105:e1-e9, 2007

106. Ricardo SD, Ding G, Eufemio M, Diamond JR: Antioxidant expression in experimental hydronephrosis: role of mechanical stretch and growth factors. *Am J Physiol* 272:F789-F798, 1997

107. Kawada N, Moriyama T, Ando A, Fukunaga M, Miyata T, Kurokawa K, Imai E, Hori M: Increased oxidative stress in mouse kidneys with unilateral ureteral obstruction. *Kidney Int* 56:1004-1013, 1999

108. Klahr S, Morrissey J: Obstructive nephropathy and renal fibrosis. *Am J Physiol Renal Physiol* 283:F861-F875, 2002

109. Diamond JR, Kees-Folts D, Ding G, Frye JE, Restrepo NC: Macrophages, monocyte chemoattractant peptide-1, and TGF-beta 1 in experimental hydronephrosis. *Am J Physiol* 266:F926-F933, 1994

110. Pimentel JL, Jr., Sundell CL, Wang S, Kopp JB, Montero A, Martinez-Maldonado M: Role of angiotensin II in the expression and regulation of transforming growth factor-beta in obstructive nephropathy. *Kidney Int* 48:1233-1246, 1995

111. Reyes AA, Klahr S: Renal function after release of ureteral obstruction: role of endothelin and the renal artery endothelium. *Kidney Int* 42:632-638, 1992

112. Kaneto H, Morrissey J, Klahr S: Increased expression of TGF-beta 1 mRNA in the obstructed kidney of rats with unilateral ureteral ligation. *Kidney Int* 44:313-321, 1993

113. Rodriguez-Pena AB, Grande MT, Eleno N, Arevalo M, Guerrero C, Santos E, Lopez-Novoa JM: Activation of Erk1/2 and Akt following unilateral ureteral obstruction. *Kidney Int* 74:196-209, 2008

114. Wang Y, Durkin JP: alpha-Amino-3-hydroxy-5-methyl-4-isoxazolepropionic acid, but not N-methyl-D-aspartate, activates mitogen-activated protein kinase through G-protein beta gamma subunits in rat cortical neurons. *J Biol Chem* 270:22783-22787, 1995

115. Ahn YM, Oh SW, Kang UG, Park J, Kim YS: An N-methyl-D-aspartate antagonist, MK-801, preferentially reduces electroconvulsive shock-induced phosphorylation of p38 mitogen-activated protein kinase in the rat hippocampus. *Neurosci Lett* 296:101-104, 2000

116. Cammarota M, Bevilaqua LR, Ardenghi P, Paratcha G, Levi dS, Izquierdo I, Medina JH: Learning-associated activation of nuclear MAPK, CREB and Elk-1, along with Fos production, in the rat hippocampus after a one-trial avoidance learning: abolition by NMDA receptor blockade. *Brain Res Mol Brain Res* 76:36-46, 2000

117. Chandler LJ, Sutton G, Dorairaj NR, Norwood D: N-methyl D-aspartate receptor-mediated bidirectional control of extracellular signal-regulated kinase activity in cortical neuronal cultures. *J Biol Chem* 276:2627-2636, 2001

118. Haddad JJ: N-methyl-D-aspartate (NMDA) and the regulation of mitogen-activated protein kinase (MAPK) signaling pathways: a revolving neurochemical axis for therapeutic intervention? *Prog Neurobiol* 77:252-282, 2005

119. Jiang Q, Gu Z, Zhang G, Jing G: N-methyl-D-aspartate receptor activation results in regulation of extracellular signal-regulated kinases by protein kinases and phosphatases in glutamate-induced neuronal apototic-like death. *Brain Res* 887:285-292, 2000

120. Zeng L, Lu L, Muller M, Gouaux E, Zhou MM: Structure-based functional design of chemical ligands for AMPA-subtype glutamate receptors. *J Mol Neurosci* 19:113-116, 2002

121. Barnstable CJ, Wei JY, Han MH: Modulation of synaptic function by cGMP and cGMP-gated cation channels. *Neurochem Int* 45:875-884, 2004

122. Monaghan DT, Bridges RJ, Cotman CW: The excitatory amino acid receptors: their classes, pharmacology, and distinct properties in the function of the central nervous system. *Annu Rev Pharmacol Toxicol* 29:365-402, 1989

123. Hollmann M, O'Shea-Greenfield A, Rogers SW, Heinemann S: Cloning by functional expression of a member of the glutamate receptor family. *Nature* 342:643-648, 1989

124. Gladding CM, Fitzjohn SM, Molnar E: Metabotropic glutamate receptor-mediated long-term depression: molecular mechanisms. *Pharmacol Rev* 61:395-412, 2009

125. Takagi N, Shinno K, Teves L, Bissoon N, Wallace MC, Gurd JW: Transient ischemia differentially increases tyrosine phosphorylation of NMDA receptor subunits 2A and 2B. *J Neurochem* 69:1060-1065, 1997

126. Adamchik Y, Baskys A: Glutamate-mediated neuroprotection against N-methyl-D-aspartate toxicity: a role for metabotropic glutamate receptors. *Neuroscience* 99:731-736, 2000

127. Sze C, Bi H, Kleinschmidt-DeMasters BK, Filley CM, Martin LJ: N-Methyl-D-aspartate receptor subunit proteins and their phosphorylation status are altered selectively in Alzheimer's disease. *J Neurol Sci* 182:151-159, 2001

128. Conn PJ: Physiological roles and therapeutic potential of metabotropic glutamate receptors. *Ann N Y Acad Sci* 1003:12-21, 2003

129. Sung B, Lim G, Mao J: Altered expression and uptake activity of spinal glutamate transporters after nerve injury contribute to the pathogenesis of neuropathic pain in rats. *J Neurosci* 23:2899-2910, 2003

130. Lee HG, Zhu X, O'Neill MJ, Webber K, Casadesus G, Marlatt M, Raina AK, Perry G, Smith MA: The role of metabotropic glutamate receptors in Alzheimer's disease. *Acta Neurobiol Exp (Wars)* 64:89-98, 2004

131. Trudeau LE: Glutamate co-transmission as an emerging concept in monoamine neuron function. *J Psychiatry Neurosci* 29:296-310, 2004

132. Nong Y, Huang YQ, Salter MW: NMDA receptors are movin' in. *Curr Opin Neurobiol* 14:353-361, 2004

133. Dingledine R, Borges K, Bowie D, Traynelis SF: The glutamate receptor ion channels. *Pharmacol Rev* 51:7-61, 1999

134. Cull-Candy SG, Brickley SG, Misra C, Feldmeyer D, Momiyama A, Farrant M: NMDA receptor diversity in the cerebellum: identification of subunits contributing to functional receptors. *Neuropharmacology* 37:1369-1380, 1998

135. Perez-Otano I, Ehlers MD: Learning from NMDA receptor trafficking: clues to the development and maturation of glutamatergic synapses. *Neurosignals* 13:175-189, 2004

136. Paoletti P, Neyton J: NMDA receptor subunits: function and pharmacology. *Curr Opin Pharmacol* 7:39-47, 2007

137. Magnusson KR: The aging of the NMDA receptor complex. *Front Biosci* 3:e70-e80, 1998

138. Guttmann RP, Sokol S, Baker DL, Simpkins KL, Dong Y, Lynch DR: Proteolysis of the N-methyl-d-aspartate receptor by calpain in situ. *J Pharmacol Exp Ther* 302:1023-1030, 2002

139. Meguro H, Mori H, Araki K, Kushiya E, Kutsuwada T, Yamazaki M, Kumanishi T, Arakawa M, Sakimura K, Mishina M: Functional characterization of a heteromeric NMDA receptor channel expressed from cloned cDNAs. *Nature* 357:70-74, 1992

140. Le Bourdelles B, Wafford KA, Kemp JA, Marshall G, Bain C, Wilcox AS, Sikela JM, Whiting PJ: Cloning, functional coexpression, and pharmacological characterisation of human cDNAs encoding NMDA receptor NR1 and NR2A subunits. *J Neurochem* 62:2091-2098, 1994

141. Karp SJ, Masu M, Eki T, Ozawa K, Nakanishi S: Molecular cloning and chromosomal localization of the key subunit of the human N-methyl-D-aspartate receptor. *J Biol Chem* 268:3728-3733, 1993

142. Yamazaki M, Mori H, Araki K, Mori KJ, Mishina M: Cloning, expression and modulation of a mouse NMDA receptor subunit. *FEBS Lett* 300:39-45, 1992

143. Ishii T, Moriyoshi K, Sugihara H, Sakurada K, Kadotani H, Yokoi M, Akazawa C, Shigemoto R, Mizuno N, Masu M, .: Molecular characterization of the family of the N-methyl-D-aspartate receptor subunits. *J Biol Chem* 268:2836-2843, 1993

144. Monyer H, Sprengel R, Schoepfer R, Herb A, Higuchi M, Lomeli H, Burnashev N, Sakmann B, Seeburg PH: Heteromeric NMDA receptors: molecular and functional distinction of subtypes. *Science* 256:1217-1221, 1992

145. Ikeda K, Nagasawa M, Mori H, Araki K, Sakimura K, Watanabe M, Inoue Y, Mishina M: Cloning and expression of the epsilon 4 subunit of the NMDA receptor channel. *FEBS Lett* 313:34-38, 1992

146. Kutsuwada T, Kashiwabuchi N, Mori H, Sakimura K, Kushiya E, Araki K, Meguro H, Masaki H, Kumanishi T, Arakawa M, .: Molecular diversity of the NMDA receptor channel. *Nature* 358:36-41, 1992

147. Bellone C, Nicoll RA: Rapid bidirectional switching of synaptic NMDA receptors. *Neuron* 55:779-785, 2007

148. Rebola N, Srikumar BN, Mulle C: Activity-dependent synaptic plasticity of NMDA receptors. *J Physiol* 588:93-99, 2010

149. Luo J, Wang Y, Yasuda RP, Dunah AW, Wolfe BB: The majority of N-methyl-D-aspartate receptor complexes in adult rat cerebral cortex contain at least three different subunits (NR1/NR2A/NR2B). *Mol Pharmacol* 51:79-86, 1997

150. Chazot PL: The NMDA receptor NR2B subunit: a valid therapeutic target for multiple CNS pathologies. *Curr Med Chem* 11:389-396, 2004

151. Leung JC, Travis BR, Verlander JW, Sandhu SK, Yang SG, Zea AH, Weiner ID, Silverstein DM: Expression and developmental regulation of the NMDA receptor subunits in the kidney and cardiovascular system. *Am J Physiol Regul Integr Comp Physiol* 283:R964-R971, 2002

152. Loftis JM, Janowsky A: The N-methyl-D-aspartate receptor subunit NR2B: localization, functional properties, regulation, and clinical implications. *Pharmacol Ther* 97:55-85, 2003

153. Hollmann M, Boulter J, Maron C, Beasley L, Sullivan J, Pecht G, Heinemann S: Zinc potentiates agonist-induced currents at certain splice variants of the NMDA receptor. *Neuron* 10:943-954, 1993

154. Hardingham GE: Coupling of the NMDA receptor to neuroprotective and neurodestructive events. *Biochem Soc Trans* 37:1147-1160, 2009

155. Durand GM, Bennett MV, Zukin RS: Splice variants of the N-methyl-D-aspartate receptor NR1 identify domains involved in regulation by polyamines and protein kinase C. *Proc Natl Acad Sci U S A* 90:6731-6735, 1993

156. Lynch DR, Guttmann RP: NMDA receptor pharmacology: perspectives from molecular biology. *Curr Drug Targets* 2:215-231, 2001

157. Nakanishi S: Molecular diversity of glutamate receptors and implications for brain function. *Science* 258:597-603, 1992

158. Ciabarra AM, Sullivan JM, Gahn LG, Pecht G, Heinemann S, Sevarino KA: Cloning and characterization of chi-1: a developmentally regulated member of a novel class of the ionotropic glutamate receptor family. *J Neurosci* 15:6498-6508, 1995

159. Das S, Sasaki YF, Rothe T, Premkumar LS, Takasu M, Crandall JE, Dikkes P, Conner DA, Rayudu PV, Cheung W, Chen HS, Lipton SA, Nakanishi N: Increased NMDA current and spine density in mice lacking the NMDA receptor subunit NR3A. *Nature* 393:377-381, 1998

160. Nishi M, Hinds H, Lu HP, Kawata M, Hayashi Y: Motoneuron-specific expression of NR3B, a novel NMDA-type glutamate receptor subunit that works in a dominant-negative manner. *J Neurosci* 21:RC185, 2001

161. Matsuda K, Fletcher M, Kamiya Y, Yuzaki M: Specific assembly with the NMDA receptor 3B subunit controls surface expression and calcium permeability of NMDA receptors. *J Neurosci* 23:10064-10073, 2003

162. Mayer ML: Glutamate receptors at atomic resolution. *Nature* 440:456-462, 2006

163. Mayer ML: Glutamate receptor ion channels. *Curr Opin Neurobiol* 15:282-288, 2005

164. Meddows E, Le Bourdelles B, Grimwood S, Wafford K, Sandhu S, Whiting P, McIlhinney RA: Identification of molecular determinants that are important in the assembly of N-methyl-D-aspartate receptors. *J Biol Chem* 276:18795-18803, 2001

165. Niethammer M, Kim E, Sheng M: Interaction between the C terminus of NMDA receptor subunits and multiple members of the PSD-95 family of membrane-associated guanylate kinases. *J Neurosci* 16:2157-2163, 1996

166. Bi R, Bi X, Baudry M: Phosphorylation regulates calpain-mediated truncation of glutamate ionotropic receptors. *Brain Res* 797:154-158, 1998

167. Wechsler A, Teichberg VI: Brain spectrin binding to the NMDA receptor is regulated by phosphorylation, calcium and calmodulin. *EMBO J* 17:3931-3939, 1998

168. Lynch DR, Guttmann RP: Excitotoxicity: perspectives based on N-methyl-D-aspartate receptor subtypes. *J Pharmacol Exp Ther* 300:717-723, 2002

169. Johnson JW, Ascher P: Glycine potentiates the NMDA response in cultured mouse brain neurons. *Nature* 325:529-531, 1987

170. Kleckner NW, Dingledine R: Requirement for glycine in activation of NMDA-receptors expressed in Xenopus oocytes. *Science* 241:835-837, 1988

171. Mony L, Kew JN, Gunthorpe MJ, Paoletti P: Allosteric modulators of NR2B-containing NMDA receptors: molecular mechanisms and therapeutic potential. *Br J Pharmacol* 157:1301-1317, 2009

172. Akazawa C, Shigemoto R, Bessho Y, Nakanishi S, Mizuno N: Differential expression of five N-methyl-D-aspartate receptor subunit mRNAs in the cerebellum of developing and adult rats. *J Comp Neurol* 347:150-160, 1994

173. Morhenn VB, Waleh NS, Mansbridge JN, Unson D, Zolotorev A, Cline P, Toll L: Evidence for an NMDA receptor subunit in human keratinocytes and rat cardiocytes. *Eur J Pharmacol* 268:409-414, 1994

174. Nahm WK, Philpot BD, Adams MM, Badiavas EV, Zhou LH, Butmarc J, Bear MF, Falanga V: Significance of N-methyl-D-aspartate (NMDA) receptor-mediated signaling in human keratinocytes. *J Cell Physiol* 200:309-317, 2004

175. Miglio G, Dianzani C, Fallarini S, Fantozzi R, Lombardi G: Stimulation of N-methyl-D-aspartate receptors modulates Jurkat T cell growth and adhesion to fibronectin. *Biochem Biophys Res Commun* 361:404-409, 2007

176. Patton AJ, Genever PG, Birch MA, Suva LJ, Skerry TM: Expression of an N-methyl-D-aspartate-type receptor by human and rat osteoblasts and osteoclasts suggests a novel glutamate signaling pathway in bone. *Bone* 22:645-649, 1998

177. Mentaverri R, Kamel S, Wattel A, Prouillet C, Sevenet N, Petit JP, Tordjmann T, Brazier M: Regulation of bone resorption and osteoclast survival by nitric oxide: possible involvement of NMDA-receptor. *J Cell Biochem* 88:1145-1156, 2003

178. Parisi E, Almaden Y, Ibarz M, Panizo S, Cardus A, Rodriguez M, Fernandez E, Valdivielso JM: N-methyl-D-aspartate receptors are expressed in rat parathyroid gland and regulate PTH secretion. *Am J Physiol Renal Physiol* 296:F1291-F1296, 2009

179. Deng A, Valdivielso JM, Munger KA, Blantz RC, Thomson SC: Vasodilatory N-methyl-D-aspartate receptors are constitutively expressed in rat kidney. *J Am Soc Nephrol* 13:1381-1384, 2002

180. Nasstrom J, Boo E, Stahlberg M, Berge OG: Tissue distribution of two NMDA receptor antagonists, [3H]CGS 19755 and [3H]MK-801, after intrathecal injection in mice. *Pharmacol Biochem Behav* 44:9-15, 1993

181. Lin YJ, Bovetto S, Carver JM, Giordano T: Cloning of the cDNA for the human NMDA receptor NR2C subunit and its expression in the central nervous system and periphery. *Brain Res Mol Brain Res* 43:57-64, 1996

182. Seeber S, Becker K, Rau T, Eschenhagen T, Becker CM, Herkert M: Transient expression of NMDA receptor subunit NR2B in the developing rat heart. *J Neurochem* 75:2472-2477, 2000

183. Deng A, Thomson SC: Renal NMDA receptors independently stimulate proximal reabsorption and glomerular filtration. *Am J Physiol Renal Physiol* 296:F976-F982, 2009

184. Anderson M, Suh JM, Kim EY, Dryer SE: Functional NMDA receptors with atypical properties are expressed in podocytes. *Am J Physiol Cell Physiol* 300:C22-C32, 2011

185. Giardino L, Armelloni S, Corbelli A, Mattinzoli D, Zennaro C, Guerrot D, Tourrel F, Ikehata M, Li M, Berra S, Carraro M, Messa P, Rastaldi MP: Podocyte Glutamatergic Signaling Contributes to the Function of the Glomerular Filtration Barrier. *J Am Soc Nephrol* 20:1929-1940, 2009

186. Sproul AD, Steele SL, Thai TL, Yu SP, Klein JD, Sands JM, Bell PD: N-Methyl-D-Aspartate Receptor Subunit NR3a Expression and Function in Principal Cells of the Collecting Duct. *Am J Physiol Renal Physiol* 2011

187. Corsi M, Fina P, Trist DG: Co-agonism in drug-receptor interaction: illustrated by the NMDA receptors. *Trends Pharmacol Sci* 17:220-222, 1996

188. Hood WF, Sun ET, Compton RP, Monahan JB: 1-Aminocyclobutane-1-carboxylate (ACBC): a specific antagonist of the N-methyl-D-aspartate receptor coupled glycine receptor. *Eur J Pharmacol* 161:281-282, 1989

189. Grosshans DR, Browning MD: Protein kinase C activation induces tyrosine phosphorylation of the NR2A and NR2B subunits of the NMDA receptor. *J Neurochem* 76:737-744, 2001

190. Chen BS, Roche KW: Regulation of NMDA receptors by phosphorylation. *Neuropharmacology* 53:362-368, 2007

191. Chen L, Huang LY: Protein kinase C reduces Mg2+ block of NMDA-receptor channels as a mechanism of modulation. *Nature* 356:521-523, 1992

192. Lan JY, Skeberdis VA, Jover T, Grooms SY, Lin Y, Araneda RC, Zheng X, Bennett MV, Zukin RS: Protein kinase C modulates NMDA receptor trafficking and gating. *Nat Neurosci* 4:382-390, 2001

193. Ghosh A: Neurobiology. Learning more about NMDA receptor regulation. *Science* 295:449-451, 2002

194. Salter MW, Kalia LV: Src kinases: a hub for NMDA receptor regulation. *Nat Rev Neurosci* 5:317-328, 2004

195. Kupper J, Ascher P, Neyton J: Internal Mg2+ block of recombinant NMDA channels mutated within the selectivity filter and expressed in Xenopus oocytes. *J Physiol* 507 (Pt 1):1-12, 1998

196. Kuner T, Schoepfer R: Multiple structural elements determine subunit specificity of Mg2+ block in NMDA receptor channels. *J Neurosci* 16:3549-3558, 1996

197. Vissel B, Krupp JJ, Heinemann SF, Westbrook GL: Intracellular domains of NR2 alter calcium-dependent inactivation of N-methyl-D-aspartate receptors. *Mol Pharmacol* 61:595-605, 2002

198. Traynelis SF, Burgess MF, Zheng F, Lyuboslavsky P, Powers JL: Control of voltage-independent zinc inhibition of NMDA receptors by the NR1 subunit. *J Neurosci* 18:6163-6175, 1998

199. Duguid IC, Smart TG: Retrograde activation of presynaptic NMDA receptors enhances GABA release at cerebellar interneuron-Purkinje cell synapses. *Nat Neurosci* 7:525-533, 2004

200. Kashiwagi K, Tanaka I, Tamura M, Sugiyama H, Okawara T, Otsuka M, Sabado TN, Williams K, Igarashi K: Anthraquinone polyamines: novel channel blockers to study N-methyl-D-aspartate receptors. *J Pharmacol Exp Ther* 309:884-893, 2004

201. Paoletti P, Vergnano AM, Barbour B, Casado M: Zinc at glutamatergic synapses. *Neuroscience* 158:126-136, 2009

202. Omelchenko IA, Nelson CS, Allen CN: Lead inhibition of N-methyl-D-aspartate receptors containing NR2A, NR2C and NR2D subunits. *J Pharmacol Exp Ther* 282:1458-1464, 1997

203. Guilarte TR, McGlothan JL: Selective decrease in NR1 subunit splice variant mRNA in the hippocampus of Pb2+-exposed rats: implications for synaptic targeting and cell surface expression of NMDAR complexes. *Brain Res Mol Brain Res* 113:37-43, 2003

204. Nagy J: The NR2B subtype of NMDA receptor: a potential target for the treatment of alcohol dependence. *Curr Drug Targets CNS Neurol Disord* 3:169-179, 2004

205. Huettner JE, Bean BP: Block of N-methyl-D-aspartate-activated current by the anticonvulsant MK-801: selective binding to open channels. *Proc Natl Acad Sci U S A* 85:1307-1311, 1988

206. Fagg GE: Phencyclidine and related drugs bind to the activated N-methyl-D-aspartate receptor-channel complex in rat brain membranes. *Neurosci Lett* 76:221-227, 1987

207. Williams K: Ifenprodil discriminates subtypes of the N-methyl-D-aspartate receptor: selectivity and mechanisms at recombinant heteromeric receptors. *Mol Pharmacol* 44:851-859, 1993

208. Perin-Dureau F, Rachline J, Neyton J, Paoletti P: Mapping the binding site of the neuroprotectant ifenprodil on NMDA receptors. *J Neurosci* 22:5955-5965, 2002

209. Malherbe P, Mutel V, Broger C, Perin-Dureau F, Kemp JA, Neyton J, Paoletti P, Kew JN: Identification of critical residues in the amino terminal domain of the human NR2B subunit involved in the RO 25-6981 binding pocket. *J Pharmacol Exp Ther* 307:897-905, 2003

210. MacDermott AB, Mayer ML, Westbrook GL, Smith SJ, Barker JL: NMDA-receptor activation increases cytoplasmic calcium concentration in cultured spinal cord neurones. *Nature* 321:519-522, 1986

211. Cull-Candy S, Brickley S, Farrant M: NMDA receptor subunits: diversity, development and disease. *Curr Opin Neurobiol* 11:327-335, 2001

212. Sheng M, Pak DT: Ligand-gated ion channel interactions with cytoskeletal and signaling proteins. *Annu Rev Physiol* 62:755-778, 2000

213. Shorte SL: N-methyl-D-aspartate evokes rapid net depolymerization of filamentous actin in cultured rat cerebellar granule cells. *J Neurophysiol* 78:1135-1143, 1997

214. Forrest D, Yuzaki M, Soares HD, Ng L, Luk DC, Sheng M, Stewart CL, Morgan JI, Connor JA, Curran T: Targeted disruption of NMDA receptor 1 gene abolishes NMDA response and results in neonatal death. *Neuron* 13:325-338, 1994

215. Scheetz AJ, Constantine-Paton M: Modulation of NMDA receptor function: implications for vertebrate neural development. *FASEB J* 8:745-752, 1994

216. Hardingham GE, Bading H: The Yin and Yang of NMDA receptor signalling. *Trends Neurosci* 26:81-89, 2003

217. Choi DW: Calcium-mediated neurotoxicity: relationship to specific channel types and role in ischemic damage. *Trends Neurosci* 11:465-469, 1988

218. Lipton SA, Rosenberg PA: Excitatory amino acids as a final common pathway for neurologic disorders. *N Engl J Med* 330:613-622, 1994

219. Budd SL, Nicholls DG: Mitochondria, calcium regulation, and acute glutamate excitotoxicity in cultured cerebellar granule cells. *J Neurochem* 67:2282-2291, 1996

220. White RJ, Reynolds IJ: Mitochondria accumulate Ca2+ following intense glutamate stimulation of cultured rat forebrain neurones. *J Physiol* 498 (Pt 1):31-47, 1997

221. Stout AK, Raphael HM, Kanterewicz BI, Klann E, Reynolds IJ: Glutamate-induced neuron death requires mitochondrial calcium uptake. *Nat Neurosci* 1:366-373, 1998

222. Papadia S, Soriano FX, Leveille F, Martel MA, Dakin KA, Hansen HH, Kaindl A, Sifringer M, Fowler J, Stefovska V, McKenzie G, Craigon M, Corriveau R, Ghazal P, Horsburgh K, Yankner BA, Wyllie DJ, Ikonomidou C, Hardingham GE: Synaptic NMDA receptor activity boosts intrinsic antioxidant defenses. *Nat Neurosci* 11:476-487, 2008

223. Kihara M, Yoshioka H, Hirai K, Hasegawa K, Kizaki Z, Sawada T: Stimulation of N-methyl-D-aspartate (NMDA) receptors inhibits neuronal migration in embryonic cerebral cortex: a tissue culture study. *Brain Res Dev Brain Res* 138:195-198, 2002

224. Chaudhuri P, Colles SM, Damron DS, Graham LM: Lysophosphatidylcholine inhibits endothelial cell migration by increasing intracellular calcium and activating calpain. *Arterioscler Thromb Vasc Biol* 23:218-223, 2003

225. Schwab A: Function and spatial distribution of ion channels and transporters in cell migration. *Am J Physiol Renal Physiol* 280:F739-F747, 2001

226. Janmey PA: Phosphoinositides and calcium as regulators of cellular actin assembly and disassembly. *Annu Rev Physiol* 56:169-191, 1994

227. Schwab A, Schuricht B, Seeger P, Reinhardt J, Dartsch PC: Migration of transformed renal epithelial cells is regulated by K+ channel modulation of actin cytoskeleton and cell volume. *Pflugers Arch* 438:330-337, 1999

228. Chitaev NA, Troyanovsky SM: Adhesive but not lateral E-cadherin complexes require calcium and catenins for their formation. *J Cell Biol* 142:837-846, 1998

229. Cristofanilli M, Akopian A: Calcium channel and glutamate receptor activities regulate actin organization in salamander retinal neurons. *J Physiol* 575:543-554, 2006

230. Rakic P, Komuro H: The role of receptor/channel activity in neuronal cell migration. *J Neurobiol* 26:299-315, 1995

231. Itzstein C, Espinosa L, Delmas PD, Chenu C: Specific antagonists of NMDA receptors prevent osteoclast sealing zone formation required for bone resorption. *Biochem Biophys Res Commun* 268:201-209, 2000

232. Ryan MJ, Johnson G, Kirk J, Fuerstenberg SM, Zager RA, Torok-Storb B: HK-2: an immortalized proximal tubule epithelial cell line from normal adult human kidney. *Kidney Int* 45:48-57, 1994

233. Carmichael J, DeGraff WG, Gazdar AF, Minna JD, Mitchell JB: Evaluation of a tetrazolium-based semiautomated colorimetric assay: assessment of chemosensitivity testing. *Cancer Res* 47:936-942, 1987

234. Valster A, Tran NL, Nakada M, Berens ME, Chan AY, Symons M: Cell migration and invasion assays. *Methods* 37:208-215, 2005

235. de Rooij J, Kerstens A, Danuser G, Schwartz MA, Waterman-Storer CM: Integrin-dependent actomyosin contraction regulates epithelial cell scattering. *J Cell Biol* 171:153-164, 2005

236. Chuang E, Barnard D, Hettich L, Zhang XF, Avruch J, Marshall MS: Critical binding and regulatory interactions between Ras and Raf occur through a small, stable N-terminal domain of Raf and specific Ras effector residues. *Mol Cell Biol* 14:5318-5325, 1994

237. Taylor SJ, Shalloway D: Cell cycle-dependent activation of Ras. *Curr Biol* 6:1621-1627, 1996

238. Garraway SM, Xu Q, Inturrisi CE: Design and evaluation of small interfering RNAs that target expression of the N-methyl-D-aspartate receptor NR1 subunit gene in the spinal cord dorsal horn. *J Pharmacol Exp Ther* 322:982-988, 2007

239. Brummelkamp TR, Bernards R, Agami R: A system for stable expression of short interfering RNAs in mammalian cells. *Science* 296:550-553, 2002

240. Hammad FT, Wheatley AM, Davis G: Long-term renal effects of unilateral ureteral obstruction and the role of endothelin. *Kidney Int* 58:242-250, 2000

241. Chevalier RL, Thornhill BA, Wolstenholme JT, Kim A: Unilateral ureteral obstruction in early development alters renal growth: dependence on the duration of obstruction. *J Urol* 161:309-313, 1999

242. Cao Y, Baig MR, Hamm LL, Wu K, Simon EE: Growth factors stimulate kidney proximal tubule cell migration independent of augmented tyrosine phosphorylation of focal adhesion kinase. *Biochem Biophys Res Commun* 328:560-566, 2005

243. Bonventre JV: Dedifferentiation and proliferation of surviving epithelial cells in acute renal failure. *J Am Soc Nephrol* 14 Suppl 1:S55-S61, 2003

244. White DP, Caswell PT, Norman JC: alpha v beta3 and alpha5beta1 integrin recycling pathways dictate downstream Rho kinase signaling to regulate persistent cell migration. *J Cell Biol* 177:515-525, 2007

245. Kroening S, Stix J, Keller C, Streiff C, Goppelt-Struebe M: Matrix-independent stimulation of human tubular epithelial cell migration by Rho kinase inhibitors. *J Cell Physiol* 223:703-712, 2010

246. Danen EH: Integrins: regulators of tissue function and cancer progression. *Curr Pharm Des* 11:881-891, 2005

247. Horwitz R, Webb D: Cell migration. *Curr Biol* 13:R756-R759, 2003

248. Gallant ND, Michael KE, Garcia AJ: Cell adhesion strengthening: contributions of adhesive area, integrin binding, and focal adhesion assembly. *Mol Biol Cell* 16:4329-4340, 2005

249. Nigam S, Weston CE, Liu CH, Simon EE: The actin cytoskeleton and integrin expression in the recovery of cell adhesion after oxidant stress to a proximal tubule cell line (JTC-12). *J Am Soc Nephrol* 9:1787-1797, 1998

250. Tian YC, Phillips AO: TGF-beta1-mediated inhibition of HK-2 cell migration. *J Am Soc Nephrol* 14:631-640, 2003

251. Hara-Chikuma M, Verkman AS: Aquaporin-1 facilitates epithelial cell migration in kidney proximal tubule. *J Am Soc Nephrol* 17:39-45, 2006

252. De Filippo AB, Ellen RP, McCulloch CA: Induction of cytoskeletal rearrangements and loss of volume regulation in epithelial cells by Treponema denticola. *Arch Oral Biol* 40:199-207, 1995

253. Moriyoshi K, Masu M, Ishii T, Shigemoto R, Mizuno N, Nakanishi S: Molecular cloning and characterization of the rat NMDA receptor. *Nature* 354:31-37, 1991

254. Jan CR, Ho CM, Wu SN, Tseng CJ: Mechanism of rise and decay of thapsigargin-evoked calcium signals in MDCK cells. *Life Sci* 64:259-267, 1999

255. Schratt GM, Nigh EA, Chen WG, Hu L, Greenberg ME: BDNF regulates the translation of a select group of mRNAs by a mammalian target of rapamycin-phosphatidylinositol 3-kinase-dependent pathway during neuronal development. *J Neurosci* 24:7366-7377, 2004

256. Bai G, Kusiak JW: Nerve growth factor up-regulates the N-methyl-D-aspartate receptor subunit 1 promoter in PC12 cells. *J Biol Chem* 272:5936-5942, 1997

257. Krainc D, Bai G, Okamoto S, Carles M, Kusiak JW, Brent RN, Lipton SA: Synergistic activation of the N-methyl-D-aspartate receptor subunit 1 promoter by myocyte enhancer factor 2C and Sp1. *J Biol Chem* 273:26218-26224, 1998

258. Bai G, Hoffman PW: Transcriptional Regulation of NMDA Receptor Expression. In: Biology of the NMDA Receptor edited by Antonius M Van Dongen, Boca Raton (FL): CRC Press, Taylor & Francis Group, LLC, 2009,

259. Racusen LC, Monteil C, Sgrignoli A, Lucskay M, Marouillat S, Rhim JG, Morin JP: Cell lines with extended in vitro growth potential from human renal proximal tubule: characterization, response to inducers, and comparison with established cell lines. *J Lab Clin Med* 129:318-329, 1997

260. Nigam SK, Rodriguez-Boulan E, Silver RB: Changes in intracellular calcium during the development of epithelial polarity and junctions. *Proc Natl Acad Sci U S A* 89:6162-6166, 1992

261. Stuart RO, Nigam SK: Regulated assembly of tight junctions by protein kinase C. *Proc Natl Acad Sci U S A* 92:6072-6076, 1995

262. Lau CG, Takeuchi K, Rodenas-Ruano A, Takayasu Y, Murphy J, Bennett MV, Zukin RS: Regulation of NMDA receptor Ca2+ signalling and synaptic plasticity. *Biochem Soc Trans* 37:1369-1374, 2009

263. Parisi E, Bozic M, Ibarz M, Panizo S, Valcheva P, Coll B, Fernandez E, Valdivielso JM: Sustained activation of renal N-methyl-D-aspartate receptors decreases vitamin D synthesis: a possible role for glutamate on the onset of secondary HPT. *Am J Physiol Endocrinol Metab* 299:E825-E831, 2010

264. Masszi A, Fan L, Rosivall L, McCulloch CA, Rotstein OD, Mucsi I, Kapus A: Integrity of cell-cell contacts is a critical regulator of TGF-beta 1-induced epithelial-to-myofibroblast transition: role for beta-catenin. *Am J Pathol* 165:1955-1967, 2004

265. Behrens J, Vakaet L, Friis R, Winterhager E, van Roy F, Mareel MM, Birchmeier W: Loss of epithelial differentiation and gain of invasiveness correlates with tyrosine phosphorylation of the E-cadherin/beta-catenin complex in cells transformed with a temperature-sensitive v-SRC gene. *J Cell Biol* 120:757-766, 1993

266. Muller T, Choidas A, Reichmann E, Ullrich A: Phosphorylation and free pool of beta-catenin are regulated by tyrosine kinases and tyrosine phosphatases during epithelial cell migration. *J Biol Chem* 274:10173-10183, 1999

267. Gilles C, Polette M, Mestdagt M, Nawrocki-Raby B, Ruggeri P, Birembaut P, Foidart JM: Transactivation of vimentin by beta-catenin in human breast cancer cells. *Cancer Res* 63:2658-2664, 2003

268. Lei S, Czerwinska E, Czerwinski W, Walsh MP, MacDonald JF: Regulation of NMDA receptor activity by F-actin and myosin light chain kinase. *J Neurosci* 21:8464-8472, 2001

269. Komuro H, Rakic P: Modulation of neuronal migration by NMDA receptors. *Science* 260:95-97, 1993

270. Namba T, Ming GL, Song H, Waga C, Enomoto A, Kaibuchi K, Kohsaka S, Uchino S: NMDA receptor regulates migration of newly generated neurons in the adult hippocampus via Disrupted-In-Schizophrenia 1 (DISC1). *J Neurochem* 2011

271. Gerber AM, Beaman-Hall CM, Mathur A, Vallano ML: Reduced blockade by extracellular Mg(2+) is permissive to NMDA receptor activation in cerebellar granule neurons that model a migratory phenotype. *J Neurochem* 114:191-202, 2010

272. Ivanov A, Pellegrino C, Rama S, Dumalska I, Salyha Y, Ben Ari Y, Medina I: Opposing role of synaptic and extrasynaptic NMDA receptors in regulation of the extracellular signal-regulated kinases (ERK) activity in cultured rat hippocampal neurons. *J Physiol* 572:789-798, 2006

273. Sutton G, Chandler LJ: Activity-dependent NMDA receptor-mediated activation of protein kinase B/Akt in cortical neuronal cultures. *J Neurochem* 82:1097-1105, 2002

274. Kim MJ, Dunah AW, Wang YT, Sheng M: Differential roles of. *Neuron* 46:745-760, 2005

275. Barrallo-Gimeno A, Nieto MA: The Snail genes as inducers of cell movement and survival: implications in development and cancer. *Development* 132:3151-3161, 2005

276. Carrozzino F, Soulie P, Huber D, Mensi N, Orci L, Cano A, Feraille E, Montesano R: Inducible expression of Snail selectively increases paracellular ion permeability and differentially modulates tight junction proteins. *Am J Physiol Cell Physiol* 289:C1002-C1014, 2005

277. Hayashida T, Decaestecker M, Schnaper HW: Cross-talk between ERK MAP kinase and Smad signaling pathways enhances TGF-beta-dependent responses in human mesangial cells. *FASEB J* 17:1576-1578, 2003

278. Horiguchi K, Shirakihara T, Nakano A, Imamura T, Miyazono K, Saitoh M: Role of Ras signaling in the induction of snail by transforming growth factor-beta. *J Biol Chem* 284:245-253, 2009

Annex

PUBLICATIONS

1. **Bozic M**, de Rooij J, Parisi E, Ruiz Ortega M, Fernandez E, Valdivielso JM. Glutamatergic signaling maintains the epithelial phenotype of proximal tubular cells. J Am Soc Nephrol 2011; 22: 1099-1111. doi: 10.1681/ASN.2010070701.
2. Parisi E, **Bozic M**, Ibarz M, Panizo S, Valcheva P, Coll B, Fernández E, Valdivielso JM. Sustained activation of renal N-methyl-D-aspartate receptors decreases vitamin D synthesis: a possible role for glutamate on the onset of secondary HPT. Am J Physiol Endocrinol Metab 2010; 299: E825-E831. doi: 10.1152/ajpendo.00428.2010.
3. Jovanovic M, **Bozic M**, Kovacevic T, Radojcic Lj, Petronijevic M, Vicovac Lj. Effects of anti-phospholipid antibodies on a human trophoblast cell line (HTR-8 SV/neo). Acta Histochem 2010; 112: 34-41.
4. Bojic-Trbojevic Z, **Bozic M**, Vicovac Lj. Steroid hormones modulate galectin-1 in the trophoblast HTR-8/SVneo cell line. Arch Biol Sci 2008; 60 (1): 11-23.
5. Vicovac Lj, **Bozic M**, Bojic-Trbojevic Z, Golubovic S. Carcinoembryonic antigen and related molecules in normal and transformed trophoblast. Placenta 2007; 28: 85-96.
6. Petronijevic M, Vrzic-Petronijevic S, Boskovic V, Bratic D, Vicovac L, **Bozic M**. Refractory metastatic choriocarcinoma treated surgically with polychemotherapy - case report. Eur J Gynaecol Oncol 2006; 27(5); 523-525.
7. **Bozic M**, Golubovic S, Petronijevic M, Vicovac Lj. Expression of galectin-3 and carcinoembryonic antigen in the trophoblast of the gestational trophoblastic disease. J BUON 2004; 9 (4): 427-432.
8. **Bozic M**, Petronijevic M, Milenkovic S, Atanackovic J, Lazic J and Vicovac Lj. Galectin-1 and galectin-3 in the trophoblast of the gestational trophoblastic disease. Placenta 2004; 25: 797-802.
9. **Bozic M**. Phenotypic characterization of invasive trophoblasts of the gestational trophoblastic diseases - *in situ* and *in vitro* expression of galectin-1 and galectin-3. MSc Thesis, University of Belgrade, Faculty of Biology 2003. (*in Serbian*).